

**PHASE TRANSITIONS AND
RELATED PROPERTIES OF
ORGANIC-INORGANIC HYBRID
MATERIALS**

K. Mattukat

A dissertation submitted to the
Faculty of Science,
University of the Witwatersrand,
Johannesburg,
in fulfillment of the requirements for
the degree of Master of Science

Supervisor: Prof. D.G. Billing
Co-supervisor: Dr. M. Rademeyer

January 2012

“Learning is a treasure that will
follow its owner everywhere”

-Chinese proverb

Declaration

I declare that this thesis is my own, unaided work. It is submitted for the Degree of Master of Science in the University of the Witwatersrand, Johannesburg. It has not been submitted before for any degree or examination in any other University.

_____.

(Signature of candidate)

____ day of _____ 20 ____ .

Table of contents

Abstract

Acknowledgements

1. Introduction.....	1
1.1 Metal-halide complexes.....	2
1.2 Organic component.....	2
1.3 Distortions within the inorganic component.....	3
1.4 Properties.....	3
1.5 Powder and Single Crystal X-ray Diffraction.....	7
1.6 Single crystal challenges.....	9
2. Literature survey.....	11
3. Experimental.....	20
3.1 Organic components.....	20
3.2 Inorganic components.....	20
3.3 Synthesis.....	20
3.4 Equipment.....	21
3.5 Differential scanning calorimetry.....	21
3.6 Luminescence.....	22
3.7 Software.....	22
4. Results.....	23
4.1 Tetrahedral coordination.....	25
4.1.1 Zinc (II) halide hybrid crystals.....	25
4.1.2 Cobalt (II) halide hybrid crystals.....	46
4.1.3 Mercury (II) halide hybrid crystals.....	53
4.2 Isolated Octahedra Coordination.....	59
4.2.1 Zinc(II) halide hybrid crystals.....	59

4.3 Octahedral Co-ordination.....	64
4.3.1 Copper (II) chloride Hybrid crystals.....	64
4.3.2 Lead (II) Halide Hybrid Crystals.....	70
5. Discussion.....	77
6. Conclusion.....	82
7. References.....	83

Abstract

Organic-inorganic hybrid perovskite materials incorporate inorganic as well as organic moieties into a single monolithic nanocomposite structure. Generally the crystals adopt a high degree of order through self-assembly which results from the various bonding interactions. Organic-inorganic aliphatic hybrid crystals are generally represented by the formula: $[(C_nH_{2n+1})NH_3]_2 MX_4$. These hybrid structures are characterized by an alternating structure where the ionic, inorganic metal halide layers are sandwiched between paraffinic alkylammonium chains (Ciajolo *et al.* 1977; Zuniga *et al.* 1983; Guo *et al.* 1995).

This study was based around hybrid materials containing a range of aliphatic amines and the divalent metals: Copper, Cobalt, Zinc, Mercury and Lead. The hybrid crystals that were synthesized in this study were structurally and thermally characterized as a majority of the structures were novel.

The coordination of the inorganic metal-halide component was determined by the divalent metal centre. The divalent zinc, mercury and cobalt centers which were ionically bonded to chlorine, bromine or iodine tended to form isolated tetrahedral units. The zinc (II) chloride hybrid crystals however had the ability to coordinate as either isolated octahedral or isolated tetrahedral units. The lead and cadmium hybrid crystals coordinated as corner sharing octahedral units which extended along two dimensions. The packing characteristics of the cationic organic chains were directly influenced by the coordination and dimensionality of the inorganic component.

The hybrid crystals were thermally characterized as they tend to exhibit a number of phase transitions such as solid-solid phase transitions and order-disorder transitions.

Some hybrid crystals proved to be more stable than others when exposed to various atmospheric conditions. Overall the iodine containing crystals were not as stable as they tended to oxidized and degraded easily. The mercury containing crystals were also quite unstable when exposed to the atmosphere.

Acknowledgements

I would like to thank Dave for taking me under his wing and introducing me to the world of crystallography and XRD. He always had a welcoming, open door policy and always ensured that I had some pocket money and an endless supply of coffee in the percolator. I'd also like to thank Caren Billing as her door was always open to Heidi when she came for a visit.

The ongoing family joke was that by the time I finished my studies at Wits I would be eligible for retirement. I would like to thank my parents, Michelle and Alfred Mattukat, for their everlasting support and encouragement throughout the long years at Wits as none of this would have been possible without you.

My grandparents, Pat and Simon, were also always willing to support, congratulate and brag about me at every opportunity.

Scott and Werner; life would not be the same without you!

Dedication

I dedicate this study to Simon and Patricia Schultz.

They that love beyond the world

cannot be separated by it.

Death cannot kill what never dies

~ William Penn

1.Introduction

Organic-inorganic hybrid perovskite materials incorporate inorganic as well as organic moieties into a single monolithic nanocomposite structure. It is hoped that the hybrids result in materials with enhanced, desirable properties. In principle these semi-conducting crystal systems can be engineered to produce various optical, electronic and magnetic properties, which depend greatly on their composition and crystal structure(Mitzi, 1999). Potential applications of the hybrid materials include electroluminescent devices, optoelectronic and electronic materials (Glavcheva, 2004).Microelectronics uses polyimide hybrids, which are heat resistant, chemically stable and exhibit various electrical properties(Mitzi, 1999). Hybrid materials occurring naturally include compounds such as mollusk shells and human teeth.

In the literature these hybrids are often referred to as layered perovskite materials. This stems from the ability of the divalent metal halide to form corner sharing octahedral layers which are sandwiched between cationic organic layers ($C_nH_{2n+1} NH_3$), refer to **Figure 1**. The entire system is then held together by a series of charge assisted hydrogen bonds between the cationic organic species and the halide atoms of the inorganic layer.

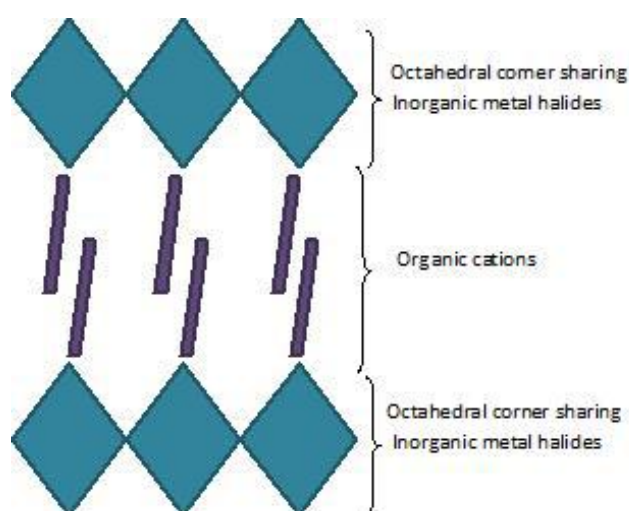


Figure 1: Schematic representation of the layered arrangement of the organic-inorganic hybrid layered perovskite crystals (Mitzi, 1999).

Generally the crystals adopt a high degree of order through self-assembly which results from the various bonding interactions. The assembly process takes place without the presence of any external interference(Mitzi, 1999).The hybrid organic-inorganic metal halide complexes are held together by a series of covalent and ionic interactions. The spatial and electronic structure of the complexed metal ions depends on their co-ordination number, geometry, oxidation state and the spin state(Zhong, 2008).

1.1 Metal halide composites

The anionic inorganic complex is comprised of a metal ionically coordinated to a halide atom. The hybrids assemble themselves into various dimensional structures. 0D (zero dimensional) structures represent isolated inorganic units. Isolated structures typically result from densely packed organic cations. As the dimensionality increases the charge of the inorganic halide complex decreases as the ligands are shared between the metal atoms. Therefore isolated units carry a greater negative charge to compensate for the densely packed organic cations. As the charge of the system is lowered the structures can vary considerably from one dimensional (chains), two (sheets) and three-dimensional structures (Dobrzycki, 2008). The larger dimensional structures result from bridging halide ions (one, two or three) between metal atoms (Billing, 2006). The metal halide component of the hybrid structure contributes to characteristics such as electrical mobility, magnetic interactions, mechanical hardness and thermal stability (Glavcheva, 2004).

1.2 Organic component

The organic molecules form cations by protonation of the amine functional group to form an ammonium molecule. The cation balances the negative charge of the anionic inorganic complex via strong charge assisted hydrogen bonds and electrostatic interactions. The ammonium groups extend right into the inorganic sub-structure and typically hydrogen bonds to the halide atoms. The organic components may interact with each other via charge assisted Van der Waals interactions (Mitzi, 1999). Stacking of the organic components can play a decisive role in regulating the network structure (Zhong, 2008). Three-dimensional systems have a defined area in which the organic cations can be placed. If the organic cation is larger than the defined area, interferences prevent the hybrids formation (Xu, 2003). The structure of the hybrid material depends on the organic component and the ions overall charge neutrality. The organic ions can influence the geometry of the inorganic structure (Mitzi, 1999).

Modifications of the organic cations influence the bonding features of the inorganic structure resulting in distortions and different packing motifs. The hybrid or powder colour is directly dependant on the exciton energy, which can be varied by having different substituted organic molecules (Xu, 2003). The organic cation component may allow for structural diversity, luminescence, polarizability and plastic mechanical properties (Mitzi, 1999).

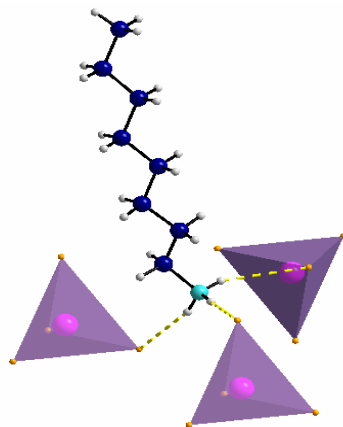


Figure 2: The hydrogen bonding arrangement of a cationic organic chain to three isolated tetrahedral inorganic metal halides (Mattukat, 2009).

1.3 Distortions within the inorganic component

Distortions within the inorganic lattice influence the electronic properties of hybrid materials. Many properties depend upon the band gap of the complex, which determines the wavelength of light emitted when stimulated electrically or optically (Knutson, 2005).

Distortions result from the relative charge density and the steric requirements of the organic cation in the hybrid complex. The band gap and conduction bands of compounds such as $(RNH_3)_2SnI_4$ are influenced by the structural requirements of the organic cation. Structural distortions result in various experimental exciton energy and calculated band gaps (Knutson, 2005). Two types of distortions occur for two dimensional hybrid systems: in plane distortions and out of plane distortions. The type of distortion is dependent on the charge density of the cation. For higher charge density the hybrid systems collapse to form in plane distortions. This results in a decrease in the width of the valence and conduction bands and increased band gaps. As the metal-halide-metal bond angle bends away from the idealized 180° there is a loss in the anti-bonding interactions of the metal's orbitals. The bottom of the conduction band determines the band gap, which is mostly non-bonding in an idealized structure. The distortions result in lower symmetrical systems where orbital mixing raises the energy of the bottom of the conduction band and therefore increases the band gap upon distortion. On the other hand cations with larger size and therefore lower charge density exhibit out-of-plane-distortions (Knutson, 2005).

1.4 Properties

1.4.1 Semi-conducting behaviour

The hybrid materials tend to exhibit semi-conducting behaviour by forming multilayered quantum well structures due to insulating organic molecules sandwiched between the inorganic layers. The inorganic halide sheets act as the wells while the organic molecules, which have a much larger band gap, represent the barrier layers. The dielectric constant of

the barrier is smaller than the quantum well structure (Mitzi, 1999; Papavassiliou, 1994; Hong, 1992).

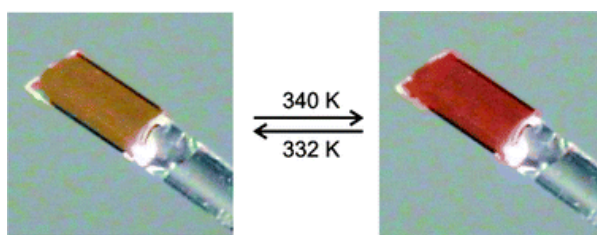
This semiconducting behaviour leads to the question whether the Organic-inorganic hybrid materials have the potential of being used in areas such as electronic devices, sensors and solar cells? Modern semiconductive devices commonly use silicon based systems due to its high mobility of the covalent network. The deposition of the semiconducting thin films involves a costly process. This leaves the market open for other easily processible semiconductors which are low cost to produce. Could the semiconducting organic-inorganic hybrid materials be the answer? (Mitzi, 2004)

If we had to consider a hybrid material for these applications we would have to determine if the carrier mobility and the band gap are suitable for any kind of electronic device. The carrier mobility is the proportionality constant between the applied electric field and the corresponding average carrier drift velocity (maximum switching speed of electronic device). The band gap relates to the carrier density of the material. When the band gap is too small it is difficult to switch off while if it's too large the device becomes impractical to switch on (Mitzi, 2004).

1.4.2 Solid-solid Phase Transitions and Thermochromism

Phase transitions result from the energetic preference of the crystal structure. Previous studies have shown that the transitions are not related by a group-subgroup transformation as previously postulated and therefore the transitions cannot be predicted. The energetic barriers between two crystal forms are different and the crystal system chosen will be the one requiring minimal amount of energy (Leoni, 2007).

Thermochromism is a property or characteristic where a compound changes colour due to a change in temperature. This is generally associated with solid-solid phase transition. The colour of a crystal is determined by the transmission of certain wavelengths from the crystal structure.



(Billing, 2008)

Figure 3: The organic-inorganic lead iodide crystal above undergoes a reversible thermochromic phase transition between the temperatures indicated. The yellow crystal transforms to a red crystal as it is heated and the reverse can be seen when cooled.

Thermochromic phase transitions have been studied in compounds such as $(\text{NH}_2(\text{C}_2\text{H}_5)_2)_2\text{CuCl}_4$ and are extensively used in optoelectronic applications. The high temperature structure was represented by a yellow crystal while the low temperature

structure became green. Once the crystal structures, at low and high temperatures, were determined it became apparent that the colour change was due to the change in the coordination environment of the copper (II) ion. It has been postulated that the thermochromic behaviour exhibited by the hybrid was greatly influenced by the hydrogen bonding within the crystal system. Phase transitions potentially result in a complete reorganization of hydrogen bonding within a crystal system; as the temperature increases so do the hydrogen bond lengths, therefore resulting in weaker hydrogen bonds. Low temperatures allow for closer interactions within a crystal system resulting in stronger hydrogen bonding. These strong hydrogen bonding interactions deform the electron cloud of the chloride ions which force the inorganic component to change geometry (Kapustyanyk, 2000).

Phase transitions are not always necessarily reversible. In some instances, once the crystal has undergone a phase transition, the transition remains permanent even if the crystal is returned to its initial temperature. A series of urethane-substituted polydiacetylene compounds with varying alkyl chain lengths were synthesized (Tachibana et al. 2001). These compounds exhibited thermochromic behaviour. The compounds showed even-odd effects where the even alkyl chain-containing polymers did not exhibit reversible thermochromic phase transitions. The odd chain lengths however did undergo a reversible phase change (Tachibana, 2001). Properties such as phase transitions and packing characteristics can depend greatly on the parity of the number of C atoms in an aliphatic chain (Zuniga *et al.* 1983). A similar effect has been identified in the present study for the zinc series of compounds where the odd and even aliphatic chains each exhibit their own packing characteristics.

1.4.3 Luminescence

Luminescence is the phenomenon where a material emits radiation in response to a previous excitation process. The materials that exhibited this phenomenon are usually semi-conducting materials where there is a radiative recombination of excited electrons and their holes (Shriver and Atkins, 1999). The exciton state is therefore associated with the band gap of the inorganic layer (Xu, 2003). The wavelength of the emitted radiation is larger in comparison with the initial radiation source as there is an energy loss of the initial radiation. This is due to the loss of energy via non-radiative decay by thermal degradation (Shriver and Atkins, 1999).

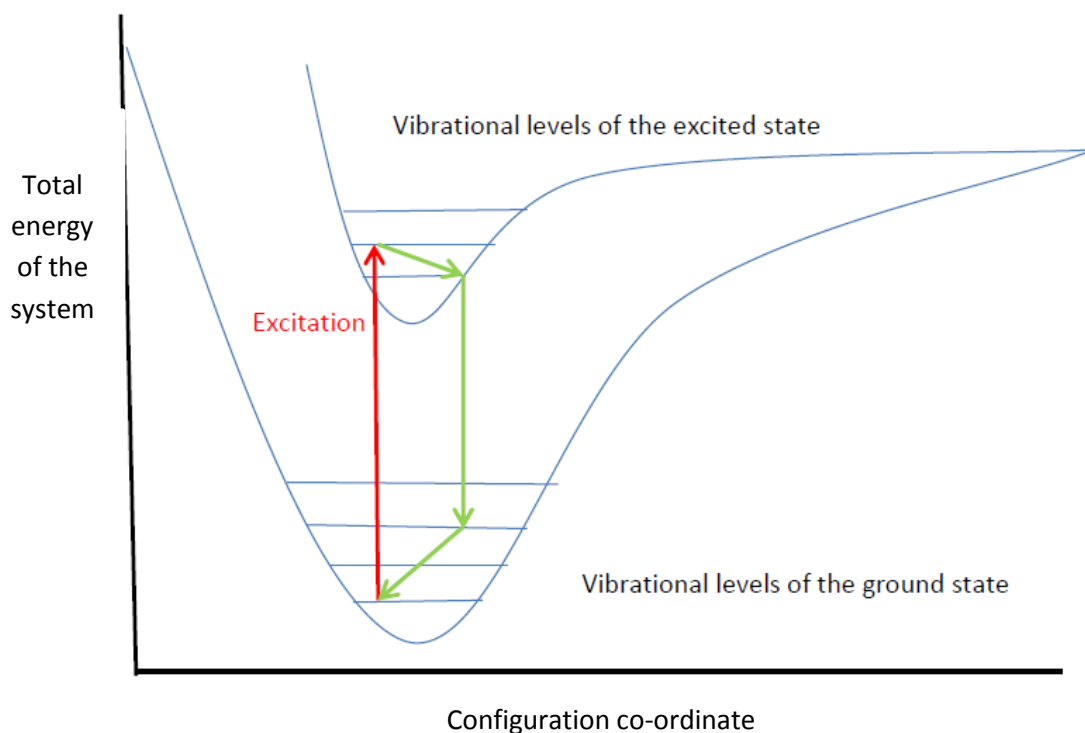


Figure 4: Processes involved in luminescence include excitation, thermal degradation and emission.

The exciton state is dependent on the binding energy of the electrons and the oscillator strength. Factors such as the dielectric constant between the organic and inorganic compounds result in exciton binding energy enhancement (Knutson, 2005).

Absorption and luminescent spectra which are in the visible wavelength region can be used as a quantitative measure of colour for the hybrid materials that exhibit any kind of thermochromic phase transition. The electronic structure of the transition metals allows the crystals to have colour, this excludes all d^{10} metals. This allows us to characterize the structure and bonding in the electronic ground state or study the photochemical and optical properties of the excited state. The photochemical properties within a crystal depend on the magnitude of the structural differences between the ground and the excited state. The wavelength or energetic differences between the absorbance and luminescent peaks in the spectra are described by the Stokes shift (Reber, 2008).

Structural properties such as the halide-metal-halide angles affect the optical properties of the compound. Larger variations in the angle result in longer wavelengths and therefore lower energies of the exciton peaks as the radiation is absorbed or emitted (Xu, 2003). The energy band gap of the hybrid materials is also dependent upon the dimensionality of the complex. The dimensionality of a hybrid is determined by the inorganic metal halide bonding scheme. Each inorganic metal halide unit can bond in various ways, where zero dimensional (isolated metal halide anions), one dimensional (anions bond along one cell axis), two dimensional (the bonding extends in two directions) and three dimensional

(anions bond in all three directions) hybrids exist. As the hybrid decreases its dimensionality, the exciton state shifts towards a higher energy state (Mousdis, 1998).

1.4.4 Magnetism

The magnetism of a compound results from metal ion interactions. Therefore the type of metal ion is important as well as the dimensionality of the system as lower dimensional systems have stronger interactions. Metal ions interact via the nonmagnetic, bridging halide ions. With each electrostatic interaction there is a dipole magnetic field associated with each spin interaction. The fields then interact with the fields of adjacent spins. The magnetic dipolar field of the crystal system is then determined by the coupling of moment's in particular crystallographic directions (Mitzi, 1999).

Hybrids such as $(RNH_3)_2CuCl_4$ where R is methyl-benzene, 1-methyl-naphthalene and 1-propyl-naphthalene show ferromagnetic properties when placed in an external electric field. The magnetization is greatly temperature dependant. π electrons in the organic component allow for electronic state mixing between the inorganic and organic units. The electronic states of the compounds were influenced by light irradiation. This implies that the magnetic properties of these compounds could be controlled (Shikoh, 2001).

1.5 Powder and Single Crystal X-ray Diffraction Methods

All forms of XRD use a monochromatic wave source for structural identification. Single crystal XRD (SC-XRD) is a qualitative technique while powder XRD (PXRD) can be used as a qualitative and quantitative technique. Both methods are used to identify unit cell dimensions and symmetry (Atkins, 1978). SC-XRD requires a crystal sample of high quality which is robust and optically clear. The single crystal is mounted onto a glass fibre. The crystal's diffraction pattern consists of regularly spaced spots or reflections. These single spots are termed Laue spots.

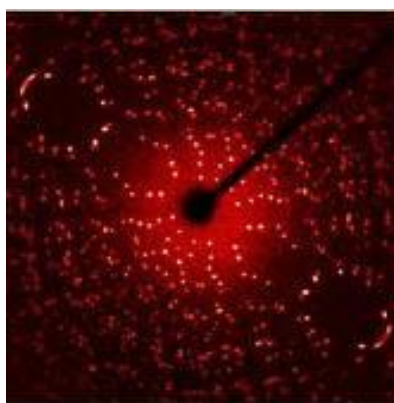


Figure 5: Diffraction pattern of a single crystal sample shows regularly spaced Laue spots which are used to solve the crystal structure. The darkened portion or line in the pattern represents the beam stop.

Powder samples are composed of a large collection of minute crystals which have random orientations. Crystal orientation is extremely important when dealing with powder samples

and therefore sample preparation is an important aspect. The crystallites of the powder sample are randomly orientated when the incoming X-ray beam interacts with the crystal planes. The deflected beams are described as cones where they are diffracted as arcs of circles. The angle of each cone is determined by the position of the image on the diffraction pattern. Each (hkl) plane gives rise to a different diffraction cone. All crystal orientations should be represented by a randomly orientated sample and therefore an averaging effect that takes place. This causes the three dimensional reciprocal space to be projected onto a single dimension. Once the diffracted radiation has been collected onto the flat plate of the detector, smooth diffraction rings result instead of the Laue spots. Indexing a diffracted image to determine (hkl) planes results in identification of the unit cell as each cell produces a recognisable and distinguishable pattern (Atkins, 1978).

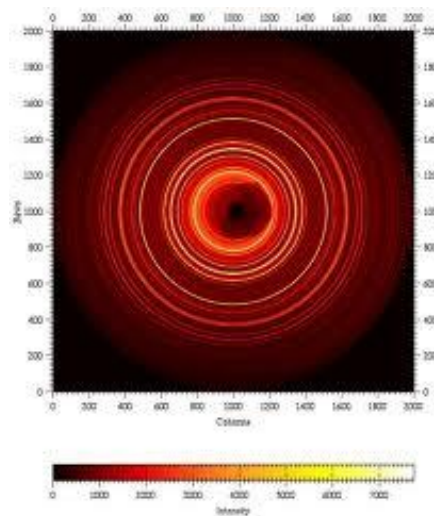


Figure 6: Diffraction pattern of a powder sample where all the hkl planes are represented as arcs of circles

The spacing between the (hkl) plane is given by the following formula:

Equation 1: $d_{hkl} = a / (h^2 + k^2 + l^2)^{1/2}$

d spacing between the planes

a is the unit cell length for a cubic unit cell (Atkins, 1978).

The angle at which the hkl planes are diffracted is given by the Bragg condition:

Equation 2:

$$\sin \Theta_{hkl} = \left[\frac{\lambda}{2a\sqrt{h^2 + k^2 + l^2}} \right]$$

This is true for the first order reflection (n=1)

Θ is the angle of incidence

λ is the wavelength

a is the unit cell length of a cubic unit cell (Atkins, 1978).

Once the diffraction pattern of any sample has been collected the images are analysed and converted into structural data.

1.6 Single Crystal Challenges

This study focuses mainly on the structural characterization by single crystal X-ray diffraction. Fortunately experience has taught us that the organic-inorganic hybrids that are the focus of the current study are crystallographically challenging materials (Lemmerer 2006; Black; Mattukat). That means that most of the “single-crystals” prepared do not result in diffraction data that are amenable to treatment via routine chemical crystallographic methods. In particular the materials are susceptible to twinning, disorder and the formation of modulated structures.

1.6.1 Twinning

A twinned crystal can be described as ‘regular aggregates consisting of crystals of the same species which are joined together in some definite mutual orientation’ (Giacovazzo, 1992). There are four categories of twinning:

The first type of twinning is merohedral twinning which only occurs in tetragonal, trigonal, hexagonal and cubic space groups. There is an exact overlap of the reciprocal lattices of the twinned crystals during diffraction. The structure solution of these twins can often be difficult. Twinning by pseudo-merohedry occurs when there is a complete but approximate overlap of reciprocal lattices. The crystals often belong to a higher crystal system than the structure predicted. Recticular merohedral twinning occurs in the rhombohedral space group. The structure solution is not as difficult as the other types of twinning. The final type of twinning is non merohedral twinning. The reciprocal lattices do not overlap exactly. These twins result in cell determination problems, cell refinement problems, integration complications and difficult structure solutions. The diffraction patterns of the twins have reflections which are too sharp or tend to split (Nespolo, 2003; Herbst-Irmer R, 2008).

In practice twinning within a crystal is often checked using the APEX 2 software, TwinRotMat or Rotax programs which can be found within the suite of programs. The twin laws can then be determined and applied to the structures (SHELXL) (Herbst-Irmer, 2008).

1.6.2 Disorder

Disorder occurs when the orientations of the molecules differ randomly within the crystal structure. The structure as determined by standard single crystal methods is therefore an average over the whole crystal. The disordered structures can be identified by distorted anisotropic displacement parameters (ADPs) and high residual electron density peaks or holes.

Two types of disorder exist:

Discrete or continuous positional disorder occurs when one atom occupies more than one site. The position of that disordered atom is therefore split between two or more sites and the actual fractional degree with which the atom occupies each site, is given by the site occupancy factor (partial occupancy model).

Static substantial disorder. The same site in two separate unit cells is occupied by different types of atoms (Muller P, Refinement of disorder with SHELXL).

1.6.3 Modulated structures

Modulated structures contain atoms or molecules that are shifted or rotated with respect to their neighbours. These distortions within the crystal cannot be explained by the crystal space group and results in the three dimensional crystal structures being destroyed. The shifts and rotations are not random but follow distinct rules. The modulated structures are identified by additional satellites surrounding the main reflections in the diffraction pattern. The modulated structure cannot therefore be indexed by only 3 reciprocal lattice vectors, the additional peaks require $3 + d$ indices where d is completely dependent on the crystal structure (Wagner, 2009).

The modulated structures can be solved in three ways:

- **The basic cell and average structure** method requires us to only index the main reflections and ignore all the satellite reflections. This will result in the basic cell which is also termed the subcell. The contents of the unit cell will be an average structure over several unit cells. The crystal structure is characterized by large anisotropic displacement parameters (ADP), unrealistic bond lengths and angles (Wagner, 2009). This method is in many ways similar to disordered structures.
- **Supercell and Superstructure** drops the distinction between the main and satellite reflections therefore using them equivalently. This results in a smaller reciprocal unit cell and reciprocal lattice. In direct space the unit cell is larger and referred to as a supercell and the structure as a superstructure. The superstructure will then be an approximation. The crystal structure is characterized by poor agreement factors, large standard deviations of refined parameters, split atoms and large ADPs (Wagner, 2009).
- **Moving into Superspace** uses all the reflections but there is a distinction between the main and satellite reflections. The first step requires the determination of the reciprocal unit cell from the main reflections. The distribution of satellite reflections are not random and therefore are divided into groups which are equidistant from each other and the main reflections. This distribution allows for a fourth vector termed the modulation wave vector q . The use of q implies a transition into four dimensional space. Therefore the reflections are described by four integers $h, k, l,$ and m . The higher dimension will therefore affect all subsequent steps (Wagner, 2009).

2. Literature survey

Organic-inorganic aliphatic hybrids are generally represented by the formula:

$[(C_nH_{2n+1})NH_3]_2 MX_4$. These hybrid structures are characterized by an alternating structure where the ionic, inorganic metal halide layers are sandwiched between paraffinic alkylammonium chains (Ciajolo *et al.* 1977; Zuniga *et al.* 1983; Guo *et al.* 1995).

Hybrid structures have been extensively studied but the majority of the work is based on systems with octahedral inorganic metal halides such as M= Pb, Mn, Fe and Cu which form corner sharing, two dimensional layers which alternate with the organic layers (Ciajolo *et al.* 1977). The divalent metal ions in the hybrid are not necessarily all octahedrally coordinated as the metal ions can coordinate in various arrangements and geometries. The inorganic metal halide's coordination is dependent upon the bonding orbitals of the metal and the size of the halide ion present. The inorganic structure is also greatly influenced by various factors such as thermodynamics and kinetics. The identity and the steric requirements of the organic cation affect the efficiency of the packing or the packing arrangement adopted.

2.1 Inorganic Tetrahedral Coordination

Cobalt, zinc and certain mercury containing hybrid's inorganic component do not conform to the usual 2 dimensional, octahedral, corner sharing units. The divalent metal ion coordinates to four halide ions forming zero dimensional, isolated, tetrahedral units which pack in a two dimensional arrangement. The crystal system is then stabilized by a series of charge assisted hydrogen bonds between the anionic inorganic and the cationic organic units (Guo *et al.* 1995; Ciajolo *et al.* 1977; Zuniga *et al.* 1983). The crystal structure consists of ionic, inorganic layers which are sandwiched between paraffinic alkylammonium layers (Zuniga *et al.* 1981).

2.1.1 Zinc Organic-Inorganic Hybrid Systems

The inorganic tetrahedra show small distortions which are usually within 5° of the recommended bond angles for crystals such as bis(n-dodecylammonium) tetrachlorozincate and bis(n-heptylamine) tetrachlorozincate (Ciajolo *et al.* 1977; Guo *et al.* 1992). Distortions usually result from the hydrogen bonding scheme of the crystal (Guo *et al.* 1992). There is usually a small deviation in the halide metal bond distances of the tetrahedra as well, reported deviations have been as small as 0.02 Å (Ciajolo *et al.* 1977). The length of the metal halide distance can also be affected by the length of the aliphatic organic chain used in the hybrid complex. This was identified when the average bonding distance for the heptylammonium hybrid was 2.26 Å which is shorter than the 2.27 Å reported for the decylammonium hybrid (Guo *et al.* 1992).

The organic chains of the hybrids all have a zigzag conformation with torsion angles which are close to 180°. Slight distortions of the internal rotation angle occur due to the close

packing arrangement of the aliphatic chains (Ciajolo *et al.* 1977). The torsion angle of the aliphatic chains stays relatively similar except for hybrids such as bis(n-heptylamine)tetrachlorozincate where the C-C bond near the polar head (NH₃) rotates to insert itself into the inorganic layer (Guo *et al.* 1995). The majority of the structural differences, for these hybrids, will be identified in the packing of the aliphatic organic chains. From here on in we can start to identify an odd-even effect of the organic chains where the parity of the organic chain determines the effect on the structure (Zuniga *et al.* 1983; Ning *et al.* 1992). Bis(n-dodecylamine)tetrachlorozincate's aliphatic chains are parallel in respect to each other and slightly tilted with respect to the inorganic layer. The chains are related by a centre of inversion. Odd numbered carbon chains such as bis(n-heptylamine)tetrachlorozincate and bis(n-tridecylamine)tetrachlorozincate's have organic layers which are not parallel and therefore no inversion centre could be identified (Avitabile *et al.* 1983; Guo *et al.* 1995; Wu *et al.* 2005).

All the aliphatic organic chains of the zinc chloride hybrid series form intercalated layers which achieves an optimal packing arrangement over the largest part of the organic chains. The interpenetrating chains result from organic layers which are attached alternately to adjacent ZnCl₄ layers. Intercalation of the chains was only found for compounds containing M= Co and Zn (Ciajolo *et al.* 1977).

The even-odd effect seems to have a great influence on the structural and thermal behaviour of the zinc hybrid series (Zuniga *et al.* 1983). The work done on these hybrids is not complete as a majority of these series of crystals have not been characterized.

Phase transitions

These hybrids exhibit a wide range of phase transitions over wide temperature ranges. These transitions are dependent upon the energetic requirements of the crystal itself while the number of transitions can depend on the number of carbon atoms included in the organic chains. The solid-solid phase transitions that take place before the melting of the organic chains include conformational and order-disorder changes (Ciajolo *et al.* 1977; Zuniga *et al.* 1981). Disorder appears between 293 and 323K for the zinc chloride series of organic-inorganic hybrids while conformational changes resulting from partial melting of the hydrocarbon chains are usually found above 335K (Fenryan 1993). The hybrid systems therefore undergo phase transitions which are governed by the dynamic of the alkylammonium groups (Ning *et al.* 1992).

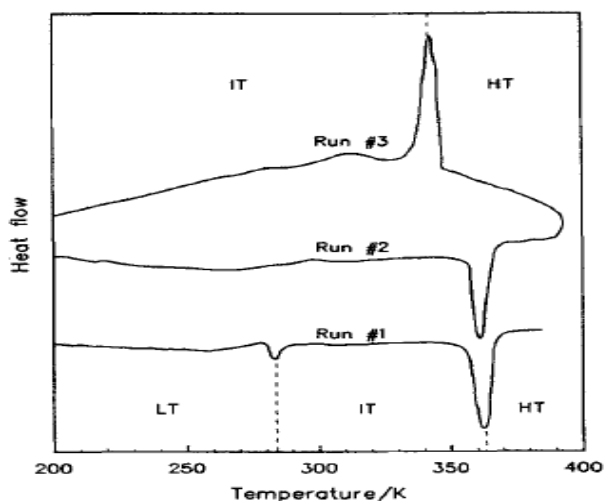
Order-disorder transitions appears when the alkyl chains possess a large degree of motional freedom, while retaining their three dimensional ordering of the chains (Landi *et al.* 1975; Ciajolo *et al.* 1977; Wu *et al.* 2010). A majority of the disorder found in these hybrids tends to be discrete or continuous positional disorder (Zuniga *et al.* 1983; Wu *et al.* 2010). A transition that involves a crystal system migrating from a disordered to an ordered system forces disordered atoms to favour one of the disordered positions or alternatively the

disordered atom would lie in an average position of the previously disordered positions (Zuniga *et al.* 1983; Ciajolo *et al.* 1977).

The carbon atoms of the alkyl chains which lie closer to the inorganic layer have a greater chance of becoming disordered as there is more space available at that position allowing for motional freedom (Zuniga *et al.* 1983). Order-disorder transitions are dependent on the temperature and are unique to each crystal studied. Therefore to obtain a better structural model of a hybrid the temperature must be controlled to obtain a more ordered structure. The temperature of the system should be maintained at a value at which the hybrid is stable and does not undergo any sort of phase transition. A decrease in the temperature of the system minimises the energy within a crystal structure, thereby reducing vibrational motions. Disorder within the structure should therefore be theoretically reduced as the temperature is lowered. This is not always the case as can be seen in the bis(*n*-heptylamine) zinc chlorate structure which becomes disordered below room temperature while structures such as bis(*n*-propylamine) zinc chlorate becomes more ordered when reducing the temperature (Guo *et al.* 1995; Zuniga *et al.* 1983). Therefore it is imperative that we should study each case individually before making any assumptions. High temperature phases on the other hand follow a general rule that the organic layers become conformationally disordered as the temperature is increased (Wu *et al.* 2010).

Odd-even effects can be identified when dealing with phase transitions. All aliphatic chains that contain an odd number of carbon atoms introduce a torsion angle close to the polar head (NH₃) which deviates from 180°. This configuration is energetically unfavourable and generates an additional phase transition which can be found in all odd members of the series or even chains where *n* is greater than 12 (Zuniga *et al.* 1983; Guo *et al.* 1995, Zuniga *et al.* 1981).

Bis(*n*-decylamine) zinc tetrachloride is an interesting compound as it experiences two phase transitions at 284 and 363K. These transitions were studied using PXRD, DSC and NMR (Fenryan 1993). The low (LT) and intermediate (IT) temperature phases both formed intercalated organic layers with no large structural differences. There is an increase of approximately 16% in the length of the *c* axis in the high temperature phase (HT). The authors assumed that the higher temperature phase formed a non-intercalated organic layer which is approximately parallel to the normal of the inorganic layer. The transition is due to the large degree of motional freedom that the organic chains acquire at the higher temperature. When cooling the hybrid we find that the LT phase is not observed. This was also found in the bis(*n*-tridecylamine) tetrachlorozincate where the room temperature phase was not observed upon cooling (Fenryan 1993).



(Fenryan 1993)

Figure 7: DSC scan of the Decylamine zinc (II) chloride hybrid where the two phase transitions are evident. The low temperature phase is not observed when cooling the crystal.

Table 1: Published zinc(II)chloride hybrid structures of bis(n-decylamine) tetrachlorozincate (C10 ZnCl), bis(n-dodecylamine) tetrachlorozincate (C12ZnCl) and bis(n-tetradecylamine) tetrachlorozincate (C14ZnCl)

	C10ZnCl (Fenryan <i>et al.</i> 1993)	C10ZnCl (Fenryan <i>et al.</i> 1993)	C10ZnCl (Fenryan <i>et al.</i> 1993)	C12ZnCl (Ciajolo <i>et al.</i> 1977)	C14ZnCl (Ciajolo <i>et al.</i> 1977)	C14ZnCl (Ciajolo <i>et al.</i> 1977)
T (K)	Below 284K Low temperature phase	284K-363K Intermediate temperature phase	Above 363K High temperature phase	Room temp	Below 362K	Above 362K
Unit cell	There was no structural difference observed for the two hybrid structures. The organic layers form intercalated layers		High temperature phase showed a large increase in the dimensions of the c axis. The organic layers became non-intercalated	Monoclinic	Monoclinic	Orthorhombic
Symmetry				$P2_1/c$	$P2_1/c$	$Pnma$
Dimensions Å				$a = 7.409$ $b = 10.379$ $c = 44.399$ $\beta = 105.56^\circ$	$a = 10.254$ $b = 7.3980$ $c = 47.659$	$a = 10.3$ $b = 7.5$ $c = 47.8$
					Phase transition at 362K	

Table 2: Table representing all odd numbered carbon chains of the aliphatic zinc hybrid series and their transitions.

	C3 ZnCl	C3 ZnCl	C3 ZnCl	C5 ZnCl	C5 ZnCl	C7 ZnCl	C13 ZnCl	C13 ZnCl	C13 ZnCl
Temperature (K)	295 K	Above 310K	298 K	Above 263 K			295 K	318 K	362 K
Unit cell	Monoclinic	Orthorhombic	Orthorhombic	Orthorhombic	Orthorhombic	Orthorhombic	Monoclinic	Orthorhombic	Orthorhombic
Symmetry	P21/n	Pnma	Pnma	-	P21nb	-	P21	Ph21a	-
Dimensions	10.219 7.3632 20.077 $\alpha=92.65$	10.243 7.3828 20.213	10.323 7.405 25.171	10.19 7.09 27.90	7.447 10.387 30.082	10.271 7.413 45.411 $\beta=94.24$	10.316 7.200 45.320	10.300 10.300 54.100	
	This hybrid crystal has a single phase transition at 310K. The organic cations are disordered in the higher temperature structure.		An order-disorder transition occurs at 256 K. the organic cations become disordered						

2.1.2 Cobalt hybrids

A number of aliphatic cobalt hybrids have already been structurally determined. Most of the work done has been based on diprotonated organic species with ammonium groups at both ends of the carbon chain (Criado *et al.* 1999).

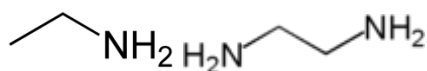


Figure 8: The organic molecules of ethylamine (monoprotonated) and ethylenediamine (diprotonated) respectively.

Table 3: Previously published diamine aliphatic cobalt hybrids

	$(\text{NH}_3 \text{ C}_2\text{H}_6 \text{ NH}_3)_2$ $(\text{CoCl}_4)_2(\text{Cl})^-$ (Smith, 1977)	$(\text{NH}_3 \text{ C}_3\text{H}_6 \text{ NH}_3)$ CoCl_4 (Ning, 1992)	$(\text{NH}_3 \text{ C}_5\text{H}_{10} \text{ NH}_3)$ CoCl_4 (Criado, 1999)	$(\text{NH}_3 \text{ C}_6\text{H}_{12} \text{ NH}_3)$ CoCl_4 (Mahmoudkhani, 2002)
T° (K)	295K	295K	295K	183K
Unit cell	Orthorhombic	Monoclinic	Monoclinic	Triclinic
Symmetry	$Pnma$	$P2_1/c$	$P2_1/c$	P_{-1}
Dimensions	$a=12.884\text{Å}$ $b=6.151\text{Å}$ $c=19.291\text{Å}$	$a=10.703\text{Å}$ $\alpha=90.00^\circ$ $b=10.663\text{Å}$ $\beta=118.46^\circ$ $c=10.852\text{Å}$ $\gamma=90.00^\circ$	$a=7.163\text{Å}$ $\alpha=90.00^\circ$ $b=15.940\text{Å}$ $\beta=96.44^\circ$ $c=11.137\text{Å}$ $\gamma=90.00^\circ$	$a=7.280\text{Å}$ $\alpha=75.68^\circ$ $b=9.948\text{Å}$ $\beta=87.49^\circ$ $c=9.957\text{Å}$ $\gamma=88.79^\circ$

The inorganic metal halide complexes of the cobalt hybrids have a similar structure to the zinc hybrids. The inorganic component is coordinated into isolated tetrahedra. The inorganic tetrahedra can exhibit small distortions in the bonding angles and distances which result from the hydrogen bonding within the crystal structure (Ning *et al.* 1992; Criado *et al.* 1999). In each inorganic layer the $[\text{CoCl}_4]^{2-}$ adopts a head to tail packing arrangement which extends in two dimensions (Mahmoudkhani *et al.* 2002). The tetrahedra are interconnected via charge assisted hydrogen bonds to the organic cations (Criado *et al.* 1999). The bond lengths of the reported species such as $(\text{NH}_3 \text{ C}_5\text{H}_{10} \text{ NH}_3) \text{CoCl}_4$ showed small deviations in the Co-Cl bond lengths where the largest value was quoted as 0.029Å. The bonding angles of the inorganic component do become slightly distorted due to the hydrogen bonding scheme within the crystal structure (Criado, 1999; Ning, 1992).

The organic chains have a nearly planar, zigzag conformation. The organic chains bridge the isolated inorganic units which stabilizes the structure (Ning *et al.* 1992). The alkylammonium groups are hydrogen bonded to three of the four coordinated chlorine atoms. Two of the hydrogen bonds are strong while the third is relatively weak in comparison. The degree of strength can be determined by the bonding distance (Mahmoudkhani *et al.* 2002). These

organic molecules are diprotonated which results in both ends forming hydrogen bonds. One aliphatic chain would therefore hydrogen bond to two separate inorganic layers which means that the organic layer consists of one row of organic molecules. The organic layers which are monoprotated consist of two organic chains extending from the alternating layers with interpenetrating carbon chains.

Thermal behaviour of some of the hybrids showed some chain-melting transitions. Hybrids such as $(\text{NH}_3 \text{C}_n\text{H}_{2n} \text{NH}_3) \text{CoCl}_4$ for $n= 10$ and 8 exhibited solid-solid phase transitions when characterized thermally. The actual crystal structures were not determined as the sample could not be crystallized (Criado *et al.* 1999).

2.1.3 Mercury hybrids

The mercury containing organic-inorganic hybrid structures consists of a wide range of structures. This is due to the mercury's ability to form various coordinated inorganic units. The inorganic component can coordinate as isolated tetrahedra, corner sharing octahedra, square pyramidal structures etc. The majority of the crystal structures have an inorganic component which is either octahedral or tetrahedral. The mercury hybrids containing methylammonium have been extensively studied where the chloride, bromide and iodide inorganic layers tend to form octahedra (Bats 1982; Salah 1982).

The diprotonated aliphatic hybrid systems of bis(ethanediammonium) dichloride tetrachloromercurate and ethylenediammonium tetrabromidomercury(II)monohydrate both exhibit tetrahedral coordination within the inorganic layer (R.Spengler 1998; Godwa, 2009). The tetrachloromercurate structure has an asymmetric unit consisting of one organic chain one chloride ion and one isolated tetrahedral unit. The hybrid structure crystallizes in an orthorhombic unit cell, $Pnma$, with the structural formula $[(\text{C}_2\text{H}_{10}\text{N}_2)_2\text{HgCl}_4] \cdot 2\text{Cl}^-$. The metal halide bonding distances of Hg-Cl range between 2.378 and 2.860 Å (Spengler, 1998). The bromide structure forms an asymmetric unit consisting of one isolated tetrahedral unit one organic chain and one water molecule. The organic chains therefore hydrogen bond directly to the inorganic halide ions or via the water molecule. The metal halide bonding distances range between 2.5597 and 2.6923 Å (Godwa, 2009).

Table 4: Published aliphatic mercury (II) halide crystals

Halide ion		Cl	Br	I
Organic chain length	C1	(Bats1982) (Salah1982)	(Pabst, 1986)	(Korfer, 1985)
	C3	(Salah, 1984)		

2.2 Inorganic Octahedral Coordination

2.2.1 Copper Hybrid Structures

A number of copper halide hybrid structures have been previously published. The crystal structures are the typical alternating, layered arrangement as previously discussed. The inorganic component consists of corner sharing octahedra which extend infinitely in two dimensions. The octahedra can reduce the symmetry within the unit cell as the inorganic components experience Jahn-Teller distortions at various temperatures (Doudin,1990).

The two dimensional structure is described as quantum well structures which have the ability to produce various optical phenomena. This is due to the large exciton binding energy which is dependent on the divalent metal and halide ions used. The divalent copper ion is also known for its paramagnetic abilities(Aruta C, 2005).

The bis(propylamine) tetrachlorocuprate structure has been extensively studied by Doudin B *et al.* This is due to the hybrid having four phase transitions above room temperature where three phases are commensurate while the fourth phase is a modulated structure (Doudin 1990, Doudin B 1990).

The bis(butylamine) tetrachlorocuprate hybrid structure was structurally characterized via PXRD while the phase transitions were determined during thermal characterization. The hybrid structure undergoes one phase transition at 51°C which was identified as an order-disorder transition. The lower temperature structure was ordered while the high temperature structure was disordered as the organic component could not be identified. The organic component started to evaporate at 237°C while the structure decomposed between 254°C and 278°C (Aruta C, 2005; Xiao Z, 2005).

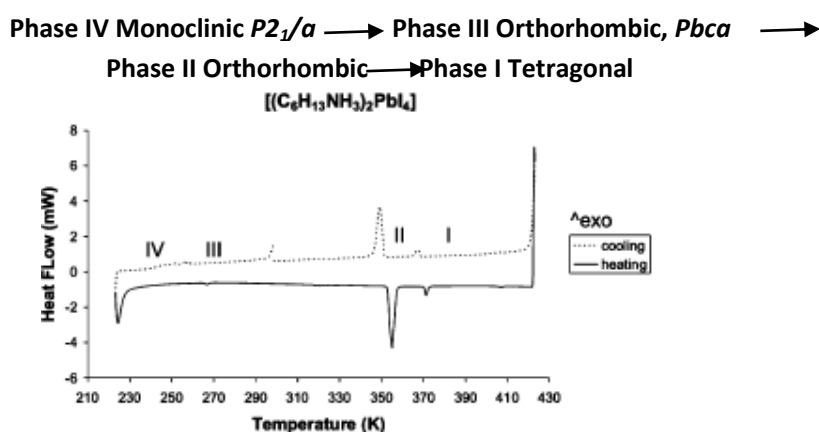
Table 5:Previously published aliphatic copper (II) halide hybrids

	CuCl₂	CuBr₂
C₃H₁₀N	(Fu, 2006; Doudin, 1990)	
C₃H₁₂N₂	(Phelps, 1976; Zhang, 2004)	(Halvorson, 1988)
C₄H₁₄N₂	(Garland,1990; Maris 1996)	(Garland, 1990)
C₅H₁₆N₂	(Garland, 1990)	(Garland, 1990)

2.2.2 Lead Hybrid Structures

The lead containing hybrids tend to form corner sharing octahedral inorganic species which extend infinitely in two dimensions. The lead halide structures tend to be effective light emitting devices due to the two dimensional layered structure as the electronic band structure is determined by the inorganic metal halide and the fluorescence is determined by the organic cation used (Billing D.G, 2007).

The lead iodide hybrid structures containing the aliphatic chains $n = 4, 5, 6$ were determined by Billing *et al.* The hybrid systems undergo phase transitions which are temperature dependent. The Butylammonium crystal has one phase transitions while pentylammonium has two and finally the hexylammonium crystal undergoes 3 phase transitions. The hybrid systems experience thermochromic phase transitions. There tends to be movement of the organic chains relative to the inorganic layer during a phase transition. The inorganic component can also experience some degree of movement when the crystal system is changed i.e. monoclinic to orthorhombic system (Billing D.G, 2007).



(Billing D.G, 2007)

Figure 9: DSC scan of bis(hexylamine) tetraiodoplumbvate

Table 6: Table representing all the previously published aliphatic lead hybrids

	Halide ion	Cl	I
ORGANIC	1		(Vincent, 1987)
	2	(Geselle, 1997)	
	3	(Meresse, 1989)	(Billing, 2006)
	4		(Mitzi, 1996)
	5		(Billing, 2007)
	6		(Billing, 2007)
	9		(Nagapetyan, 1998)
	10		(Billing, 2008)
	14		(Billing, 2008)
	16		(Billing, 2008)
n=	18		(Billing, 2008)

3. Experimental

3.1 Organic components

A series of relatively simple organic aliphatic amine chains were used as the base of this study. By using a wide range of organic cations within the hybrid structure we could then determine the effects of a change in the organic cation on the crystal structure. The list of organic amines included:

Propylamine C₃H₇NH₂ Heptylamine C₇H₁₅NH₂

Butylamine C₄H₉NH₂ Octylamine C₈H₁₇NH₂

Pentylamine C₅H₁₁NH₂ Nonylamine C₉H₁₉NH₂

Hexylamine C₆H₁₃NH₂ Decylamine C₁₀H₂₁NH₂

3.2 Inorganic components

The inorganic component of the hybrid structure is composed of a divalent metal halide (MX₂). The metal ions included in this study were: copper, cobalt, zinc, mercury and lead. The majority of the crystals contained either chlorine or bromine as their halide ion, while a few hybrids contained iodine. The reason for this is that the chlorine and bromine metal salts were the most stable reagents while the iodine metal salts and hybrids tend to oxidize easily. An inorganic acid was also added to the mixture as the acidic environment of the solution lead to the protonation of the amine group on the organic component. The acidic medium used included simple acids such as hydrogen chloride, hydrogen bromide and hydrogen iodide. The acid and metal (II) halide reagents used in this study had corresponding halide ions so that single halide compounds were prepared. The electronegativity of the halide ions results in substitutional reactions between the metal halide ions and the ionic species of the acid.

3.3 Synthesis

The reagent solutions prepared contain a metal halide (M(II)X₂), an aliphatic organic compound, an inorganic acid (HX) and a solvent or mixture of solvents which allows all the reagents to become solubilised. A wide variety of solvents were used such as ethanol, methanol, water, hexane and acetonitrile. The type and ratio of solvents were specific for each synthesis. An ultrasound bath was also used to ensure complete solubilisation. The reagents were mixed in very specific ratios given by the equation below:



The crystallization process is very important when dealing with organic-inorganic hybrid systems. To avoid any unwanted products two techniques were used to control the crystallization process in this study:

1. Slow cooling:

The sample solutions were placed in a temperature controlled oil bath. The oil bath's controller can be programmed to the requirements needed for your experiment. These controllers allow the scientist full control of the maximum and minimum temperatures as well as the heating and cooling rates. The maximum temperatures are determined by the solvent system used. Slow heating and cooling rates usually produce optimal reaction conditions.

2. Slow evaporation

The reagent solutions were prepared and kept in a controlled environment where they were left to evaporate slowly, at room temperature. The solutions were often exposed to air as it allowed for an efficient evaporation rate unless the solutions oxidized easily.

- Both techniques worked relatively well but the slow evaporation route tended to produce a higher quantity of hybrids.

3.4 Equipment

Two single crystal diffractometers were available for single crystal structural characterization, the Smart-NT and Apex 2 (Bruker, 1998; Bruker 2005). Both of these systems have the ability to do variable temperature studies with the help of suitable cryostat equipment. Additionally two powder diffractometers were available, a Bruker D5000 and a Bruker-AXSD8ADVANCE diffractometer.

Phase transitions were characterized using a Mettler Toledo differential scanning calorimeter while the actual phase transitions were visually studied using a hot stage for the light microscope that was constructed specifically for this project.

3.5 Differential Scanning Calorimetry

Phase transitions are identified by a process known as differential scanning calorimetry (DSC). This variable temperature technique involves measuring the heat absorbed or released by a sample as a function of temperature. The sample is measured in relation to a reference sample which allows the system to identify any variations in the sample. Positive peaks represent any exothermic transition where energy is released from the sample. Negative peaks are represented by endothermic transitions where the sample absorbs heat from the environment. Solid-solid phase transitions can lead to major unit cell adjustments, or just cause slight shifts in the unit cell size which corresponds to the energy requirements.

The samples were measured in the following temperature cycle:

Room temperature (25°C) → cooled -60°C → 300°C → Room temperature (25°C)

The samples were cooled then heated in a cycle so that any reversible or non-reversible phase transitions could be identified.

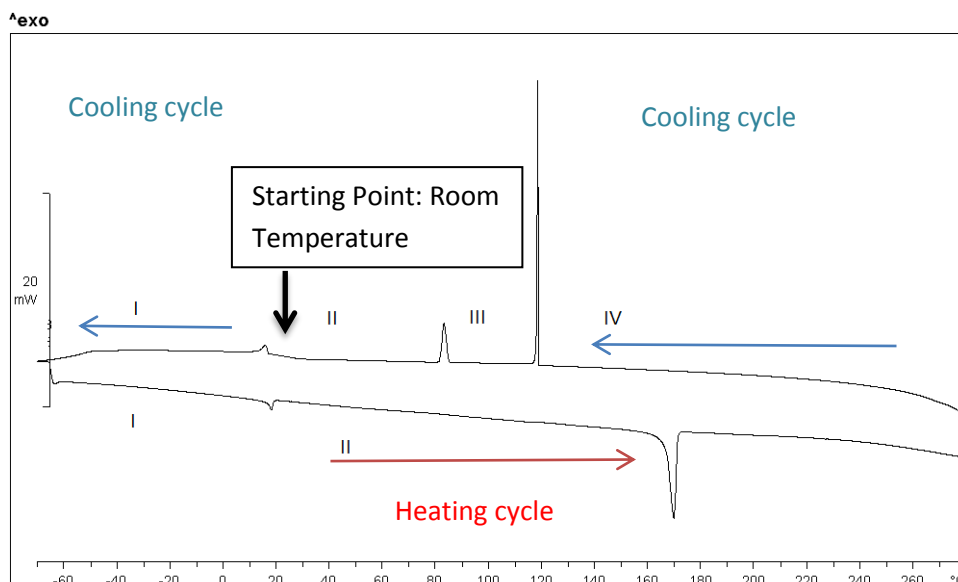


Figure 10: Example of a DSC scan which indicates the initial starting room temperature. The crystal is then cooled to below 60°C then heated to 270°C and finally cooled back to room temperature.

3.6 Luminescence

In order to obtain luminescent data the samples are cooled using a Linkam (THMS350V) cryostat system. The data was collected via a multiline UV (333.6 – 363.8nm) of an argon ion laser as the excitation source. The power of the applied radiation is kept low as to not cause degradation of the crystal sample. The excitation process is quantitatively determined during the excitation process which is associated with the band gap of the inorganic layer.

3.7 Software

A wide variety of programs helped to analyze all the data collected.

The *Apex 2* software includes a whole suite of programs which is used for the interpretation of single crystal diffraction data (Bruker, 2005). This list includes *SAINT-Plus* which is used for cell refinement and the reduction of the data (Bruker, 1999). *SHELXS97* is used to solve and *SHELXL97* to refine the crystal structures (Sheldrick, 1997). *ORTEP-3* for windows helps with structure visualization (Farrungia, 1997). *DIAMOND* is also used for structure visualization, particularly for the polyhedral representation of inorganic structural components (Brandenburg, 1999). *WINGX* is the software used to prepare the data for publications (Farrungia, 1999). Finally *PLATON* is used for structure validation and checking (Spek,

2003). Modulated structures would however need specialized programs such as *JANA2006* (Petricek *et al.* 2006) for analysis of the single crystal data.

Powder diffraction data is interpreted by either *EVA* which is the basic powder evaluation package or *TOPAS* which allows for a more in-depth study which includes unit cell determination, quantitative and qualitative analysis of various samples (Coelho A. A, 2000).

4. Results

Organic-inorganic hybrid compounds investigated in this study are comprised of aliphatic amines which typically form alternating, layered crystal structures which extend infinitely in two dimensions. The alternating layers consist of anionic, inorganic metal halide units and cationic aliphatic, organic chains which are held together by charge assisted hydrogen bonds.

The coordination and dimensionality of the inorganic metal halide layer is directly dependent on the divalent metal ion used but may show variability for the same metal. The metal halide units can exhibit some distortion in their bond lengths and angles, this is due to the hydrogen bonding network within the crystal structure, and as a result of the packing requirements.

The organic ions hydrogen bond via the cationic ammonium portion of the chain. The polar head usually inserts itself directly into the inorganic layers to ensure better hydrogen bonding interactions. The organic units extending from opposite inorganic layers can either experience no intercalation or alternatively can form intercalated species were the carbon chains extend into the same area. This factor is directly dependant on the charge density of the hybrid system.

The hybrid structure can undergo a number of temperature dependent phase transitions. These transitions have proved to be either order-disorder or solid-solid phase transitions. The phase transitions are governed by the thermodynamics of the crystallite structure.

Table 7: Organic-inorganic hybrids where the crystal structures were determined for the first time in this study are highlighted in blue for inorganic reagents and $C_nH_{2n+1}NH_2$.

		Inorganic Metal (II) Halide									
		Tetrahedral coordination						Octahedral coordination			
		ZnCl ₂	ZnBr ₂	ZnI ₂	CoCl ₂	HgBr ₂	HgI ₂	ZnCl ₂	CuCl ₂	PbBr ₂	PbI ₂
O R G A N I C (n)	C3										
	C4										
	C5										
	C6										
	C7										
	C8										
	C9										
	C10										

The organic-inorganic hybrid structures have been divided into the two categories according to the coordination of the metal ion. The metal halide complex is coordinated either as a tetrahedral or octahedral complex. The results have been colour coded for simplification. Coloured dividers represent the divalent metal ion while the hybrids names are highlighted to represent the halide ion used.

Table 8: Colour coded metal sections and halide title sections

Tetrahedral coordination		Halide ion	
	Zinc		Chloride
	Cobalt		Bromide
	Mercury		Iodide
Octahedral coordination			
	Copper		
	Lead		

4.1 Tetrahedral coordination

The divalent metal halides such as zinc(II), cobalt(II) and mercury(II) tend to form isolated tetrahedra in the organic-inorganic hybrid structure. The isolated units are essentially zero dimensional but pack in a manner that extends in a two dimensional arrangement. With no bonding interactions occurring between the inorganic units the structure would be reliant on the charge assisted hydrogen bonds of the organic cations for overall stability of the compound.

4.1.1 Zinc (II) Halide Hybrids

This series of Zinc (II) hybrids tend to form isolated tetrahedral inorganic units. The isolated units results in a large charge density within the crystal structure. Efficient packing is therefore essential when dealing with the organic units as they stabilize the structure by forming charge assisted hydrogen bonds. The hydrogen bonding scheme can affect the tetrahedra resulting in some degree of distortion. The isolated tetrahedra extend in a two dimensional layer formation where they exhibit head to tail packing along a certain direction.

1. Bis(Butylamine) Tetrachlorozincate

The crystal structure was determined at room temperature. Upon cooling to -100°C , the organic cations became disordered resulting in poor diffraction data that made structure solution and refinement impossible. However, unit cell parameters are reported and a tentative space group symbol assigned. The room temperature structure showed some degree of disorder in one of its organic molecules where a carbon atom was split between two positions. The structure was determined without any hydrogen atoms due to the disorder of the carbon and nitrogen atoms within the structure. The room temperature structure was situated close to a phase transition; this resulted in the instability of the structure.

The crystal's asymmetric unit consists of an incomplete isolated tetrahedral ZnCl_4 unit and two cationic organic chains (refer to **Figure 11**). The tetrahedral unit is completed by the symmetry operator of the unit cell.

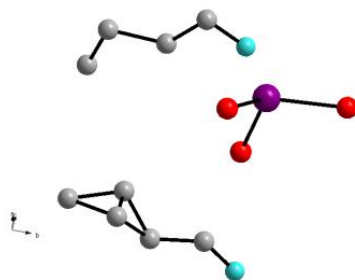


Figure 11: Asymmetric unit

The hybrid forms an alternating layered structure where the aliphatic, organic chains are sandwiched between inorganic layers. The inorganic layers extend along the ac -direction with a head to tail packing arrangement which extends along the c plane. The inorganic tetrahedra have an average zinc chloride bond distance of 2.251\AA . The bond angles are only slightly distorted from the ideal value of 109° which results from the hydrogen bonding within the hybrid.

The carbon chains extend at a slight angle relative to the inorganic layer (refer to **Figure 12**). The torsion angles of the two organic chains indicate a relatively planar conformation.

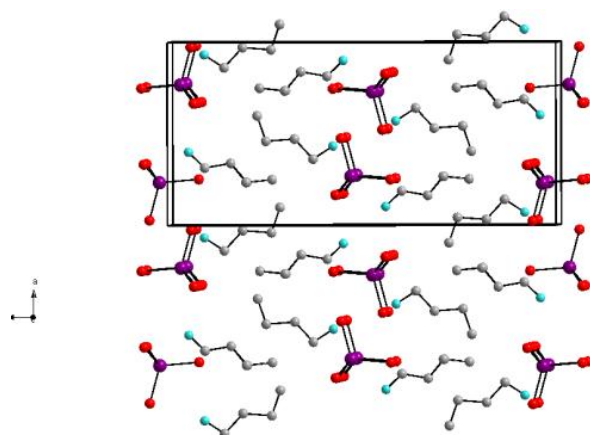


Figure 12: Crystal packing arrangement

The entire system is stabilized by charge assisted hydrogen bonding between the cationic ammonium groups and the anionic chloride ions. The hydrogen bonding could not be discussed as the inclusion of hydrogen atoms cause the structure refinement to become unstable.

Thermal characterization

The hybrid structure undergoes two reversible phase transitions as the sample is heated, and an additional third transition appears as the sample is cooled. The structure of phase II (between 20 °C and 80°C) and the unit cell of phase I was identified. The first phase transition peak (near room temperature) resulted in a unit cell transformation: monoclinic (phase I) to orthorhombic (phase II) for both of the heating and cooling cycles. There is an additional third phase transition present when cooling the hybrid from 270°C. The additional transition exists between 81-84°C. No phase transitions are evident below room temperature in the temperature range studied by DSC. The second solid-solid phase transition during heating was not determined so the final transition could not be identified as phase II or IV.

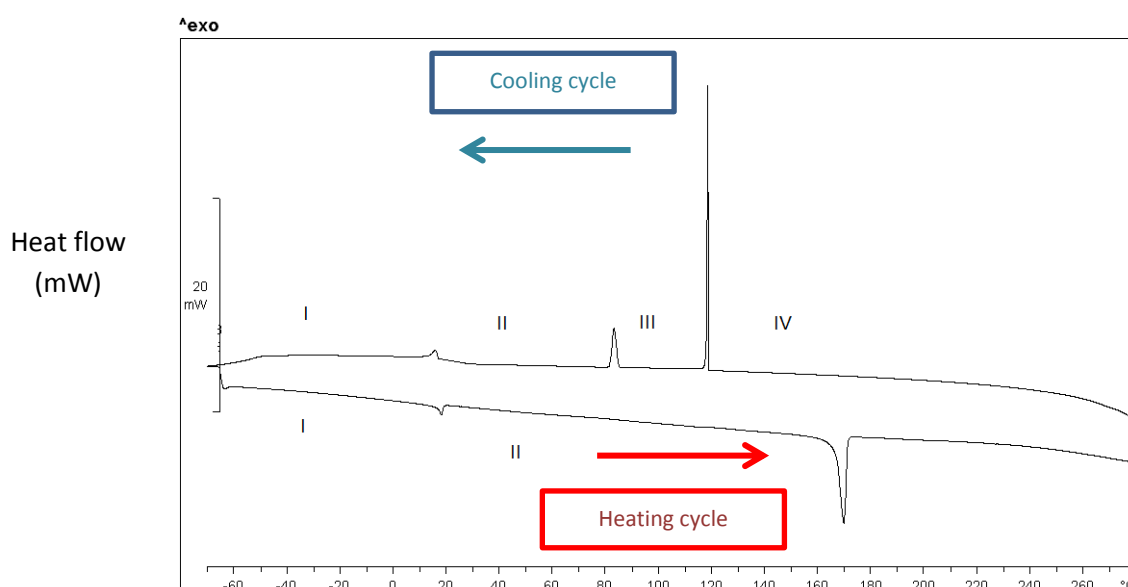


Figure13: DSC scan of the bis(butylamine) tetrachlorozincate

Synthesis

0.05g (0.37mmol) Zinc(II)chloride and 0.052g (0.70 mmol) Butylamine were dissolved in a solution containing 1ml concentrated HCl, 2mlethanol and 2ml acetone. Once all the reagents had dissolved the solution was left to slowly evaporate which resulted in crystallization.

Crystal data

Table 9: Experimental data

$(C_4H_{11}NH_3)_2ZnCl_4$	
$T = 20^\circ C$ PHASE II	$T = -100^\circ C$ PHASE I
<p>Crystal data Orthorhombic, $Pnma$ $a = 10.449 \text{ \AA}$ $b = 7.372 \text{ \AA}$ $c = 22.223 \text{ \AA}$ $V = 1711.8 \text{ \AA}^3$ $Z = 4$</p> <p>Refinement data $F_{000} = 664$ $D_x = 1.332 \text{ Mg m}^{-3}$ Mo $K\alpha$ radiation $\lambda = 0.71073 \text{ \AA}$ Cell parameters from 2720 reflections $\theta = 2.7\text{--}23.5$ $\mu = 2.04 \text{ mm}^{-1}$ Block, clear $0.67 \times 0.43 \times 0.26 \text{ mm}$ $R_{int} = 3.35$</p>	<p>Crystal data Triclinic, $P\bar{1}$ $a = 7.3203 \text{ \AA}$ $\alpha = 90.28^\circ$ $b = 21.655 \text{ \AA}$ $\beta = 94.90^\circ$ $c = 42.040 \text{ \AA}$ $\gamma = 90.02^\circ$ $V = 6640 \text{ \AA}^3$</p> <p>Refinement data $F_{000} = 3892$ Mo $K\alpha$ radiation $\lambda = 0.71073 \text{ \AA}$</p> <p>Block, clear $0.67 \times 0.43 \times 0.26 \text{ mm}$</p>
Structure, refined without H	Unit cell data

2. Bis(Hexylamine) Tetrachlorozincate

The title compound, $(C_6H_{16}N)_2 [ZnCl_4]$, was structurally characterized at -100°C . The asymmetric unit of the crystal consists of two n-hexylammonium cations and one isolated, inorganic tetrahedral $ZnCl_4^{2-}$ unit (refer to **Figure 14**).

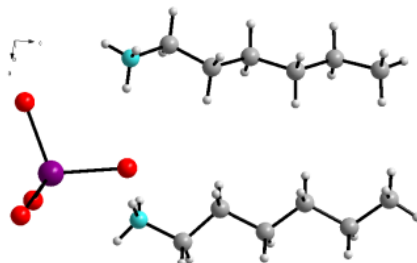


Figure 14: Asymmetric unit

The inorganic tetrahedra pack in two dimensional layers which extend infinitely along the *ab*-plane with a head to tail packing arrangement along the *b*-direction. The tetrahedra have an average bond distance Zn-Cl of 2.272\AA with a standard deviation of 0.018\AA . The inorganic Cl-Zn-Cl bond angles are slightly distorted from the ideal value which results from the hydrogen bonding within the crystal structure.

The organic chains in a layer hydrogen bond to both of the alternating inorganic layers within a sandwiched area, the chain lengths therefore extend into the same space to form relatively planar, intercalated species which is common for aliphatic zinc chloride hybrids (refer to **Figure 15**). The organic chains extend in a manner that is approximately perpendicular with respect to the inorganic layer.

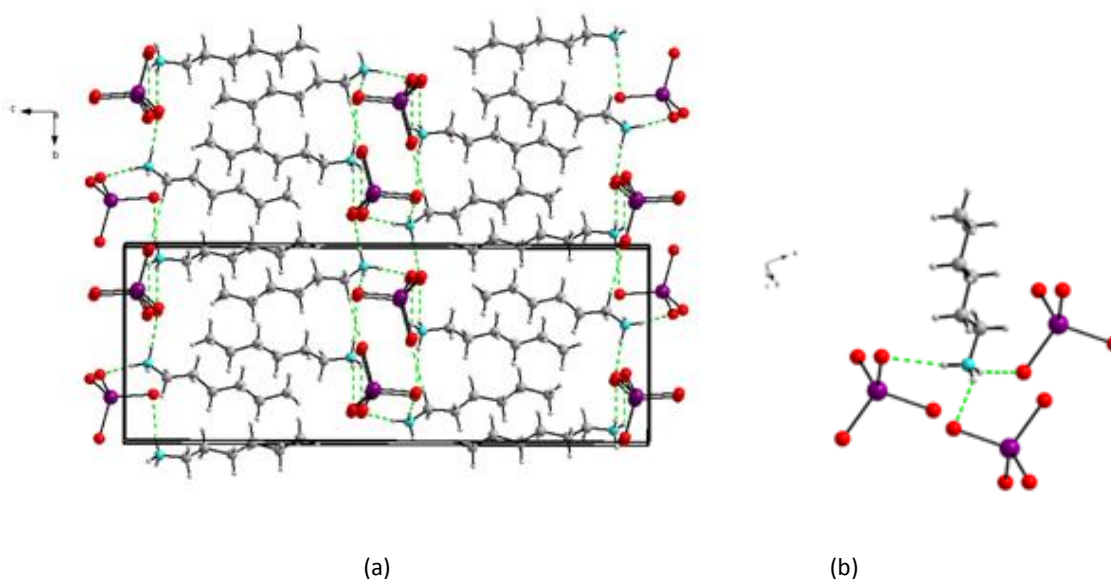


Figure 15: Crystal packing arrangement and the associated hydrogen bonding (a) in the cell structure (b) of the cationic organic chain

Thermal characterization

The hybrid structure experiences two phase transitions above 0°C. It might seem as though there are more transitions due to the presence of many peaks. A transition is classified by the position of the peak relative to the base line. If the base line is imposed on the DSC we can see that some of the peaks are included within the same transition (Schubnell, 2010). Therefore there are only two transitions that are present which are reversible when heating and cooling. As the sample is heated from -40°C to 240°C the transitions take place between 5°C to 35°C and 65°C to 160°C as indicated in the figures above. Phase transitions are largely governed by the organic cations of the hybrid complex.

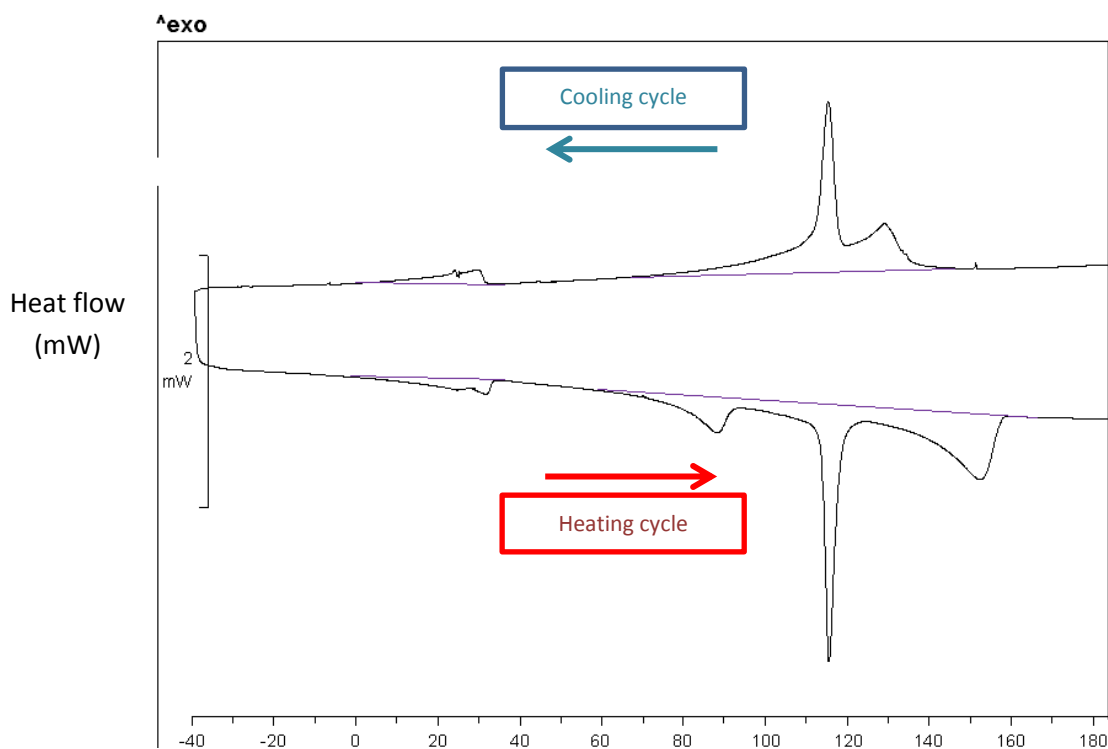


Figure 16: DSC scan of bis(hexylamine) tetrachlorozincate with the imposed baseline image

Synthesis

0.05g (0.37 mmol) of zinc(II)chloride and 0.08g (0.78 mmol) hexylamine were dissolved in 2ml of HCl. The solution was slowly heated in a closed vessel to 90°C in a temperature controlled oil bath. As the sample was cooled back to room temperature crystallization occurred.

Crystal data

Table 10: Experimental data

(C₆H₁₃NH₃)₂ZnCl₄
T = 0°C
Crystal data
Monoclinic <i>P</i> 2 ₁ / <i>n</i>
<i>a</i> = 7.2910(15) Å
<i>b</i> = 10.283(2) Å <i>β</i> = 95.25(3)°
<i>c</i> = 27.586(6) Å
<i>V</i> = 2059.5(7) Å ³
<i>Z</i> = 4
Refinement data
<i>F</i> ₀₀₀ = 864
<i>D</i> _x = 1.327 Mg/m ³
Mo <i>K</i> α radiation
λ = 0.71073 Å
θ = 1.48 to 23.32°.
μ = 1.703 mm ⁻¹
Plate, colourless
0.58 x 0.048 x 0.06 mm
<i>R</i> _{int} = 2.67

3. Bis(Pentylamine) Tetrabromozincate

The organic-inorganic hybrid was structurally characterised at three different temperatures. The unit cell data was collected at 0°C while the crystal structures were determined for both of the low temperatures -50°C and -100°C.

The asymmetric unit of the crystal consists of two n-pentylammonium cations which are hydrogen bonded to an isolated inorganic tetrahedral ZnBr_4^{-2} unit.

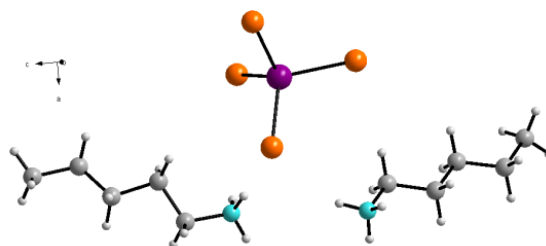


Figure 17: Asymmetric unit

The organic and inorganic species form an alternating two dimensional layered structure. These two dimensional layers extend infinitely along the *ab*-plane while the inorganic tetrahedra adopt a head to tail packing arrangement along the *b*-direction. The average Zn-Br distance for the -50°C structure was calculated to be 2.406Å with a standard deviation of 0.005Å while the -100°C structure had an average bonding distance of 2.405 Å with a standard deviation of 0.009Å. The lower temperature structure had a shorter average bonding distance due to the decrease in motional freedom with decreasing temperature.

The organic cations form intercalated species which extend from the alternating inorganic layers. The lower temperature structure contained a carbon chain which exhibited a small deviation in the internal rotation angle. The higher temperature structure exhibited a larger deviation of the internal rotation angle between the carbon atoms.

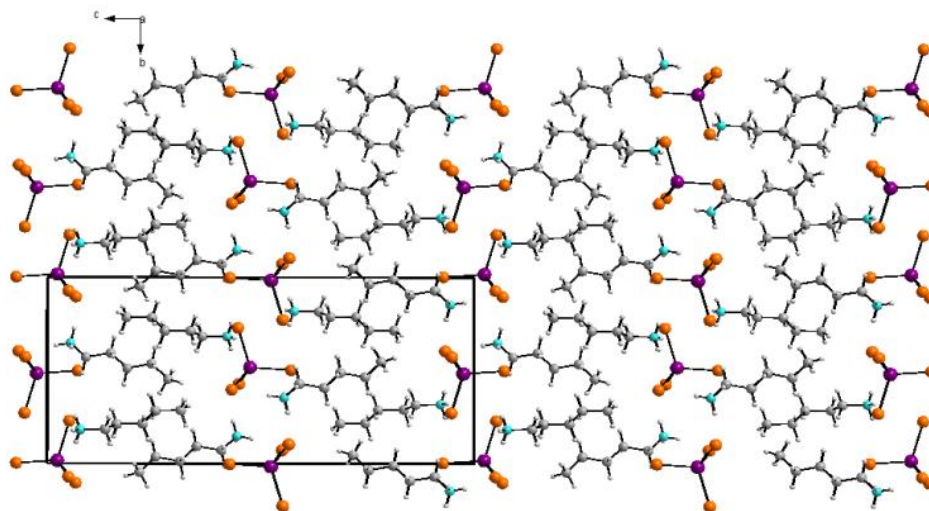


Figure 18:Crystal packing arrangement

Thermal characterization

The hybrid showed no evidence of any phase transitions between 0°C and -100°C. There was therefore no need for any thermal characterization and the sample was not analysed via differential scanning calorimetry.

Synthesis

The same hybrid was produced via two different methods:

- 0.05g (0.22 mmol) Zinc(II)bromide and 0.04g (0.45 mmol) pentylamine were dissolved in a solution containing 2 drops of HBr and 2ml hexane. The solution was then left to evaporate which resulted in crystallization.
- The second method involved the dissolution of 0.05g (0.22 mmol) zinc(II)bromide and 0.04g (0.45 mmol) pentylamine in a solution containing HBr and 2ml acetonitrile. The solution was heated to 72°C in a closed vessel and then slowly cooled back to room temperature. Crystallization occurred once the solution was cooled.

Crystal data

Table 11: Experimental data

(C₅H₁₁NH₃)₂ZnBr₄		
T = 0°C	T = -50°C	T = -100°C
Crystal data Orthorhombic <i>a</i> = 7.674 Å <i>b</i> = 10.464 Å <i>c</i> = 25.525 Å <i>V</i> = 2049.72 Å ³	Crystal data Orthorhombic, <i>P</i> 2 ₁ 2 ₁ 2 ₁ <i>a</i> = 7.589 Å <i>b</i> = 10.799 Å <i>c</i> = 24.794 Å <i>V</i> = 2031.8 Å ³ <i>Z</i> = 4	Crystal data Orthorhombic, <i>P</i> 2 ₁ 2 ₁ 2 ₁ <i>a</i> = 7.566 Å <i>b</i> = 10.749 Å <i>c</i> = 24.714 Å <i>V</i> = 2031.8 Å ³ <i>Z</i> = 4
Refinement data Mo Kα radiation λ = 0.71073 Å Plate, colourless 0.70 x 0.38 x 0.38 mm ³ <i>R</i> _{int} = 60.38	Refinement data <i>F</i> ₀₀₀ = 1404 <i>D</i> _x = 2.299 mg/m ³ Mo Kα radiation λ = 0.71073 Å θ = 1.64 to 23.37° μ = 9.418 mm ⁻¹ Plate, colourless 0.70 x 0.38 x 0.38 mm ³ <i>R</i> _{int} = 7.83	Refinement data <i>F</i> ₀₀₀ = 1088 Mo Kα radiation λ = 0.71073 Å θ = 0.82 to 23.44° μ = 9.12 mm ⁻¹ Plate, colourless 0.70 x 0.38 x 0.38 mm ³ <i>R</i> _{int} = 25.23
Unit cell data	Structure	Structure

4. Bis(Hexylamine) Tetrabromozincate

The hybrid was characterized at two different temperatures. The unit cell data was collected at $-100\text{ }^{\circ}\text{C}$ while the crystal structure was solved at $-50\text{ }^{\circ}\text{C}$. The asymmetric unit of the crystal consists of one isolated inorganic tetrahedral ZnBr_4^{2-} unit and two n-hexylammonium cations.

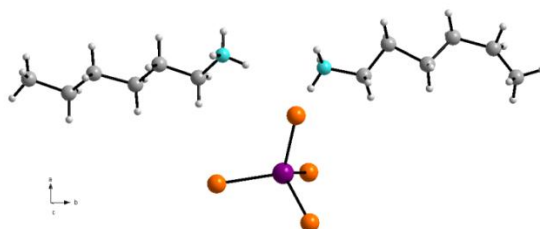


Figure 19: Asymmetric unit

The hybrid forms an alternating, layered structure consisting of metal halide tetrahedra and aliphatic, ammonium chains. The inorganic species form 2D layers which extend along the ac -plane. The isolated tetrahedra stack in a head to tail fashion along the c -direction and overlap directly with their neighbouring unit cell equivalents along the a -axis. The average Zn-Br bond is 2.402 \AA with a standard deviation of 0.017 \AA . The Br-Zn-Br angles are slightly distorted due to the hydrogen bonding within the hybrid structure.

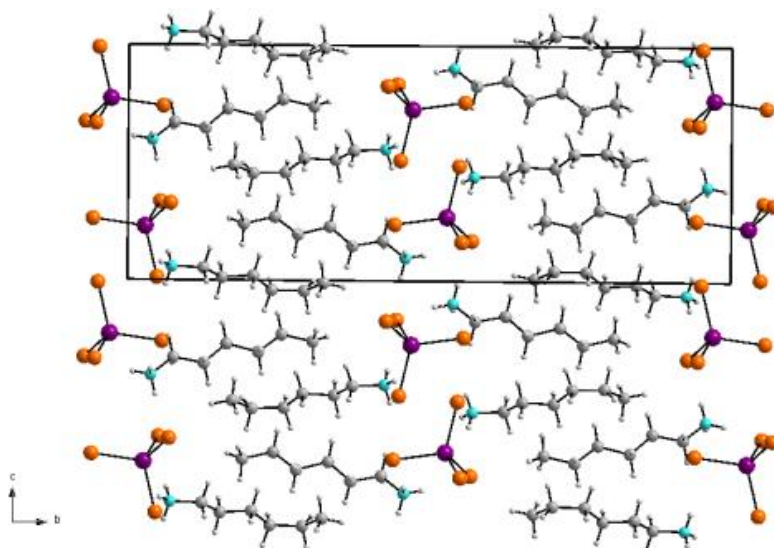


Figure 20: Crystal packing arrangement

The organic cations are sandwiched between the inorganic layers. The aliphatic organic chain lengths extend in the b direction where the carbon chains form intercalated species.

Thermal characterization

The hybrid does not exhibit any solid-solid phase transitions between -100°C and -50°C. The hybrid structure determined at -100°C seemed to contain some disorder as the structure was not completely solved. The crystal was not analysed via DSC.

Synthesis

0.05g (0.22 mmol) Zinc(II)bromide and 0.05g (0.49mmol) hexylamine were dissolved in 2ml of HBr. The solution was slowly heated to 90°C and then cooled back to room temperature. Crystallization occurred upon cooling.

Crystal data

Table 12: Experimental data

$(C_6H_{13}NH_3)_2ZnBr_4$	
$T = -100^\circ C$	$T = -50^\circ C$
Crystal data Monoclinic $a = 7.581\text{\AA}$ $b = 10.570\text{\AA}$ $\beta = 96.621^\circ$ $c = 27.690\text{\AA}$ $V = 2204.05\text{\AA}^3$	Crystal data Monoclinic, $P21/c$ $a = 7.635\text{\AA}$ $b = 27.279\text{\AA}$ $\beta = 92.074^\circ$ $c = 10.6454\text{\AA}$ $V = 2215.6\text{\AA}^3$ $Z = 4$
Refinement data Mo $K\alpha$ radiation $\lambda = 0.71073\text{\AA}$ Plate, colourless $1.30 \times 0.66 \times 0.20\text{ mm}^3$	Refinement data $F_{000} = 1152$ $D_x = 1.767\text{ Mg/m}^3$ Mo $K\alpha$ radiation $\lambda = 0.71073\text{\AA}$ $\theta = 1.49\text{ to }28.28^\circ$ $\mu = 8.315\text{ mm}^{-1}$ Plate, colourless $1.30 \times 0.66 \times 0.20\text{ mm}^3$ $R_{int} = 6.30$
Unit cell data	Structure

5. Bis(Heptylamine) Tetrabromozincate

The organic-inorganic hybrid was structurally characterized at two different temperatures. The room temperature structure's atoms could not be anisotropically refined while the structure at -100°C produced a reasonable structural model. The discrepancy between the two structures was most probably caused by an order-disorder phase transition.

The asymmetric unit of the crystal consists of an incomplete inorganic tetrahedral unit and two n-heptylammonium cations. The additional bromine atom is generated by a symmetry operator.

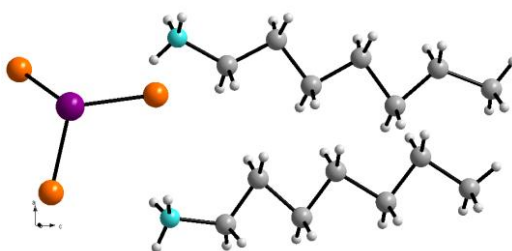


Figure 21: Asymmetric unit

The hybrid structure consists of alternating, two dimensional layers which extend infinitely along the *ab*-plane. The inorganic layers consists of isolated tetrahedra which pack in a head to tail arrangement along the *a*-direction while the unit cell equivalents stack directly on top of each other along the *b*-direction. The tetrahedra have an average Zn-Br bond distance 2.398\AA with a standard deviation of 0.007\AA while the bonding angle of the inorganic unit exhibits some distortion which results from the hydrogen bonding scheme in the unit cell.

The organic cations are sandwiched between the inorganic layers. The organic chains insert their ammonium group into the inorganic layer which allows for better hydrogen bonding interactions. The torsion angles of the organic unit had to be restrained in order to produce a reliable structure model.

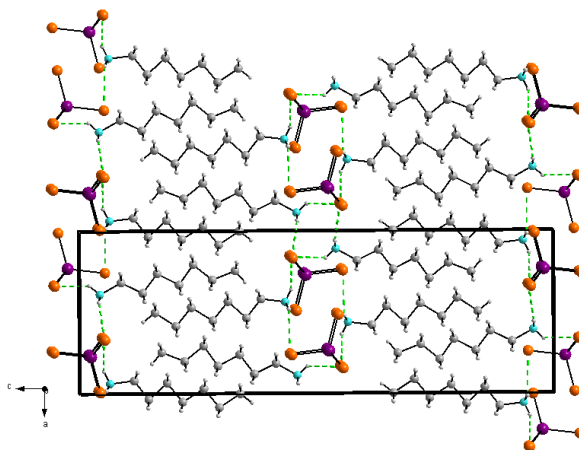


Figure 22:Crystal packing arrangement and the associated hydrogen bonding

Thermal characterization

The hybrid undergoes four phase transitions as it is heated. The initial transition occurs at approximately -50°C while the next three transitions occur between 125°C and 190°C. As the sample is heated a non-reversible transition occurs as the structure only exhibits two phase transitions upon cooling. Further studies can be done on this hybrid to identify the reversible and non-reversible phase transitions as it has not been distinguished which of the cooling peaks are the related reversible transitions of the heating cycle. Phase II was structurally characterized in this study.

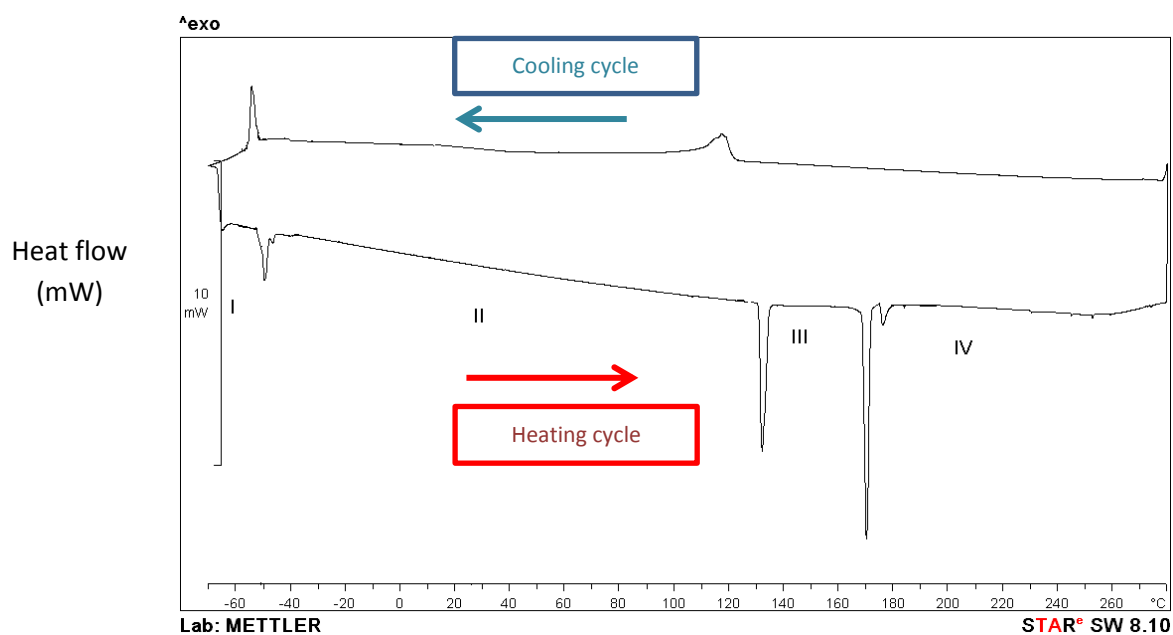


Figure 23: DSC scan of bis(heptylamine) tetrabromozincate

Synthesis

0.05g (0.22 mmol) of Zinc(II)bromide and 0.051g (0.44 mmol) of heptylamine were dissolved in 4ml of concentrated HBr. Crystallization occurred once the solution was left to evaporate.

Crystal data

Table 13: Experimental Data

$(C_7H_{15}NH_3)_2 ZnBr_4$	
$T = 20^\circ C$	$T = 0^\circ C$
<p>Crystal data Orthorhombic $a = 7.703 \text{ \AA}$ $b = 10.521 \text{ \AA}$ $c = 30.595 \text{ \AA}$ $V = 2479.2 \text{ \AA}^3$</p> <p>Refinement data $F_{000} = 1584$ Mo $K\alpha$ radiation $\lambda = 0.71073 \text{ \AA}$ $\theta = 1.33$ to 24.71°. $\mu = 7.730 \text{ mm}^{-1}$ Plate, colourless $0.44 \times 0.38 \times 0.24 \text{ mm}^3$</p>	<p>Crystal data Orthorhombic, <i>Pnma</i> $a = 10.463 \text{ \AA}$ $b = 7.7136 \text{ \AA}$ $c = 30.496 \text{ \AA}$ $V = 2461.2 \text{ \AA}^3$ $Z = 4$</p> <p>Refinement data $F_{000} = 1216$ $D_x = 1.666 \text{ Mg/m}^3$ Mo $K\alpha$ radiation $\lambda = 0.71073 \text{ \AA}$ $\theta = 2.06$ to 23.36° $\mu = 7.489 \text{ mm}^{-1}$ Plate, colourless $0.44 \times 0.38 \times 0.24 \text{ mm}^3$ $R_{int} = 10.37$</p>
Unit cell data	Structure

6. Bis(Octylamine) Tetrabromozincate

The title compound was structurally characterized at -50°C . The asymmetric unit of the crystal consists of two cationic organic chains and one isolated tetrahedral inorganic unit. The inorganic unit exhibits some degree of disorder as the bromide ion $[\text{Br}_4^-]$ is split between two positions.

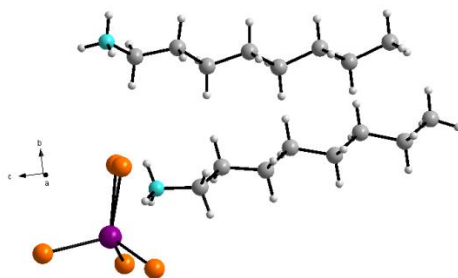


Figure 24: Asymmetric unit

The inorganic layers consist of isolated, tetrahedral metal halide units which extend infinitely along the ab -plane. The ammonium organic cations are then sandwiched between the inorganic layers (refer to **Figure 25**). The tetrahedral units form a head to tail packing formation which extends along the b -direction. The tetrahedral bonding angles are slightly distorted which results from the hydrogen bonding scheme. The average Zn-Br bonding distance is 2.407\AA with a standard deviation of 0.022\AA .

The organic cations are sandwiched between the inorganic layers of the hybrid structure. The ammonium group of the organic chains inserts itself into the inorganic layers resulting in the strongest hydrogen bonding interactions. The entire crystal structure is reliant on the hydrogen bonding scheme for stability.

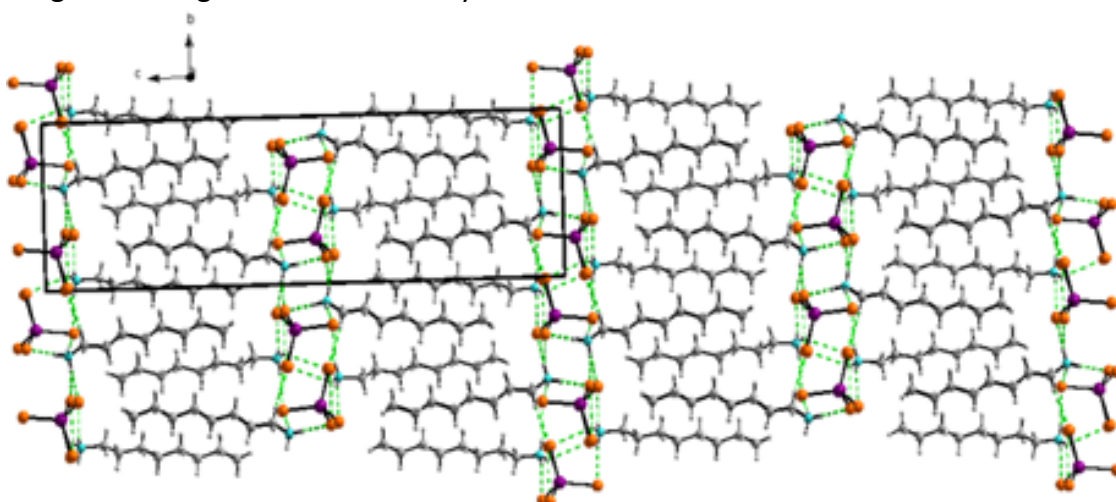


Figure 25: Crystal packing arrangement and the associated hydrogen bonding

Thermal characterization

The hybrid was initially heated from 40°C to 280°C. The crystal experienced a number of phase transitions upon heating. The resulting cooling peaks lead us to believe that some of the transitions when heating are non-reversible. Phase I was structurally characterized at -50°C.

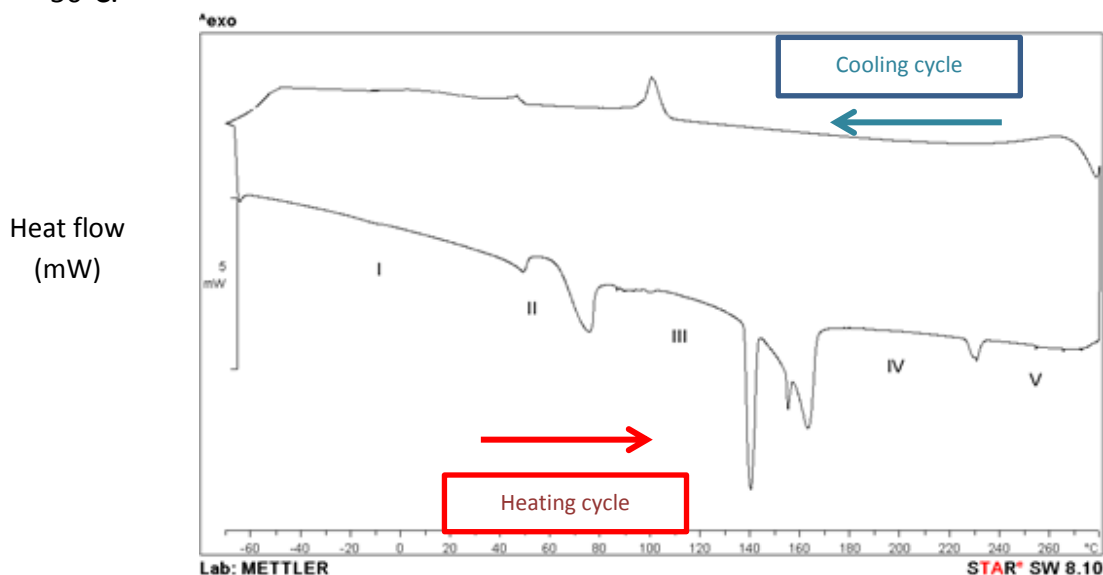


Figure 26: DSC scan of bis(octylamine) tetrabromozincate

Synthesis

0.17g (7.55 mmol) Zinc(II)bromide and 0.2g (1.54 mmol) octylamine were dissolved in 10ml of acetonitrile and 2ml of concentrated HBr. Crystallization occurred once the solution was left to slowly evaporate.

Crystal data

Table 14: Experimental data

$(C_8H_{17}NH_3)_2 ZnBr_4$
T = -50°C
<p>Crystal data Monoclinic, $P2_1/c$ $a = 7.5803 \text{ \AA}$ $b = 10.5278 \text{ \AA}$ $\beta = 96.3^\circ$ $c = 32.8535 \text{ \AA}$ $V = 2606.15 \text{ \AA}^3$ $Z = 4$</p> <p>Refinement data $F_{000} = 1280$ $D_x = 1.645 \text{ Mg/m}^3$ Mo Kα radiation $\lambda = 0.71073 \text{ \AA}$ $\theta = 2.03 \text{ to } 22.06^\circ$ $\mu = 7.077 \text{ mm}^{-1}$ Plate, colourless $0.53 \times 0.16 \times 0.01 \text{ mm}^3$ $R_{int} = 7.16$</p>

7. Bis(Nonylamine) Tetrabromozincate

The crystal structure of bis(nonylamine) tetrabromozincate was determined at room temperature and -50°C . The unit cell data was collected at -20°C and -100°C as the quality of the diffraction data was poor which made the structure solution and refinement impossible.

The asymmetric unit of the room temperature structure consists of two n-nonylammonium cations which are hydrogen bonded to an incomplete isolated inorganic tetrahedral unit (refer to **Figure 27a**). The inorganic unit is dependent upon the symmetry operator for completion. The asymmetric unit of the low temperature structure consists of four organic chains and two isolated tetrahedral units.

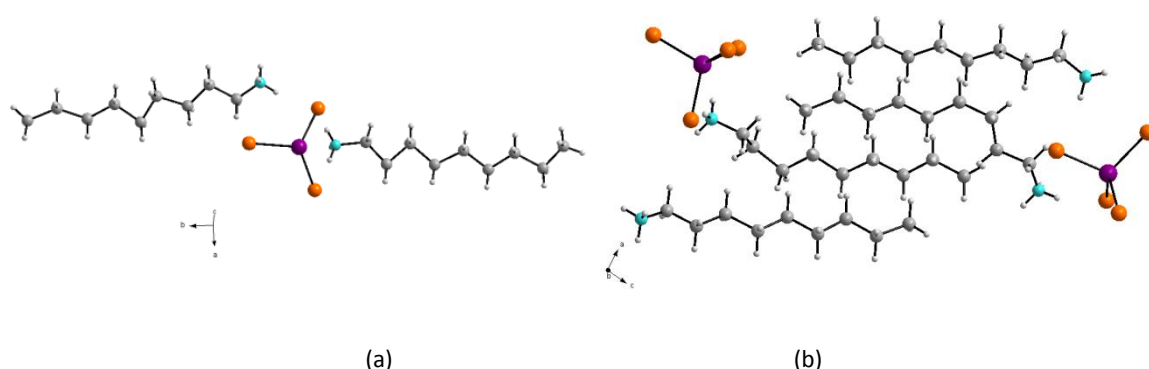


Figure 27: Asymmetric unit of (a) the room temperature or orthorhombic crystal structure and (b) the -50°C or monoclinic crystal structure

The inorganic layers extend along the ac -plane while the inorganic tetrahedra exhibit a head to tail packing conformation along the a -direction. The average metal-halide bonding distance is 2.396\AA with a standard deviation of 0.010\AA at room temperature. The low temperature structure has an average bonding distance of 2.405\AA with a standard deviation of 0.012\AA .

The organic component form intercalated species which are sandwiched between the inorganic layers. The organic chains of both of the structures were relatively planar with small variations. The high temperature structure's organic chains extended in a manner that was perpendicular to the inorganic layer while the low temperature structure tended to be at an angle relative to the inorganic layer (refer to Figure 28).

The entire structure is stabilized by the charge assisted hydrogen bonds between the cationic organic and anionic metal-halide units.

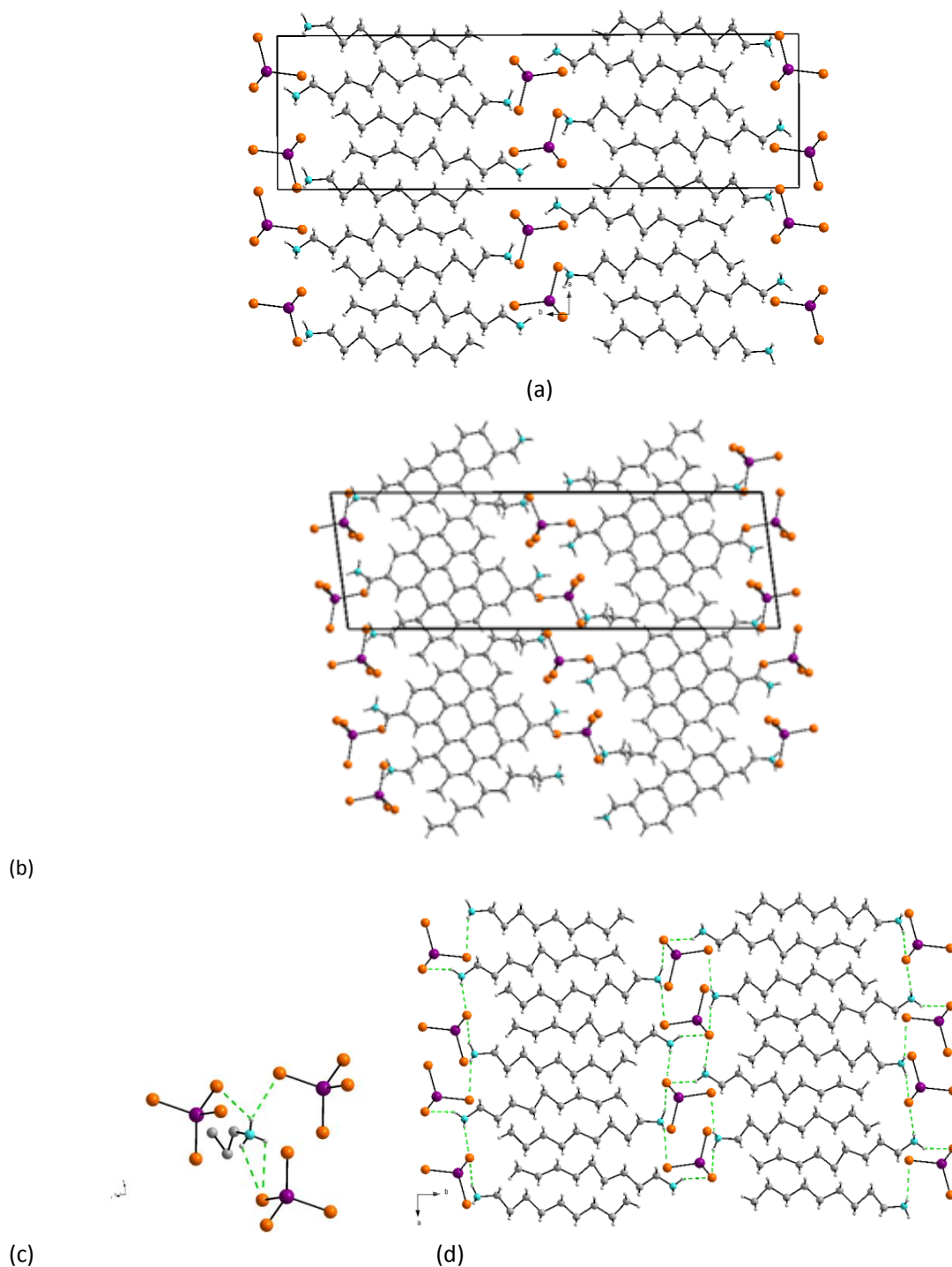


Figure 28: Crystal packing arrangement of (a) the room temperature structure, (b) the low temperature structure and the associated hydrogen bonding arrangement of (c) an organic cation and (d) the hydrogen bonding scheme associated with the high temperature structure

Thermal characterization

The DSC image reveals that there are three reversible solid-solid phase transitions. The transition between phase I and II was identified in this study. The SC-XRD data identified the transition conversion for an orthorhombic (II) to a monoclinic (I) space group. The transitions occur between -30°C to -15°C ; 60°C to 75°C and finally 95°C to 125°C when heated.

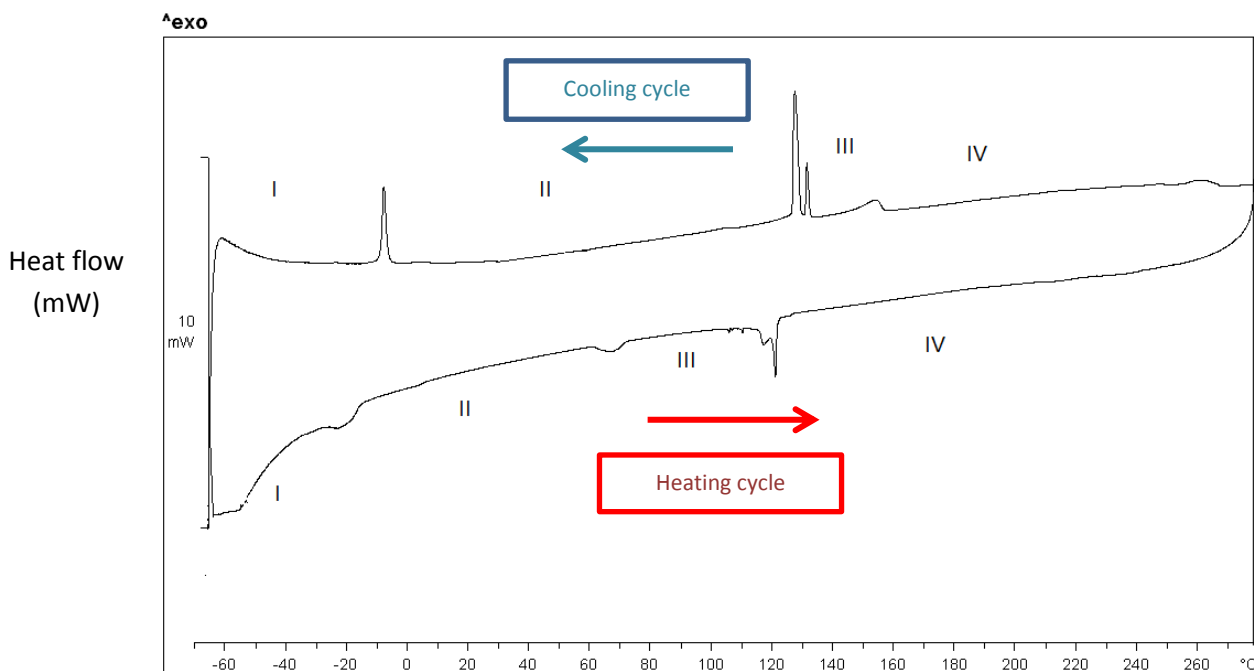


Figure 29: DSC scan of bis(nonylamine) tetrabromozincate

Synthesis

0.05g (7.55 mmol) of Zinc(II)bromide and 0.064g (4.47 mmol) of nonylamine were dissolved in a 1:1 ratio of concentrated HBr and hexane. Crystallization occurred once the solution was left to evaporate.

Crystal data

Table 15: Experimental data

$(C_9H_{19}NH_3)_2ZnBr_4$			
$T = 20^\circ C$	$T = -20^\circ C$	$T = -50^\circ C$	$T = -100^\circ C$
Crystal data Orthorhombic, $Pnam$ $a = 10.479 \text{ \AA}$ $b = 35.54 \text{ \AA}$ $c = 7.720 \text{ \AA}$ $V = 2875 \text{ \AA}^3$ $Z = 4$	Crystal data Monoclinic $a = 10.938 \text{ \AA}$ $b = 7.5212 \text{ \AA}$ $\beta = 97.6^\circ$ $c = 34.474 \text{ \AA}$ $V = 2811.2 \text{ \AA}^3$	Crystal data Monoclinic, $P2_1$ $a = 10.950 \text{ \AA}$ $b = 7.480 \text{ \AA}$ $\beta = 97.3^\circ$ $c = 34.438 \text{ \AA}$ $V = 2798.1 \text{ \AA}^3$ $Z = 4$	Crystal data Monoclinic $a = 10.923 \text{ \AA}$ $b = 7.436 \text{ \AA}$ $\beta = 97.2^\circ$ $c = 34.399 \text{ \AA}$ $V = 2772.0 \text{ \AA}^3$
Refinement data $F_{000} = 1344$ $D_x = 1.587 \text{ Mg/m}^3$ Mo $K\alpha$ radiation $\lambda = 0.71073 \text{ \AA}$ $\theta = 2.26$ to 27.00° $\mu = 6.419 \text{ mm}^{-1}$ Plate, colourless $0.84 \times 0.80 \times 0.3 \text{ mm}^3$ $R_{int} = 22.25$	Refinement data Mo $K\alpha$ radiation $\lambda = 0.71073 \text{ \AA}$ Plate, colourless $0.04 \times 0.40 \times 0.60 \text{ mm}^3$	Refinement data $F_{000} = 1344$ $D_x = 1.599 \text{ Mg/m}^3$ Mo $K\alpha$ radiation $\lambda = 0.71073 \text{ \AA}$ $\theta = 1.79$ to 23.32° $\mu = 6.595 \text{ mm}^{-1}$ Plate, colourless $0.60 \times 0.40 \times 0.04 \text{ mm}^3$ $R_{int} = 6.77$	Refinement data Mo $K\alpha$ radiation $\lambda = 0.71073 \text{ \AA}$ Plate, colourless $0.60 \times 0.40 \times 0.04 \text{ mm}^3$
Structure	Unit cell data	Structure	Unit cell data

8. Bis(Decylamine) Tetrabromozincate

The organic-inorganic hybrid was structurally characterized at two different temperatures. The unit cell data was collected at -10°C while the crystal structure was determined at -75°C . The asymmetric unit of the title compound consists of two *n*-decylammonium cation chains and one isolated ZnBr_4^{2-} tetrahedral unit.

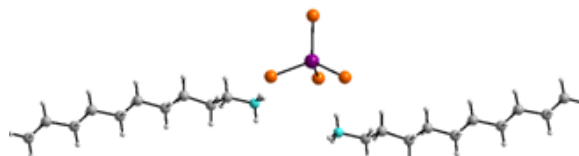


Figure 30: Asymmetric unit

The inorganic tetrahedra pack in an arrangement that extend infinitely in two dimensions along the *ab*-plane. The inorganic units form a head to tail arrangement along the *b*-direction within the 2D layer. The average Zn-Br bond distance is 2.407\AA with a standard deviation of 0.014\AA . The bonding angle deviates slightly from the standard values but this is a result of the hydrogen bonding arrangement of the hybrid.

The cationic amine chains are sandwiched between the 2D inorganic layers where they form intercalated layers. The torsion angles of the organic chains are slightly deviated from 180° toward the amine side. This allows the organic cation to orientate itself and penetrate further into the inorganic layer therefore ensuring efficient hydrogen bonding.

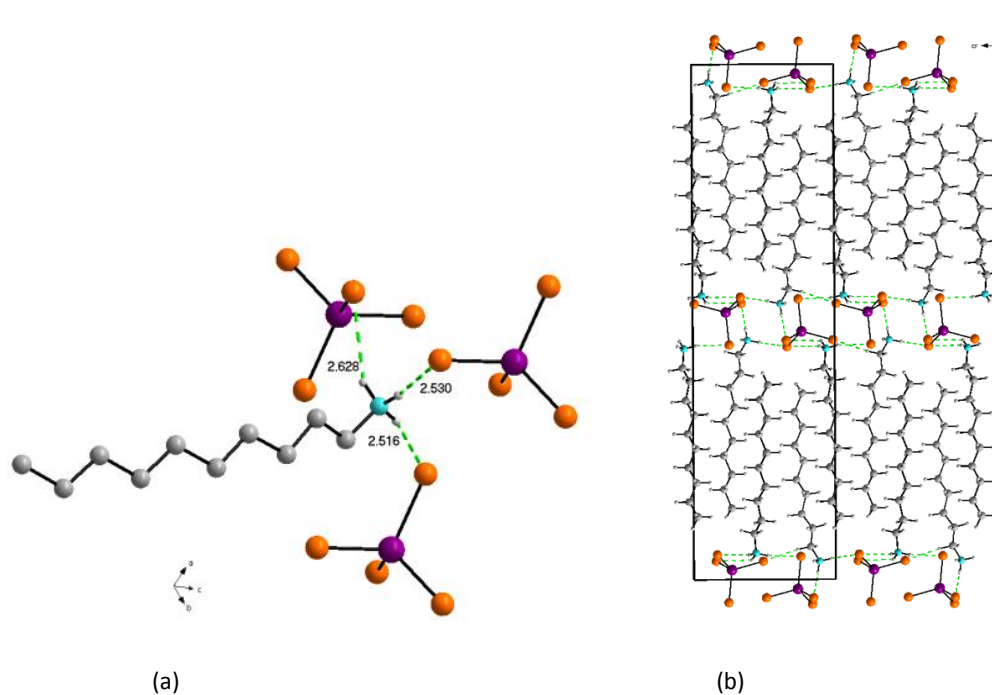


Figure 31: (a) Hydrogen bonding ability of the organic cation (b) Crystal packing arrangement with associated hydrogen bonding scheme

Thermal characterization

The hybrid undergoes three reversible solid-solid phase transitions between -40°C and 250°C. All of the phase transitions occur above room temperature. Phase I was structurally characterized in this study at -75°C. There is a glass transition present near 25°C which results from the presence of a contaminant such as amorphous materials. The bromide hybrid experiences an additional phase transition when compared to the published chloride structure. The phase transitions for both structures occur above 0°C. Phase transitions occur at approximately 60°C, 80°C and 110°C for the heating cycle.

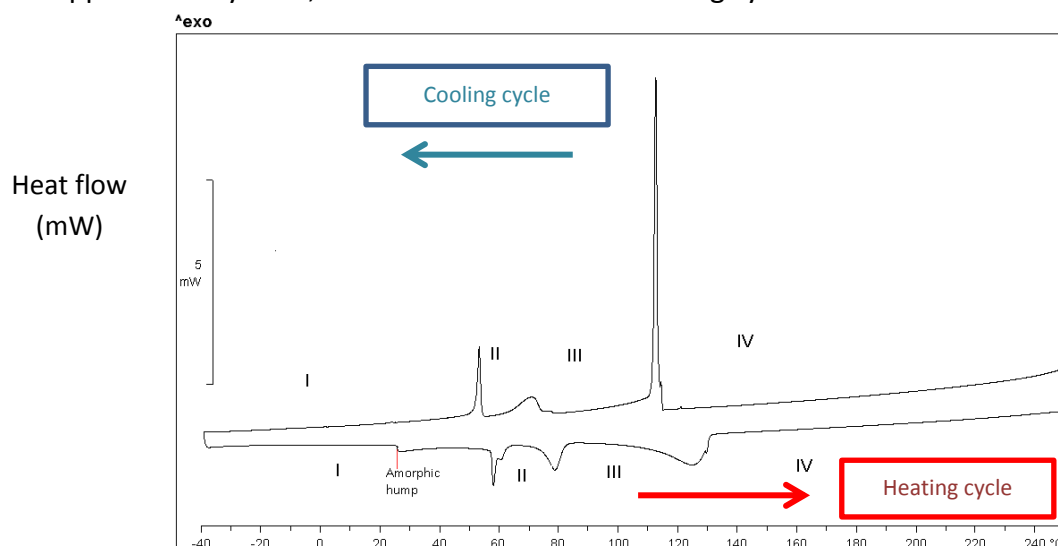


Figure 32: DSC scan of bis(decylamine) tetrachlorozincate

Synthesis

0.05g (0.22mmol) Zinc(II)bromide and 0.070g (0.44 mmol)decylamine were dissolved in 2.4ml of concentrated HBr and 3ml ethanol. Crystallization occurred once the solution was left to evaporate.

Crystal data

Table 16: Experimental data

(C₁₀H₂₁NH₃)₂ZnBr₄	
T = -10°C	T = -75°C
<p>Crystal data</p> <p>Triclinic, <i>P</i>-1 $a = 7.690\text{Å}$ $\alpha = 91.74^\circ$ $b = 10.520\text{Å}$ $\beta = 91.21^\circ$ $c = 38.38\text{Å}$ $\gamma = 90.21^\circ$ $V = 3103\text{Å}^3$</p> <p>Refinement data $F_{000} = 1667$</p> <p>Mo Kα radiation $\lambda = 0.71073\text{Å}$ $\theta = 1.06$ to 23.93°. Plate, colourless $0.46 \times 0.38 \times 0.04\text{ mm}^3$ $R_{\text{int}} = 116.6$</p> <p>Unit cell</p>	<p>Crystal data $M_r = 701.59$ Monoclinic, <i>P</i>2₁/<i>c</i> $a = 7.5615\text{Å}$ $b = 10.4250\text{Å}$ $\beta = 93.973^\circ$ $c = 37.9120\text{Å}$ $V = 2981.4\text{Å}^3$ $Z = 4$</p> <p>Refinement data $F_{000} = 1408$ $D_x = 1.563\text{ Mg/m}^3$ Mo Kα radiation $\lambda = 0.71073\text{Å}$ $\theta = 1.08$ to 23.31°. $\mu = 6.193\text{ mm}^{-1}$ Plate, colourless $0.46 \times 0.38 \times 0.04\text{ mm}^3$ $R_{\text{int}} = 14.59$</p> <p>Structure</p>

9. Bis(Pentylamine) Tetraiodozincate

The hybrid was structurally characterized at -100°C . The asymmetric unit is larger than the average unit in this series of crystals. This is due to the low symmetry operator of the triclinic unit cell, P-1. The unit consists of two isolated metal halide tetrahedra which are hydrogen bonded to four organic chains.

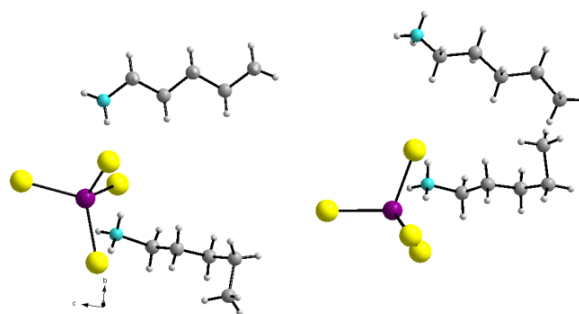


Figure 33: Asymmetric unit

The inorganic tetrahedra form two dimensional layers which extend along the ab -plane with a head to tail packing arrangement along the b -direction. The average metal-halide bonding distance is 2.632\AA and 2.635\AA for each of the isolated tetrahedra in the asymmetric unit. The bonding angles within the inorganic isolates are distorted. The distortions are a result of the hydrogen bonding scheme of the crystal.

The organic component forms intercalated chains which are sandwiched between the inorganic layers. There are two distinct types of the organic chains within the asymmetric unit. The one chain hardly deviates from its planar conformation while the second cation experiences deviations in the internal rotation angle at the end of the carbon chain. This could have resulted in the low symmetry operator of the unit cell.

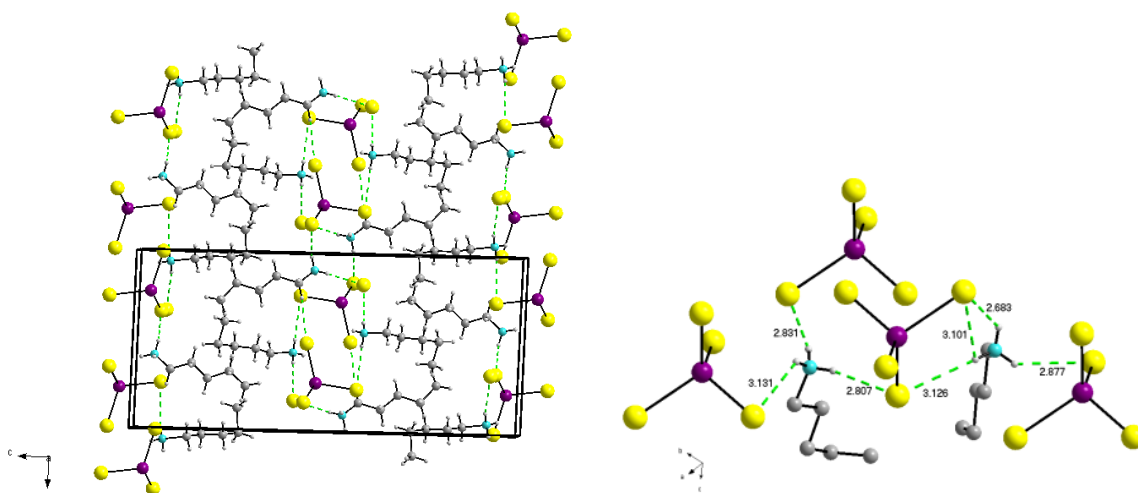


Figure 34: (a) Crystal packing arrangement with the associated hydrogen bonding scheme and (b) the hydrogen bonding possibilities of two different nitrogen atoms

Synthesis

0.05g (0.157mmol) Zinc(II)iodide and 0.028g (0.314mmol) pentylamine were dissolved in a solution containing 2ml of ethanol, 3 drops of concentrated HI and 1 drop of phosphinic acid. Crystallization occurred once the samples were left to slowly evaporate.

Crystal data

Table17:Experimental data

$(C_5H_{11}NH_3)_2ZnI_4$
$T = -100^\circ C$
Crystal data
Triclinic, <i>P</i> -1
$a = 8.1938 \text{ \AA}$ $\alpha = 88.66^\circ$
$b = 11.1501 \text{ \AA}$ $\beta = 81.66^\circ$
$c = 24.3589 \text{ \AA}$ $\gamma = 89.14^\circ$
$V = 2201.2 \text{ \AA}^3$
$Z = 2$
Refinement data
$F_{000} = 1376$
$D_x = 2.261 \text{ Mg/m}^3$
Mo $K\alpha$ radiation
$\lambda = 0.71073 \text{ \AA}$
$\theta = 0.85$ to 27.40° .
$\mu = 6.715 \text{ mm}^{-1}$
Plate, colourless
$0.25 \times 0.36 \times 0.04 \text{ mm}^3$
$R_{int} = 15.28$

10. Bis(Hexylamine) Tetraiodozincate

The hybrid was characterized at two different temperatures. The unit cell was determined at 20°C while the crystal structure was determined at -100°C. The asymmetric unit of the hybrid consisted of one isolated tetrahedral unit with two n-hexylammonium cations (refer to **figure 35**).

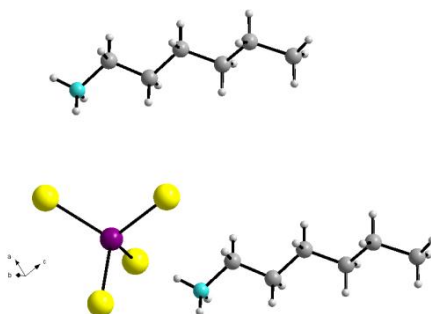


Figure 35: Asymmetric unit

The inorganic tetrahedra ZnI_4^{2-} pack in an arrangement which extends infinitely along the *ab*-plane, with a head to tail stacking arrangement along the *b*-direction. The average metal halide bonding distance is 2.613Å with a standard deviation of 0.022Å. The tetrahedral angles deviate slightly due to the hydrogen bonding scheme of the crystal structure. The hydrogen bonding distances range between 3.629Å and 3.849Å for the donor-acceptor bonds.

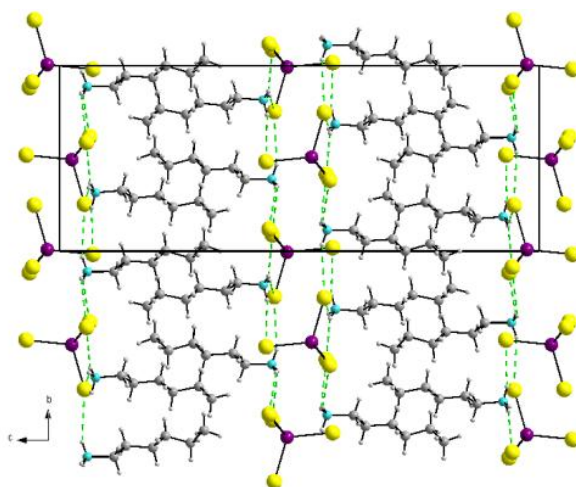


Figure 36: Crystal packing arrangement with the associated hydrogen bonding scheme

The organic cation's polar head is responsible for the charge assisted hydrogen bonds between the inorganic and organic units. The ammonium group penetrates right into the inorganic layer to achieve a better hydrogen bonding ability. The organic component of the crystal forms intercalated cations which are sandwiched between the inorganic layers. The internal rotation angle of the organic chains deviates slightly from its planar conformation.

Thermal characterization

A transition was identified between room temperature and -100°C where the crystal exhibits a solid-solid phase transition from a triclinic unit cell to an orthorhombic unit cell with space group $P2_12_12_1$. The exact transition temperature should be determined by DSC which will be left for future investigation.

Synthesis

The crystals were grown in two different solvent systems:

0.05g (0.157mmol) Zinc(II)iodide and 0.031g (0.314mmol) hexylamine were dissolved in a solution containing 3 drops of concentrated HI, 1 drop of phosphinic acid and 2ml of ethanol or 2ml of ethyl acetate. Crystallization occurred once the samples were left to slowly evaporate. Both solvent systems resulted in good quality crystals.

Crystal data

Table 18: Experimental data

$(C_6H_{16}N)_2ZnI_4$	
$T = -100^\circ C$	$T = 20^\circ C$
Crystal data	Crystal data
Orthorhombic, $P2_12_12_1$	Triclinic
$a = 8.298 \text{ \AA}$	$a = 8.131 \text{ \AA} \quad \alpha = 88.561^\circ$
$b = 10.521 \text{ \AA}$	$b = 11.119 \text{ \AA} \quad \beta = 86.075^\circ$
$c = 27.295 \text{ \AA}$	$c = 27.856 \text{ \AA} \quad \gamma = 89.772^\circ$
$V = 2382.57 \text{ \AA}^3$	$V = 2511.83 \text{ \AA}^3$
$Z = 4$	
Refinement data	Refinement data
$F_{000} = 1416$	
$D_x = 2.15 \text{ Mg/m}^3$	
Mo $K\alpha$ radiation	Mo $K\alpha$ radiation
$\lambda = 0.71073 \text{ \AA}$	$\lambda = 0.71073 \text{ \AA}$
$\theta = 2.1 \text{ to } 23.33^\circ$	
$\mu = 6.208 \text{ mm}^{-1}$	
Plate, colourless	Plate, colourless
$0.70 \times 0.13 \times 0.5 \text{ mm}^3$	$0.48 \times 0.21 \times 0.06 \text{ mm}^3$
$R_{int} = 8.06$	$R_{int} = 10.4$
Structure	Unit cell

4.1.2 Cobalt (II) Chloride

The organic-inorganic hybrids of tetrachlorocobaltate and monoprotonated aliphatic chains with the formula $(C_nH_{2n+2}N)_2 CoCl_4$ were prepared. Most of the cobalt chloride hybrids published have used diprotonated organic species. These series of crystals form a two dimensional, alternating layered structure which is stabilized by a series of charge assisted hydrogen bonds between the anionic inorganic component and the cationic organic chains (Mahmoudkhani et al. 2001). The divalent cobalt hybrids tend to form isolated tetrahedral inorganic units which results in a large charge density (Dobrzycki, 2008).

11. Bis(Hexylamine) Tetrachlorocobaltate

The hybrid structure forms a two dimensional layered structure of alternating organic and inorganic layers at 0°C. The asymmetric unit of the crystal consists of one isolated tetrahedral metal halide unit and two n-hexylammonium cations.

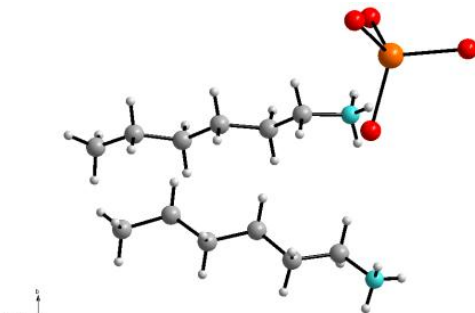


Figure 37: Asymmetric unit

The two dimensional inorganic layers extend infinitely along the *ab*-plane and pack with a head to tail packing arrangement along the *b*-direction. The average metal halide bonding distance is 2.269Å with a standard deviation of 0.011Å. The bonding angles are slightly distorted due to the hydrogen bonding of the crystal. The inorganic layers sandwich the organic cations between the inorganic layers.

The organic cations exhibit an extremely efficient form of packing where the carbon chains form intercalated species. The ammonium heads of the organic chains are inserted right into the inorganic layer which allows better hydrogen bonding interactions. The torsion angles of the organic species are only slightly distorted from a planar conformation.

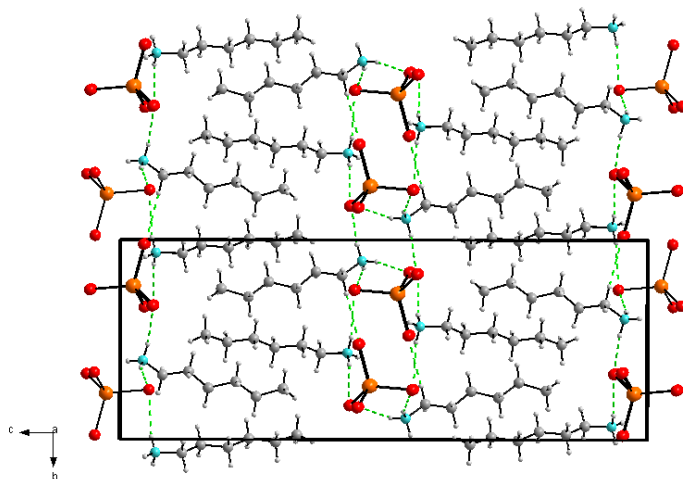


Figure 38: Crystal packing arrangement with the associated hydrogen bonding scheme

Thermal characterization

This cobalt hybrid undergoes five reversible solid-solid phase transitions between -70°C and 280°C. Phase I was structurally characterized at 0°C. All of the transitions identified occurred above room temperature at approximately 40°C, 65°C, 115°C, 195°C, and 230°C during the heating portion of the cycle.

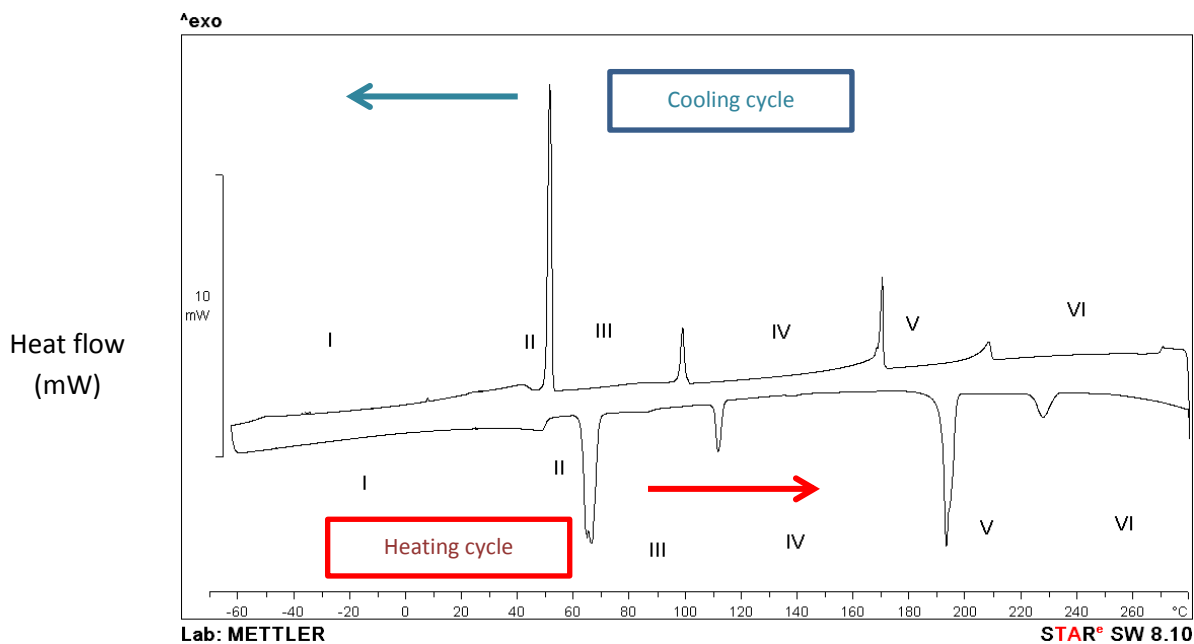


Figure 39: DSC scan of bis(hexylamine) tetrachlorocobaltate

Synthesis

0.05g (0.21mmol) Cobalt(II)chloride and 0.0366g (0.36 mmol) hexylamine were dissolved in concentrated HCl. The sample was then slowly heated to 80 °C and cooled back to room temperature. Crystallization occurred upon cooling.

Crystal data

Table 19: Experimental data

$(C_6H_{11}NH_3)_2 CoCl_4$	
$T = 0^\circ C$	
Crystal data	
Monoclinic, $P2_1/n$	
$a = 7.379 \text{ \AA}$	
$b = 10.393 \text{ \AA}$ $\beta = 94.56^\circ$	
$c = 27.539 \text{ \AA}$	
$V = 2105.2 \text{ \AA}^3$	
$Z = 4$	
Refinement data	
$F_{000} = 852$	
$D_x = 1.278 \text{ Mg/m}^3$	
Mo $K\alpha$ radiation	
$\lambda = 0.71073 \text{ \AA}$	
$\theta = 1.48$ to 23.40° .	
$\mu = 1.315 \text{ mm}^{-1}$	
Plate, blue	
$0.70 \times 0.80 \times 0.02 \text{ mm}^3$	
$R_{int} = 14.30$	

12. Bis(Octylamine) Tetrachlorocobaltate

The hybrid was structurally characterized at two different temperatures. The unit cell data was collected at -10°C while the crystal structure was determined at -50°C . The asymmetric unit deviates from the typical units seen before in this study. The asymmetric unit of bis(octylamine) tetrachlorocobaltate consists of one isolated tetrahedral unit, one chloride ion and three n-octylammonium cations. The structure is similar to the diprotonated hybrid which has been previously published $[2(\text{NH}_3 \text{C}_2\text{H}_6 \text{NH}_3)(\text{CoCl}_4)_2(\text{Cl})]$ (Smith, 1977).

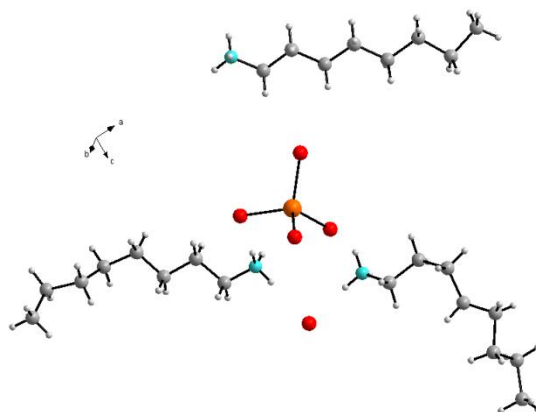


Figure 40: Asymmetric unit

The hybrid structure is comprised of the typical alternated, two dimensional layered structure. The inorganic layer infinitely extends along the c -axis and comprises of two tetrahedra with head to tail packing which is then followed by two chloride ions. The inorganic tetrahedra have an average Co-Cl bonding distance of 2.280\AA with a standard deviation of 0.022\AA . The bonding angles are slightly distorted which results from the hydrogen bonding scheme.

The hydrogen bonding scheme within the structure involves bonds between the organic cations and the inorganic component which is comprised of the tetrahedra and the isolated chloride ions. Two of the organic chains deviate from the planar internal rotation angle where the one carbon tail end deviates slightly from 180° while the other alkyl chain's torsion angle deviates drastically (refer to **Figure 41**). The polar heads of the organic chains are inserted directly into the inorganic layer which allows for better hydrogen bonding. The structure does contain some degree of intercalation.

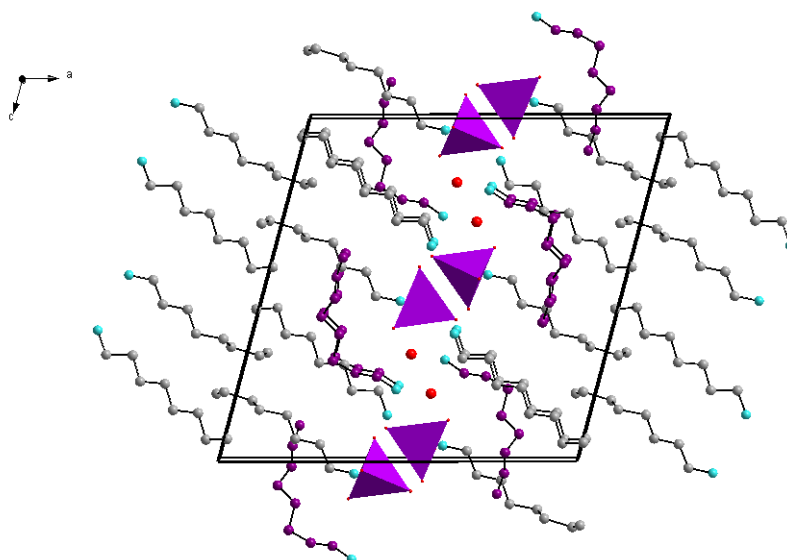


Figure 41:Crystal packing arrangement. The organic cation highlighted in purple deviates from the planar conformation of the other chains

Synthesis

0.05g (3.85 mmol) of Cobalt(II)chloride and 0.054g (4.18 mmol) of octylamine were dissolved in 2ml of concentrated HCl. The sample vial was then slowly heated to 80°C and then cooled back to room temperature over a 48 hour period. Crystallization occurred once the sample solution started to cool.

Crystal data

Table 20:Experimental data

$(C_8H_{17}NH_3)_3 CoCl_4 \cdot Cl^-$	
$T = -10^\circ C$	$T = -50^\circ C$
Crystal data	Crystal data
Monoclinic	Monoclinic, $P2_1/c$
$a = 9.847 \text{ \AA}$	$a = 19.908 \text{ \AA}$
$b = 9.884 \text{ \AA}$	$b = 9.847 \text{ \AA}$
$c = 19.823 \text{ \AA}$	$c = 19.728 \text{ \AA}$
$\beta = 103.24^\circ$	$\beta = 104.97^\circ$
$V = 1877.97 \text{ \AA}^3$	$V = 3736.0 \text{ \AA}^3$
	$Z = 4$
Refinement data	Refinement data
	$F_{000} = 1348$
	$D_x = 1.115 \text{ Mg/m}^3$
Mo K α radiation	Mo K α radiation
$\lambda = 0.71073 \text{ \AA}$	$\lambda = 0.71073 \text{ \AA}$
	$\theta = 1.06 \text{ to } 23.38^\circ$
	$\mu = 0.832 \text{ mm}^{-1}$
Plate, blue	Plate, blue
$0.46 \times 0.38 \times 0.04 \text{ mm}^3$	$0.90 \times 0.16 \times 0.04 \text{ mm}^3$
$R_{int} = 28.55$	$R_{int} = 14.05$
Unit cell data	Structure

13. Bis(Decylamine) Tetrachlorocobaltate

The hybrid was structurally characterized at two temperatures. The unit cell data was collected at 0°C while the crystal structure was determined at -100°C. This structure is very similar to the hexylammonium hybrid previously discussed.

Asymmetric unit of the low temperature structure consists of two n-decylammonium cations and one isolated tetrahedral unit.

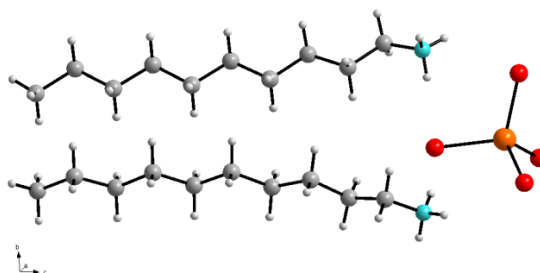


Figure 42: Asymmetric unit

The two dimensional inorganic layers extend infinitely along the *ab*-plane and pack in a head to tail packing arrangement along the *b*-direction. The average Co-Cl bonding distance is 2.272Å with a standard deviation of 0.014Å. The bonding angles are slightly distorted due to the hydrogen bonding of the crystal. The inorganic layers sandwich the organic cations.

The organic cations form intercalated species. The ammonium heads of the organic chains are inserted right into the inorganic layer which allows for better hydrogen bonding interactions. The torsion angles of the organic species are only slightly distorted from 180°.

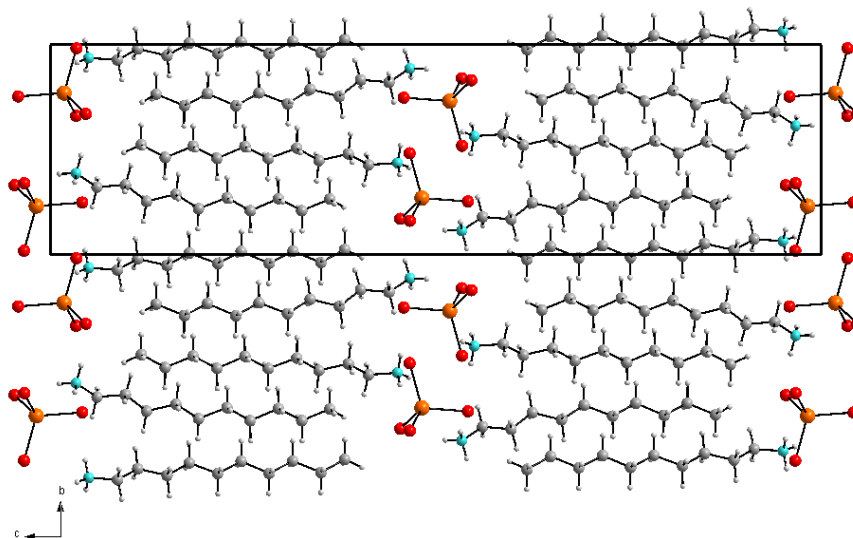


Figure 43: Crystal packing arrangement

Thermal characterization

The crystal experiences two reversible phase transitions above room temperature. Phase I was structurally characterized in this study at -100°C. There are no phase transitions present below 0°C but there is a definite shift in the unit cell size to accommodate the decrease in temperature and therefore energy. The transitions occur at approximately 70°C and 155°C during the heating portion of the cycle.

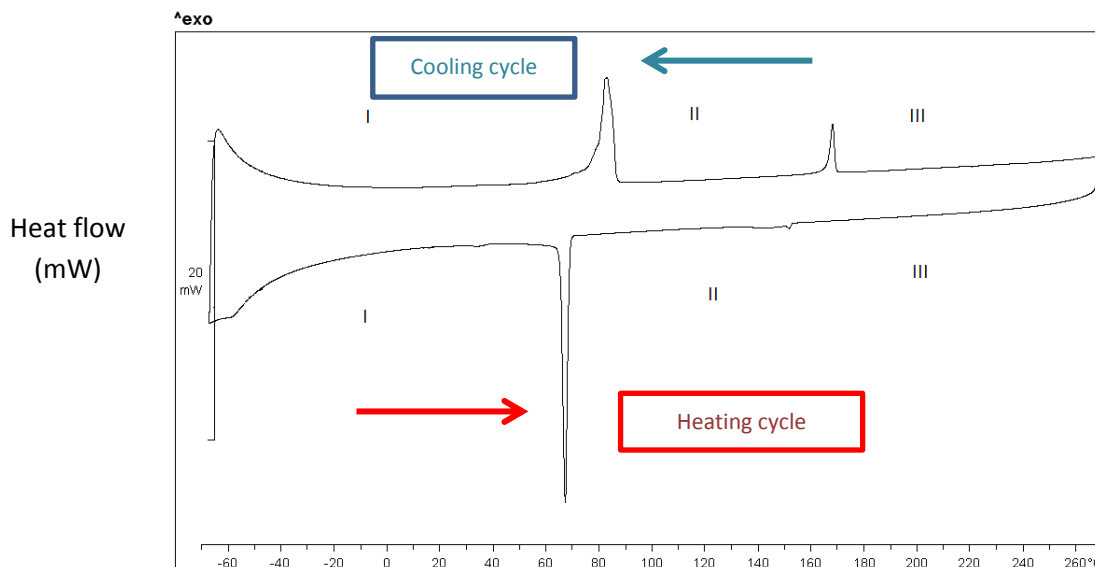


Figure 44: DSC scan of bis(decylamine) tetrachlorocobaltate

Synthesis

0.05g (0.21mmol) Cobalt(II)chloride and 0.066g (0.41mmol) decylamine were dissolved in a solution of concentrated HCl and Ethanol in a ratio of 2:1 respectively. Crystallization occurred once the solution was left to evaporate.

Crystal structure

Table 21: Experimental data

(C₁₀H₂₁NH₃)₂CoCl₄	
T = 0°C	T = -100°C
<p>Crystal data Monoclinic a = 7.368 Å b = 10.283 Å β = 95.442 ° c = 37.766 Å V = 2848.47 Å³</p> <p>Refinement data</p> <p>Mo Kα radiation λ = 0.71073 Å</p> <p>Plate, blue 0.50 x 0.18 x 0.04 mm³</p>	<p>Crystal data Monoclinic, P21/c a = 7.281 Å b = 10.200 Å β = 95.080 ° c = 37.725 Å V = 2790.6 Å³ Z = 4</p> <p>Refinement data F₀₀₀ = 1108 D_x = 1.231 Mg/m³ Mo Kα radiation λ = 0.71073 Å θ = 2.03 to 22.06° μ = 1.006 mm⁻¹ Plate, blue 0.50 x 0.18 x 0.04 mm³ R_{int} = 14.33</p>
Unit cell	Structure

4.1.3 Mercury(II) halide hybrids

The mercury based organic-inorganic hybrid structures tend to be similar to the cobalt and zinc series of hybrids in this study. The metal ions coordinate as isolated tetrahedra for both bromide and iodide structures. The charge density would therefore be large which would then require efficient packing of the organic chains in order to stabilize the charge. The organic cations therefore form intercalated species.

The mercury hybrids tend to be very unstable when exposed to the atmosphere and many of the problems caused during structure solution could have been due to degradation of the crystal.

14. Bis(Butylamine) Tetrabromomercurate

The unit cell data was collected at three different temperatures. The unit cell data was collected at -50°C and -100°C while the crystal structure was determined at room temperature. The structure contained some disorder as the organic component could not be determined.

The asymmetric unit of the crystal consists of three quarters of the isolated inorganic tetrahedron where the last bromide ion is generated by the symmetry operation. The organic components would consist of two organic chains for every isolated tetrahedral unit.

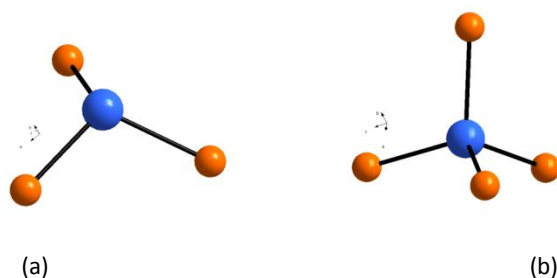


Figure 45: Inorganic asymmetric unit (a) before and (b) after the symmetry operation

The average Hg-Br bonding distance of the inorganic unit was 2.583\AA with a standard deviation of 0.017\AA . The bonding angle deviates slightly from the ideal value of 109° due to the hydrogen bonding within the crystal.

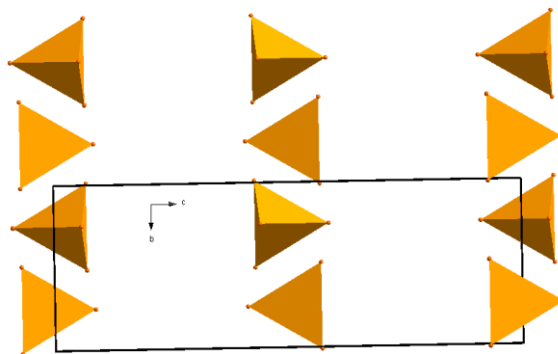


Figure 46: Crystal packing arrangement of the two dimensional inorganic units, represented as polyhedra.

Thermal characterization

The crystal experienced a solid-solid phase transition between room temperature and -50°C . The crystal system tends to lose its symmetry as the crystal is cooled as there is a transformation from an orthorhombic to a triclinic unit cell.

Synthesis

0.05g (1.39 mmol)Mercury(II)bromide and 0.02g (2.73 mmol)butylamine were dissolved in concentrated HBr. The solution was then left to slowly evaporate for an extended amount of time until the crystals formed.

Crystal structure

Table 22: Experimental data

(C₄H₁₁NH₃)₂ HgBr₄		
T = -100°C	T = -50°C	T = 20°C
Crystal data Triclinic, <i>P</i> -1 $a = 7.8790 \text{ \AA}$ $\alpha = 117.968$ $b = 12.3431 \text{ \AA}$ $\beta = 100.416$ $c = 13.0033 \text{ \AA}$ $\gamma = 97.386$ $V = 1064.85 \text{ \AA}^3$	Crystal data Triclinic, <i>P</i> -1 $a = 7.7601 \text{ \AA}$ $\alpha = 93.410$ $b = 11.2738 \text{ \AA}$ $\beta = 90.643$ $c = 21.9490 \text{ \AA}$ $\gamma = 92.756$ $V = 1914.4 \text{ \AA}^3$	Crystal data Orthorhombic, <i>Pnma</i> $a = 10.728 \text{ \AA}$ $b = 7.9160 \text{ \AA}$ $c = 22.417 \text{ \AA}$ $V = 1903.7 \text{ \AA}^3$ $Z = 4$
Refinement data Mo K α radiation $\lambda = 0.71073 \text{ \AA}$ Plate, colourless $0.06 \times 0.54 \times 0.56 \text{ mm}^3$ $R_{\text{int}} = 78$	Refinement data Mo K α radiation $\lambda = 0.71073 \text{ \AA}$ Plate, colourless $0.04 \times 0.28 \times 0.44 \text{ mm}^3$ $R_{\text{int}} = 17.46$	Refinement data $F_{000} = 1920$ $D_x = 3.733 \text{ Mg/m}^3$ Mo K α radiation $\lambda = 0.71073 \text{ \AA}$ $\theta = 2.10 \text{ to } 23.41^\circ$ $\mu = 30.429 \text{ mm}^{-1}$ Plate, colourless $0.04 \times 0.28 \times 0.44 \text{ mm}^3$ $R_{\text{int}} = 14.89$
Unit cell data	Unit cell data	Inorganic structure

15. Bis(Octylamine) Tetraiodomercurate

The hybrid system was characterized at two different temperatures, -50°C and -100°C . The -50°C structure was solved without any hydrogen atoms as the addition of the atoms caused the refinement to become unstable. The unit cell data was collected at -100°C . The problems experienced with the structures could be due to disorder or disintegration of the crystal structure as iodide hybrid structures tend to be very unstable.

The asymmetric unit consists of two n-octylammonium cations and one isolated tetrahedral unit.

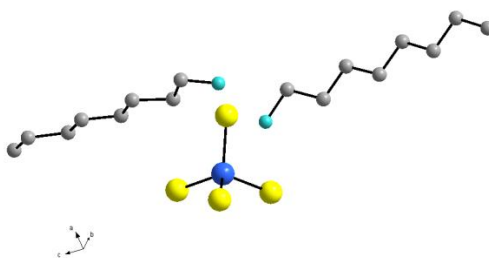


Figure 47: Asymmetric unit

The inorganic tetrahedra have a head to tail packing arrangement along the b direction. This results in two dimensional layers which extend along the *ab*-plane. The average Hg-I bonding distance for the -50°C structure is 2.261 \AA with a standard deviation of 0.016 \AA while the bonding angle for I-Hg-I range between 105.47° - 111.89° resulting in a standard deviation of 2.437° . The -100°C structure exhibited a larger degree of disorder which resulted in a larger average bonding distance with a large standard deviation of 0.370 \AA .

The organic chains deviate slightly from their planar conformation. The sandwiched organic chains form intercalated species which extend almost perpendicularly to the inorganic layer.

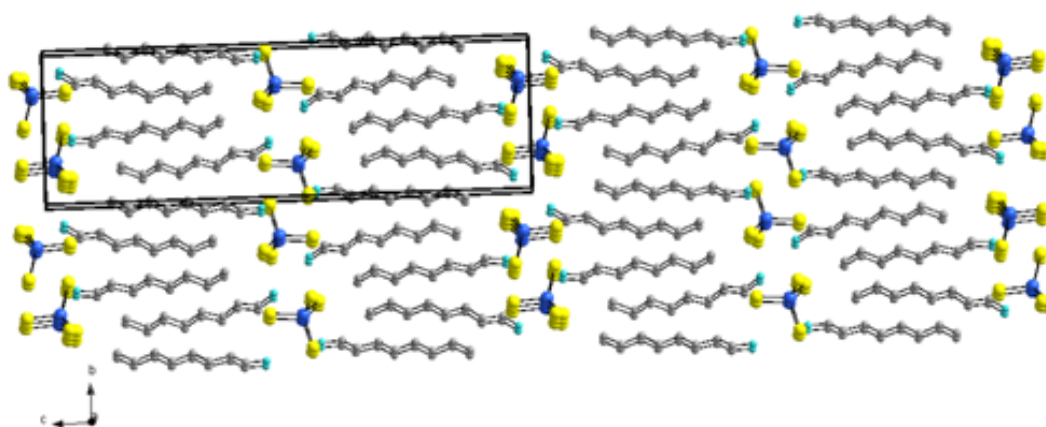


Figure 48: Crystal packing arrangement

Thermal characterization

The crystal was not thermally characterized via DSC as there was no evidence of any phase transitions at low temperatures.

Synthesis

0.0375g(0.83 mmol) mercury(II)iodide and 0.02g (0.17 mmol) Octylamine was dissolved in 3ml of concentrated HI, 2ml H₃PO₄ and 7ml of H₂O. The solution was then slowly heated to 90°C and then cooled back to room temperature over a 54hr period.

Crystal Structure

Table 23: Experimental data

(C₈H₁₉NH₃)₂HgI₄	
T = -50°C	T = -100°C
Crystal data Monoclinic, <i>P</i> 2 ₁ / <i>n</i> <i>a</i> = 7.292 Å <i>b</i> = 10.263 Å <i>β</i> = 95.65° <i>c</i> = 32.574 Å <i>V</i> = 2426.0 Å ³ <i>Z</i> = 4	Crystal data Monoclinic, <i>P</i> 2 ₁ / <i>n</i> <i>a</i> = 7.286 Å <i>b</i> = 10.235 Å <i>β</i> = 96.40° <i>c</i> = 32.672 Å <i>V</i> = 2421 Å ³
Refinement data <i>F</i> ₀₀₀ = 2088 <i>D</i> _x = 3.201 Mg/m ³ Mo Kα radiation <i>λ</i> = 0.71073 Å <i>θ</i> = 1.26 to 22.43° <i>μ</i> = 17.736 mm ⁻¹ Block, colourless 0.26 x 0.10 x 0.09 mm ³ <i>R</i> _{int} = 6.09	Refinement data <i>F</i> ₀₀₀ = 2088 <i>D</i> _x = 3.20 Mg/m ³ Mo Kα radiation <i>λ</i> = 0.71073 Å <i>θ</i> = 1.25 to 29.17° <i>μ</i> = 17.769 mm ⁻¹ Plate, colourless 0.53 x 0.50 x 0.02 mm ³ <i>R</i> _{int} = 105
Structure anisotropic with no hydrogen atoms	Inorganic structure

16. Bis(Nonylamine) Tetraiodomercurate

The hybrid was structurally characterized at -50°C . The structure contained some disorder and could not be refined with hydrogen atoms as this caused the structure to become unstable. The asymmetric unit consisted of two isolated tetrahedra and four organic chains. Disorder was prevalent in the unit as both the inorganic tetrahedra and the organic chains had atoms which were split between two positions.

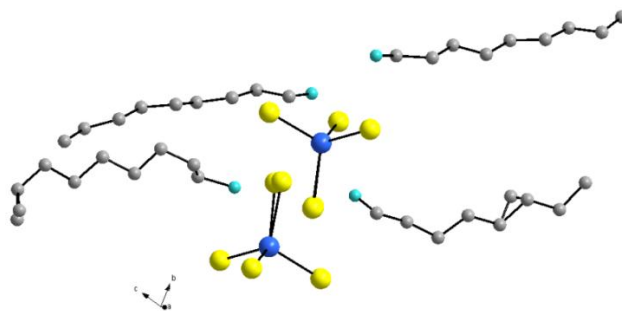


Figure 49: Asymmetric unit

The isolated inorganic tetrahedra extend infinitely along the ab -plane with a head to tail packing arrangement which extends along the b -direction. There is a disordered iodide ion in the inorganic unit. This implies that the ion is split between two sites within the same unit cell. The average Hg-I bond distance is 2.782\AA and 2.794\AA with standard deviations which range between 0.04\AA and 0.05\AA . The organic chains also exhibited some disorder in the carbon atoms of the cation. The organic chains are intercalated and extend at an angle relative to the inorganic layer.

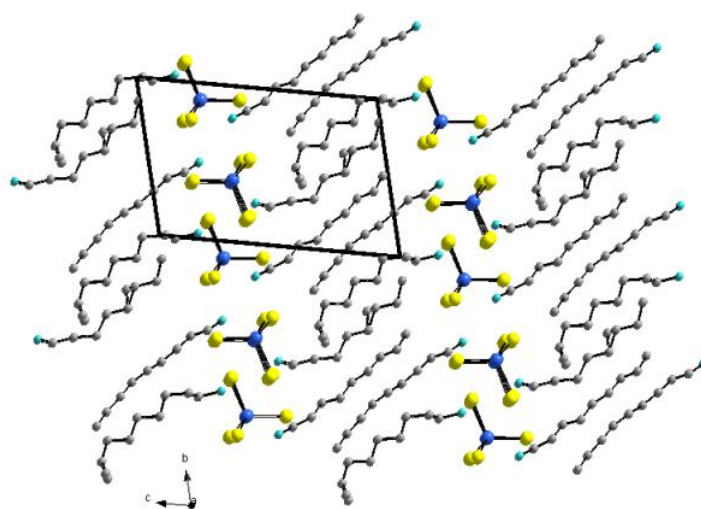


Figure 50: Crystal packing arrangement

Synthesis

0.035g (0.08 mmol)HgI₂ and 0.05g(0.34 mmol) Nonylamine were dissolved in a solution containing 2ml hexane, 2ml ethylacetate, 1ml of concentrated HI and a couple of drops of phosphinic acid. The samples were then heated to 90°C and left over night. The sample was then slowly cooled back to room temperature until crystallization occurred.

Crystal data:

Table 24:Experimental data

(C₉H₁₉NH₃)₂ HgI₄	
T = -50°C	
Crystal data	
<i>M_r</i> = 596.65	
Triclinic, <i>P</i> 1	
<i>a</i> = 8.4223Å	<i>α</i> = 76.56°
<i>b</i> = 10.9873Å	<i>β</i> = 86.15°
<i>c</i> = 16.6826Å	<i>γ</i> = 89.39°
<i>V</i> = 1498.10Å ³	
<i>Z</i> = 1	
Refinement data	
<i>F</i> ₀₀₀ = 1335	
<i>D_x</i> = 3.307 Mg/m ³	
Mo <i>Kα</i> radiation	
<i>λ</i> = 0.71073 Å	
<i>θ</i> = 1.26 to 24.74°.	
<i>μ</i> = 17.955 mm ⁻¹	
Plate, colourless	
0.40 x 0.06 x 0.04 mm ³	
<i>R</i> _{int} = 6.19	

4.2 Isolated Octahedra Coordination

4.2.1 Zinc (II) chloride - Octahedral coordination

Zinc halide hybrids tend to form isolated tetrahedral inorganic units. The isolated units are zero dimensional but adopt a packing structure which allows the formation of two dimensional layers. The zinc halide structures can however adopt a different coordination which is not as common. R.J Deeth *et al.* discovered a zinc chloride hybrid which forms a structure containing isolated octahedra. The hybrid discovered was bis(ethylenediammonium) hexachlorozincate (Deeth, 1984).

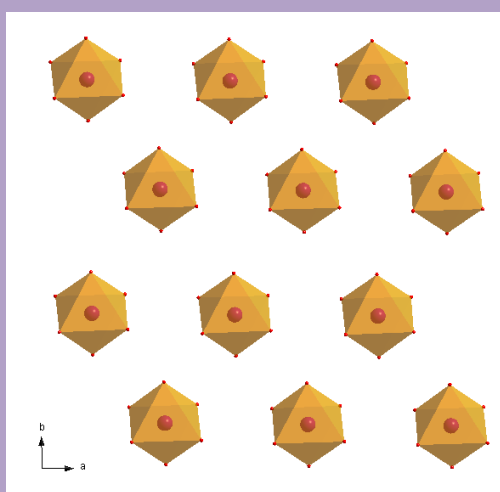


Figure 51: Isolated inorganic units

17. Bis(Butylamine) Hexachlorozincate

The crystal structure was determined at -50°C . The crystal structure asymmetric unit consists of two n-butylammonium cations and one isolated octahedral unit.

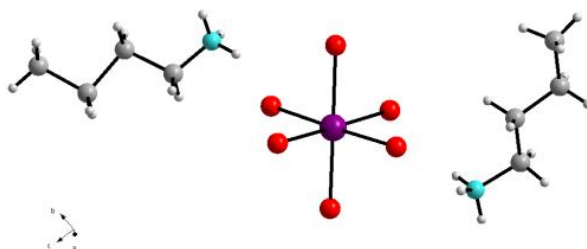


Figure 52: Asymmetric unit

The inorganic layers consist of isolated octahedra which are related by translation only. The layers extend infinitely along the *ab*-plane. The average metal halide bonding distance is 2.431\AA with a standard deviation of 0.018\AA . The bonding angles exhibit slight distortions which are related to the hydrogen bonding scheme.

Organic cations are sandwiched between the inorganic layers and tend to form intercalated species. The organic chains tend to be at an angle in relation to the inorganic layer. The organic chains are not parallel in relation to each other. The polar head of the chain penetrates right into the inorganic layer for better hydrogen bonding interactions.

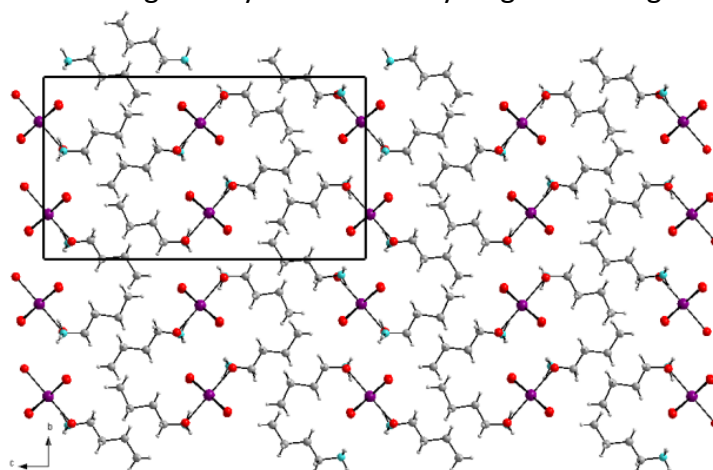


Figure 53: Crystal packing arrangement

Thermal characterization

The crystal is very unstable as the crystal structure seems to decompose as it is heated. None of the transitions seen below are reversible and a number of amorphous transitions can be seen meaning that the crystals aren't pure and are contaminated.

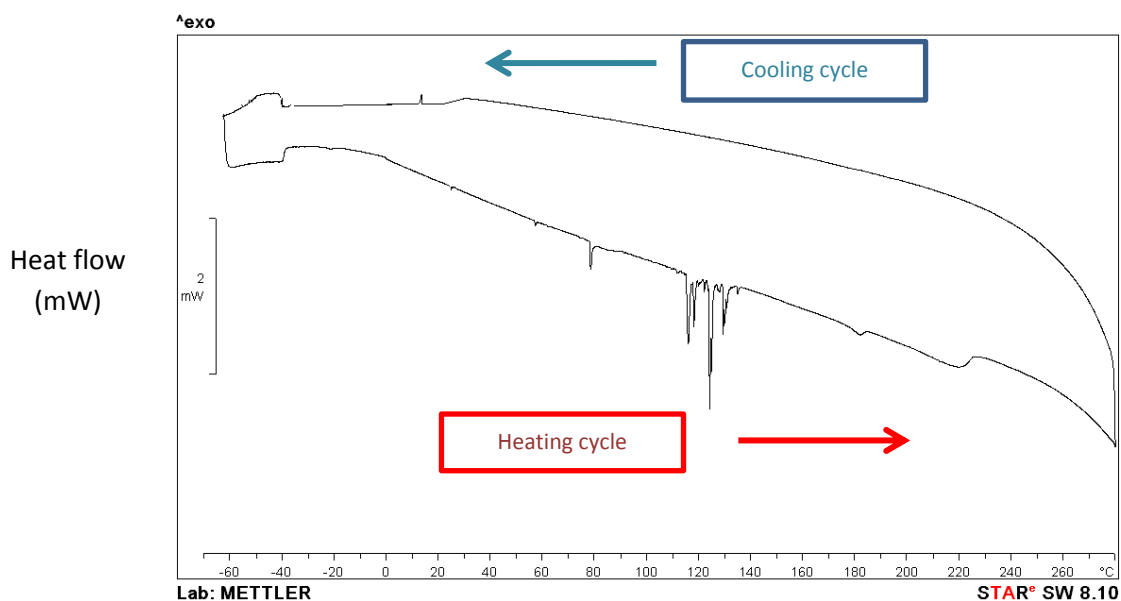


Figure 54: DSC scan of bis(butylamine) hexachlorozincate

Synthesis

0.05g (0.37 mmol) Zinc(II)chloride and 0.052g (0.70mmol) butylamine were dissolved in a solution of ethanol and concentrated HCl in a 3:1 ratio. The samples were heated to 70°C in a temperature controlled oil bath. Once all the reagents had dissolved the sample was slowly cooled back to room temperature. Crystallization then occurred once the solution was slowly evaporated.

Crystal data

Table 25: Experimental data

$(C_4H_9NH_3)_2 ZnCl_6$
$T = -50^\circ C$
<p>Crystal data Monoclinic, $P2_1/n$ $a = 7.2790 \text{ \AA}$ $b = 12.231 \text{ \AA}$ $\beta = 91.21^\circ$ $c = 21.627 \text{ \AA}$ $V = 1925.0 \text{ \AA}^3$ $Z = 4$</p> <p>Refinement data $F_{000} = 872$ $D_x = 1.471 \text{ Mg/m}^3$ Mo $K\alpha$ radiation $\lambda = 0.71073 \text{ \AA}$ $\theta = 1.88 \text{ to } 23.41^\circ$ $\mu = 2.093 \text{ mm}^{-1}$ Plate, colourless $0.52 \times 0.24 \times 0.03 \text{ mm}^3$ $R_{int} = 11.31$</p>

18. Bis(Octylamine) Hexachlorozincate

The crystal structure was determined at two different temperatures, room temperature and -100°C . A solid-solid phase transition occurs between the two temperatures.

The asymmetric unit of the room temperature structure consists of four organic chains and two incomplete inorganic units which rely on the symmetry operator to complete the isolated octahedra. The low temperature structure has a lower symmetry and therefore the asymmetric unit consists of two complete isolated inorganic octahedral and four organic chains.

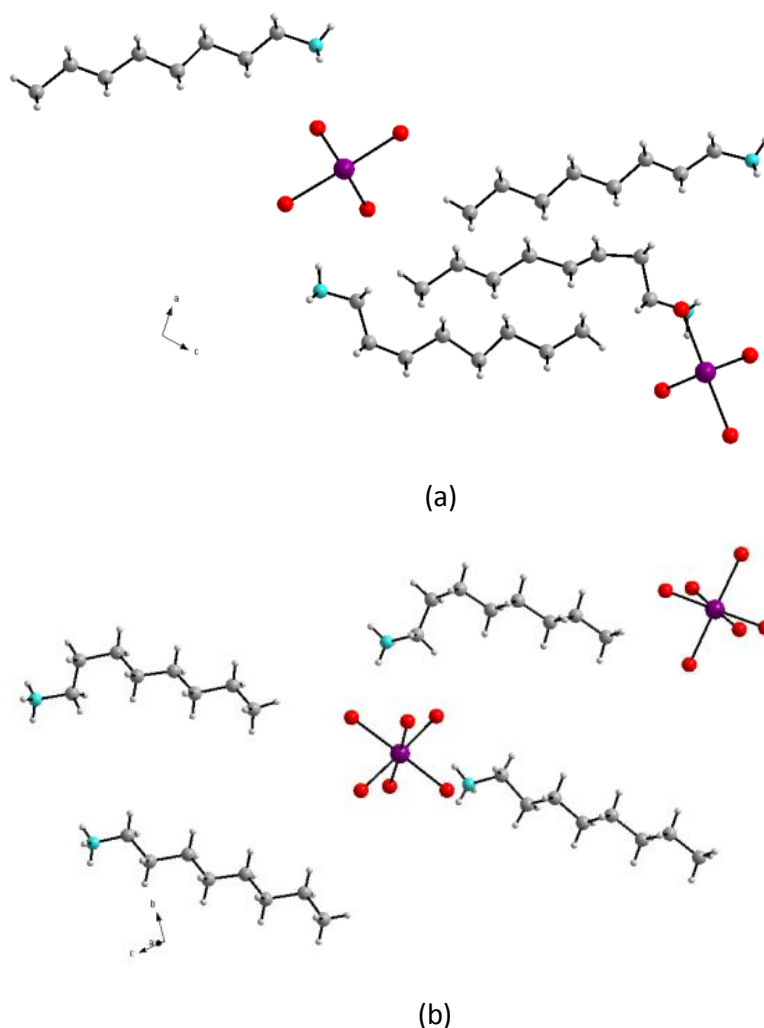


Figure 55: Asymmetric unit at (a) room temperature and (b) -100°C

The isolated inorganic octahedra pack in an arrangement forming two dimensional layers which extend along the ab -plane. The average metal halide bonding distance at -100°C is 2.43\AA for both of the inorganic asymmetric units. The average standard deviation of the bond length is 0.015\AA . The room temperature structure has an average metal halide bonding distance of 2.47\AA with a standard deviation of 0.015\AA .

The sandwiched organic layers form intercalated chains which are all relatively planar. The polar heads of some of the organic cations are bent to allow for better hydrogen bonding interactions. The organic chains extend in a manner which tends to be at an angle relative to the inorganic layers.

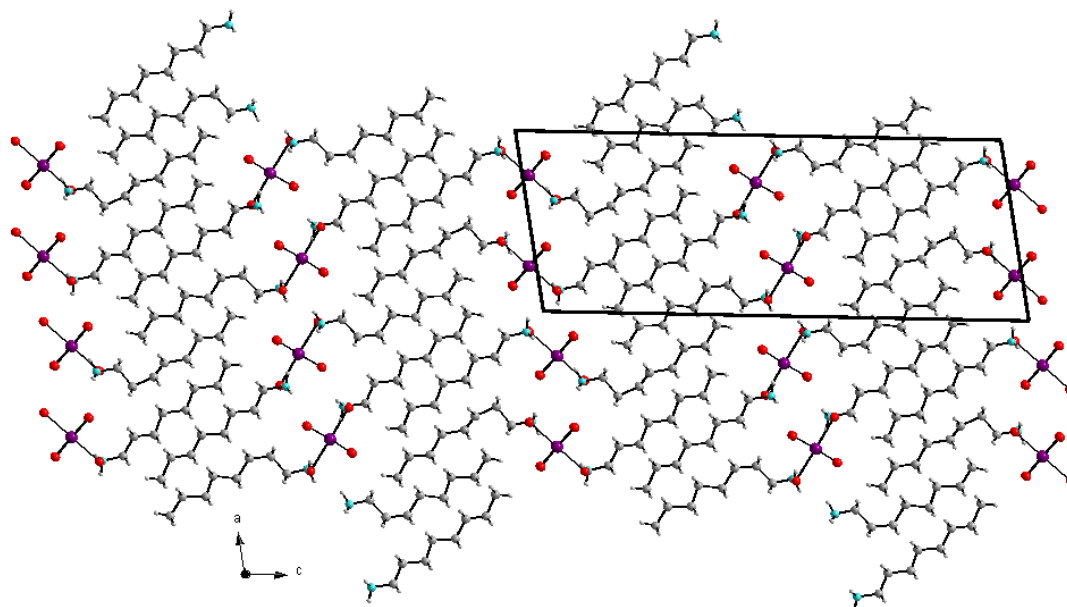


Figure 56: Crystal packing arrangement of the room temperature structure

Thermal characterization

The crystal undergoes two reversible phase transitions between -70°C and 280°C . Phase I was identified in this study at -100°C and room temperature. There is an additional phase transition which is not present on the DSC pattern the transition could have occurred below the ranges of the instrument. The additional phase was identified via SC-XRD data where phase I transforms from a monoclinic to a triclinic unit cell. The two phase transitions are relatively close to each other during the heating portion of the temperature cycle. The transitions occur at approximately 70°C and 85°C .

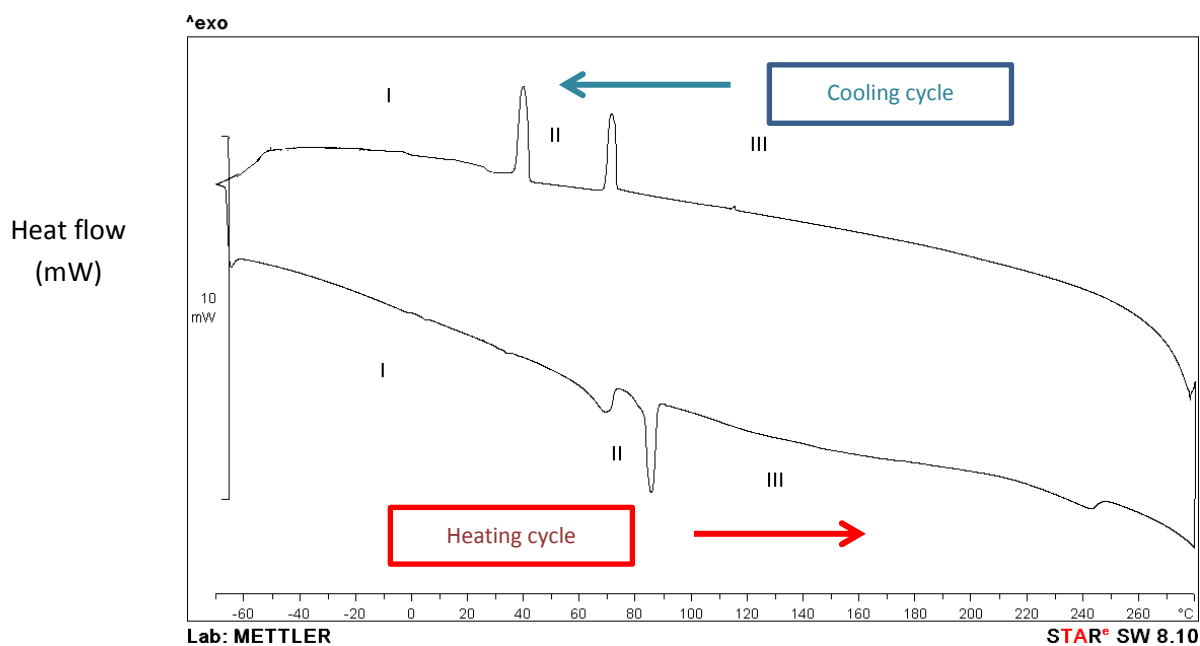


Figure 57: DSC scan of bis(octylamine) hexachlorozincate

Synthesis

0.05g (0.37mmol) of Zinc(II)chloride and 0.095g (0.73mmol) of octylamine were dissolved in an 5ml ethanol and 0.5ml of concentrated hydrochloric acid solution. The solutions were heated to 70°C to dissolve all the reagents. Crystallization occurred once the solution was left to evaporate.

Crystal data

Table 26: Experimental data

$(C_8H_{17}NH_3)_2 ZnCl_6$	
$T = -100^\circ C$	$T = 20^\circ C$
Crystal data $M_r = 538.59$ Triclinic, $P-1$ $a = 7.167\text{\AA}$ $\alpha = 98.27^\circ$ $b = 11.835\text{\AA}$ $\beta = 93.14^\circ$ $c = 31.198\text{\AA}$ $\gamma = 91.23^\circ$ $V = 2613.54\text{\AA}^3$ $Z = 4$	Crystal data $M_r = 538.59$ Monoclinic, $P2_1/m$ $a = 12.188\text{\AA}$ $b = 7.426\text{\AA}$ $\beta = 99.99^\circ$ $c = 32.372\text{\AA}$ $V = 2885.4\text{\AA}^3$ $Z = 4$
Refinement data $D_x = 1.45 \text{ Mg/m}^3$ Mo $K\alpha$ radiation $\lambda = 0.71073 \text{ \AA}$ $\theta = 0.7$ to 23.3° $\mu = 2.006 \text{ mm}^{-1}$ Plate, colourless $0.46 \times 0.38 \times 0.04 \text{ mm}^3$	Refinement data $D_x = 1.24 \text{ Mg/m}^3$ Mo $K\alpha$ radiation $\lambda = 0.71073 \text{ \AA}$ $\theta = 0.6$ - 23.5° $\mu = 1.411 \text{ mm}^{-1}$ Plate, colourless $0.46 \times 0.38 \times 0.04 \text{ mm}^3$
Structure	Structure

4.3 Octahedral Co-ordination

The divalent metal ion used in the hybrid determines the coordination of the inorganic units in the hybrid. The octahedra in this study are corner sharing and therefore produce two dimensional sheets. The charge of this type of structure is less than the isolated units seen before. This leads to different packing characteristics of the organic cations with a lower packing efficiency where no intercalation takes place. The entire system is still stabilized via charge assisted hydrogen bonds.

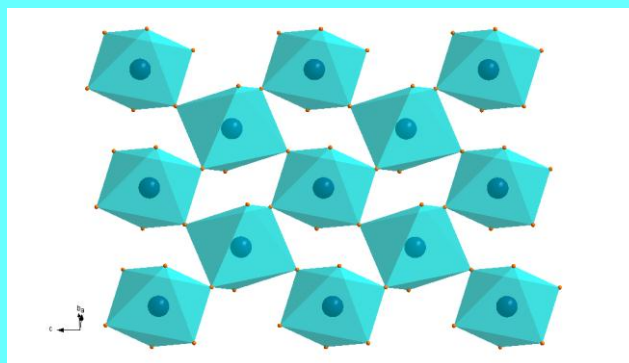


Figure 58: Corner sharing octahedra

4.3.1 Copper (II) chloride hybrids

The copper (II) hybrids form the typical layered structure as seen before. The inorganic octahedra are corner sharing and therefore produce two dimensional sheets. The organic cations are sandwiched between the inorganic sheets. The entire system is stabilized by the hydrogen bonds between the organic and inorganic units. The copper hybrid structures studied tend to undergo a number of phase transitions.

19. Bis(Butylamine) Tetrachlorocuperate

The butylammonium hybrid contains some disorder in the structure which resulted in a number of problems during refinement specifically with the organic cations. Hydrogen atoms could only be placed on the polar head of the organic chains. This specific hybrid system has been characterized before via PXRD, UV-Vis, DSC and TGA (Xiao, 2005). The hybrid structure is now characterized via SC-XRD.

The asymmetric unit of the butylammonium hybrid consists of one n-butylammonium cation and a fraction of a copper ion which is ionically bonded to two chloride ions. The rest of the structure is generated via the symmetry operator of the crystal system.

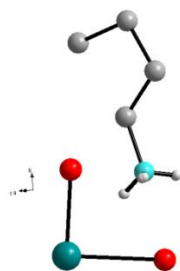


Figure 59: Asymmetric unit

The inorganic layer of the cuperate hybrids consist of corner sharing octahedra which extend infinitely along the ac plane. The average Cu-Cl bonding distance was 2.535Å with a standard deviation of 0.157Å.

The torsion angles of the cations indicates that the polar heads are rotated so that the organic chains can insert themselves into the inorganic layers which allows for better hydrogen bonding interactions. The torsion angles only deviate near the polar head while the rest of the carbon chains remain planar.

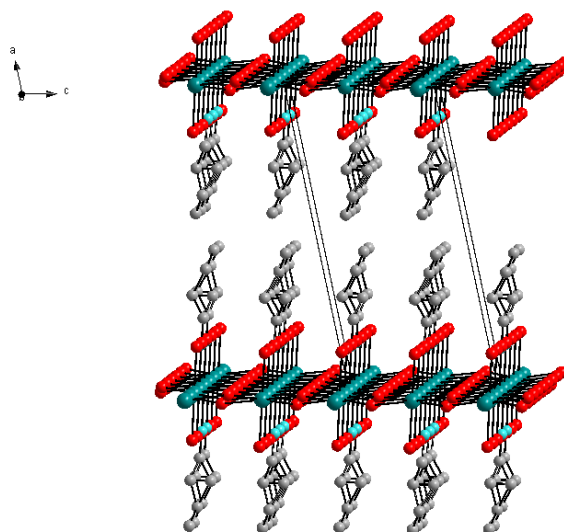


Figure 60: Crystal packing arrangement

Thermal characterization

Solid-solid phase transitions were identified in a previous study by means of DSC. The crystals experience an order-disorder transition at approximately 51°C where the lower temperature structure is ordered while the higher temperature structure results in disordered alkylammonium chains (Xiao, 2005).

Synthesis

0.05g(0.39mmol) CuCl₂ and 0.043g (0.59mmol)Butylamine were dissolved in a solution containing 1.2ml of concentrated HCl and 3 ml H₂O. Once all the reagents were dissolved the solution was left to evaporate until crystallization occurred.

Crystal data

Table 27: Experimental data

(C₄H₉NH₃)₂CuCl₄
T = 20°C
Crystal data Orthorhombic, <i>Cmca</i> <i>a</i> = 7.2976 Å <i>b</i> = 30.556 Å <i>c</i> = 7.4890 Å <i>V</i> = 1669.9 Å ³ <i>Z</i> = 4
Refinement data <i>F</i> ₀₀₀ = 664 <i>D</i> _x = 2.005 Mg m ⁻³ Mo Kα radiation <i>λ</i> = 0.71073 Å <i>θ</i> = 1.33 to 23.34°. <i>μ</i> = 5.643 mm ⁻¹ Plate, yellow 0.34 x 0.22 x 0.02 mm ³ <i>R</i> _{int} = 8.95

20. Bis(Heptylamine) Tetrachlorocuperate

The heptylammonium hybrid was structurally characterized at two different temperatures. The unit cell data was collected at room temperature while the crystal structure was determined at -100°C . The asymmetric unit of the crystal system consists of two n-heptylammonium cations and a copper ion bonded to four chloride ions in a square planar configuration. The inorganic octahedra are completed by the symmetry operations of the unit cell.

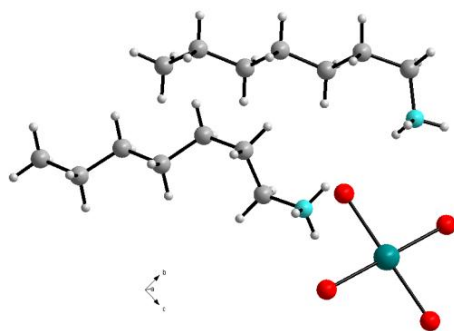


Figure 61: Asymmetric unit

The inorganic layer of the cuperate hybrids consist of corner sharing octahedra which extend infinitely along the *ab*-plane. The average Cu-Cl bonding distance was 2.297\AA with a standard deviation of 0.016\AA . The octahedra experience some tilting which is a result of the hydrogen bonding scheme.

The torsion angles of the cations indicates that the polar heads are rotated so that the organic chains can insert themselves into the inorganic layers which allows for better hydrogen bonding interactions. The torsion angles only deviate near the polar head while the rest of the carbon chains remain planar. The carbon chains are tilted with respect to the inorganic layer but are parallel with respect to each other.

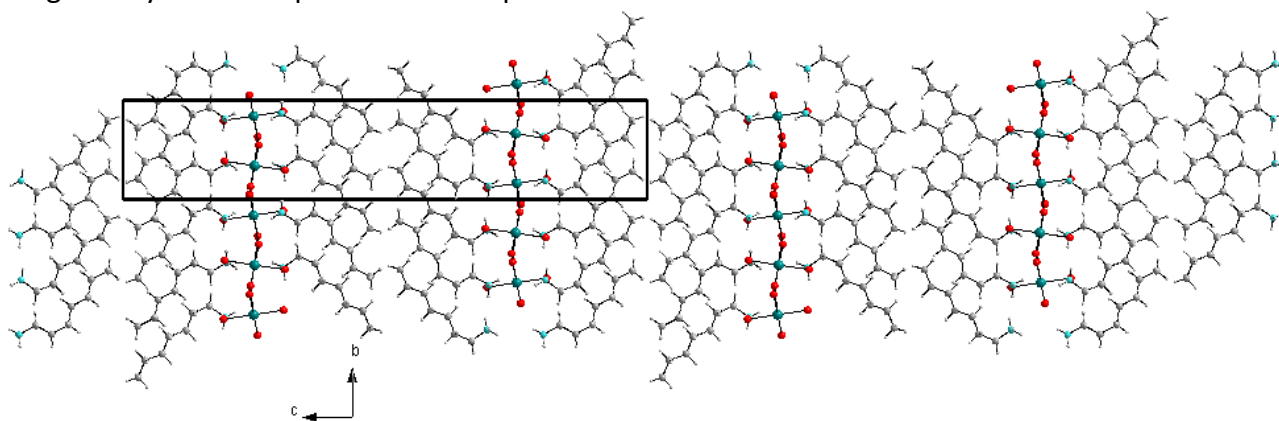


Figure 62: Crystal packing arrangement

Thermal characterization

The DSC scan of the heptylammonium hybrid resulted in a number of phase transitions present between the temperatures specified, -50°C to 300°C . There are two solid-solid phase transitions present as the sample is heated at -30°C and 50°C . Phase I proved to be a

monoclinic system with the transition being reversible. Phase II involves a phase transition as well as an order-disorder transition where:

Phase I Monoclinic, $P2_1/n$ → Phase II Orthorhombic, with a great deal of disorder

The final large exothermic peak starting at 220°C indicates the decomposition temperature.

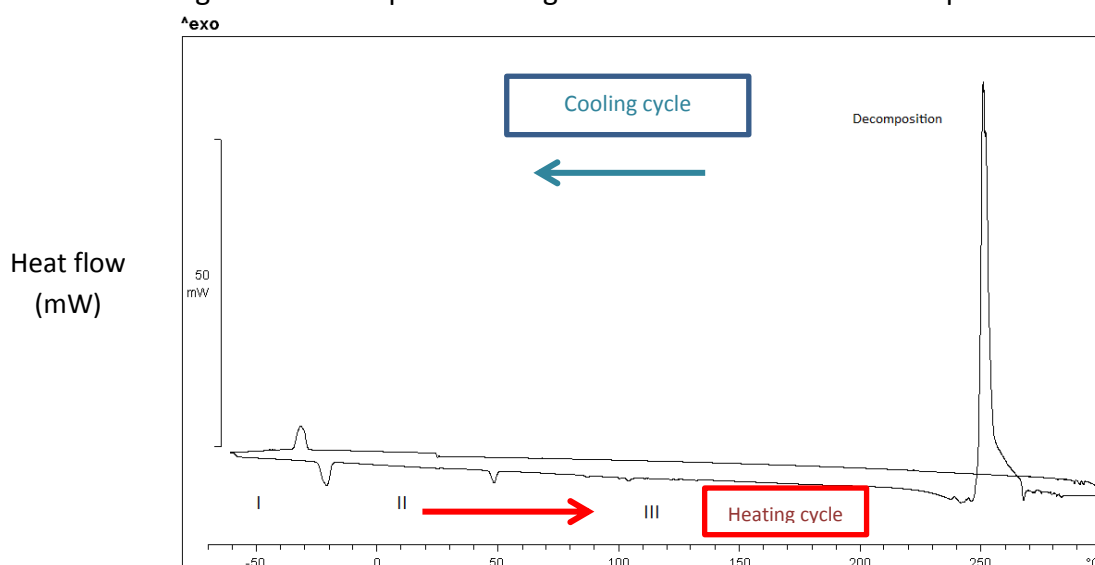


Figure 63: DSC scan of bis(heptylamine) tetrachlorocuperate

Synthesis

0.05g (0.39mmol)CuCl₂ and 0.0676g(0.59mmol)of Heptylamine were mixed in a 5:1 solution of 10 ml acetonitrile to 2 ml of concentrated HCl solution. The solutions were then left to slowly evaporate until crystallization occurred.

Crystal data

Table 28: Experimental data

$(C_7H_{15}NH_3)_2 CuCl_4$	
$T = -100^\circ C$	$T = 20^\circ C$
Crystal data	Crystal data
Monoclinic, $P2_1/n$	Orthorhombic
$a = 7.158 \text{ \AA}$	$a = 42.082 \text{ \AA}$
$b = 7.5165 \text{ \AA}$ $\beta = 91.560^\circ$	$b = 7.644 \text{ \AA}$
$c = 39.825 \text{ \AA}$	$c = 7.498 \text{ \AA}$
$V = 2141.8 \text{ \AA}^3$	$V = 2411.82 \text{ \AA}^3$
$Z = 4$	
Refinement data	Refinement data
$F_{000} = 924$	$F_{000} = 1344$
$D_x = 1.358 \text{ Mg m}^{-3}$	$D_x = 1.79 \text{ Mg m}^{-3}$
Mo $K\alpha$ radiation	Mo $K\alpha$ radiation
$\lambda = 0.71073 \text{ \AA}$	$\lambda = 0.71073 \text{ \AA}$
$\theta = 1.02$ to 23.33° .	
$\mu = 1.516 \text{ mm}^{-1}$	$\mu = 2.655 \text{ mm}^{-1}$
Plate, yellow	Plate, yellow
$0.70 \times 0.36 \times 0.06 \text{ mm}^3$	$0.64 \times 0.30 \times 0.02 \text{ mm}^3$
$R_{int} = 18.02$	$R_{int} = 17.81$
Structure	Unit cell data

4.3.2 Lead (II) halide structures

The hybrid structure is composed of corner sharing octahedra which extend infinitely in two dimensions. The organic component is sandwiched between the inorganic layers. The crystal undergoes a number of phase transitions which are temperature dependent. The phase transitions include solid-solid phase transitions and order-disorder transitions.

21. Bis(Butylamine) Tetrabromoplumbate

The hybrid was structurally characterized at -100°C . The organic component of the crystal could not be determined as the crystal experienced some degree of disorder.

The inorganic component's asymmetric unit consisted of a fraction of a lead ion which was bonded to two bromide ions. The octahedral geometry would be completed by the symmetry operations of the unit cell.

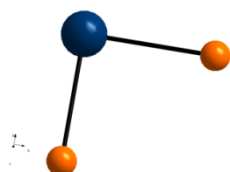


Figure 64: Asymmetric unit

The inorganic octahedra are corner sharing and form two dimensional sheets which extend infinitely along the bc -plane. The average Pb-Br bonding distance is 2.987\AA with a standard deviation of 0.005\AA .

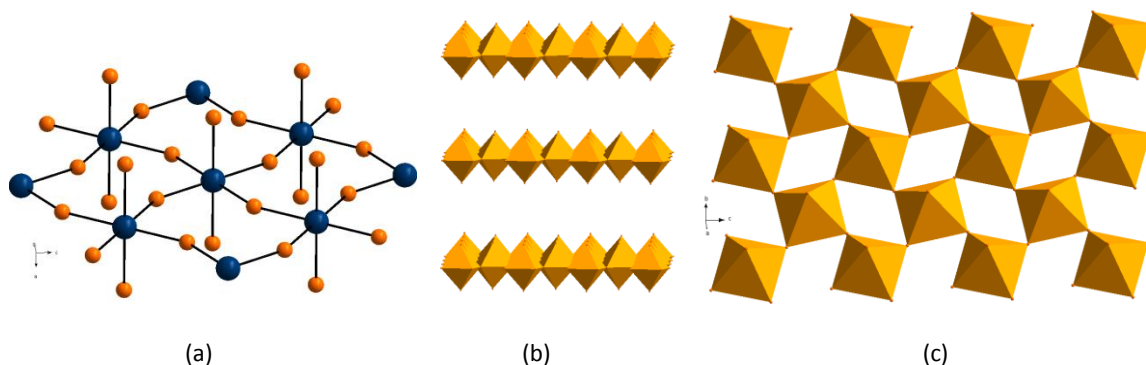


Figure 65: Inorganic two dimensional layers as (a) a ball and stick model (b) side view of the polyhedra (c) top view of the polyhedra

Thermal characterization

The crystal tends to undergo a solid-solid phase transition between -50°C and -100°C . The crystal transforms from an orthorhombic to a monoclinic space group as the crystal is heated from -100°C .

Synthesis

0.05g (0.14mmol)PbBr₂ and 0.02g (0.27mmol)of Butylamine were mixed in a 3:1 solution of water and ethanol respectively with 0.5 ml of concentrated HBr. The solutions were then left to slowly evaporate until crystallization occurred.

Crystal data

Table 29:Experimental data

(C₄H₉NH₃)₂ PbBr₄
T = -100°C
Crystal data Orthorhombic, <i>Cmca</i> <i>a</i> = 27.453 Å <i>b</i> = 8.271 Å <i>c</i> = 8.155 Å <i>V</i> = 1851.9 Å ³ <i>Z</i> = 4
Refinement data <i>F</i> ₀₀₀ = 1920 <i>D</i> _x = 3.887 Mg m ⁻³ Mo Kα radiation <i>λ</i> = 0.71073 Å <i>θ</i> = 1.48 to 28.37°. <i>μ</i> = 33.678 mm ⁻¹ Plate 0.31 x 0.22 x 0.01 mm ³ <i>R</i> _{int} = 5.39
Structure inorganic

22. Bis(Nonylamine) Tetrabromoplumbate

The crystal structure was determined at -100°C . The asymmetric unit of the lead bromide hybrid consists of one n-nonylammonium cation and a part of the octahedrally coordinated lead ion. The full octahedral coordination is generated by the inversion centre and the two fold screw axis.

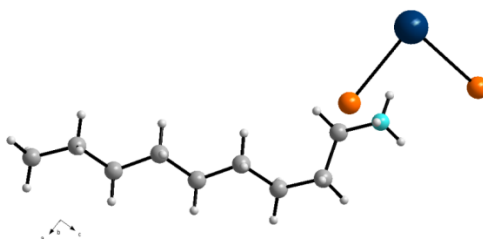
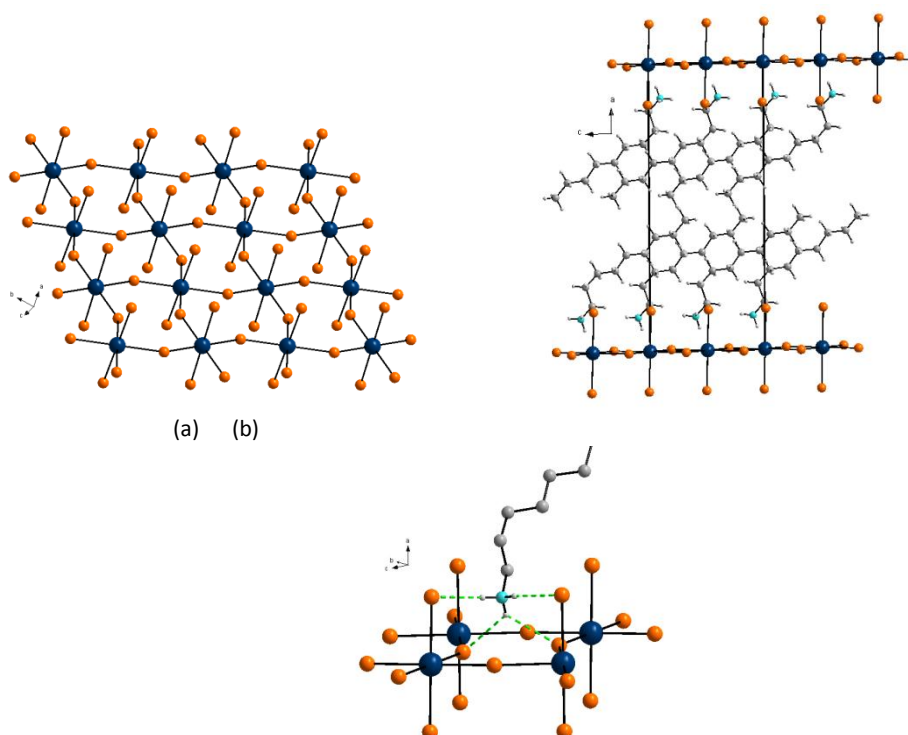


Figure 66: Asymmetric unit

The inorganic octahedra are corner sharing and extend infinitely in two dimensions along the bc -plane. The average bonding distance for the metal-halide bond is 3.004\AA with a standard deviation of 0.007\AA for all of the octahedral bonds. The monoprotic cations are sandwiched between the inorganic layers. The organic chains are tilted in relation to the inorganic layer but are parallel with respect to each other. Organic chains which are hydrogen bonded to alternate layers do not interact at all. The organic cations polar head extends right into the inorganic structure which allows for better hydrogen bonding.



(c)

Figure 67: (a) Two dimensional inorganic sheet (b) crystal packing arrangement (c) hydrogen bonding of the organic chains

Synthesis

0.27g (0.0775mmol) of PbBr_2 and 0.02g (0.155mmol) of nonylamine were dissolved in a solution comprised of 1ml of concentrated HBr and 9ml methanol. The solution was then left to slowly evaporate until crystallization occurred.

Crystal data

Table30:Experimental data

$(\text{C}_9\text{H}_{19}\text{NH}_3)_2\text{PbBr}_4$
$T = -100^\circ\text{C}$
Crystal data Monoclinic $P2_1/c$ $a = 21.275 \text{ \AA}$ $b = 7.869 \text{ \AA}$ $\beta = 91.09^\circ$ $c = 8.508 \text{ \AA}$ $V = 1424.1 \text{ \AA}^3$ $Z = 2$
Refinement data $F_{000} = 776$ $D_x = 1.901 \text{ Mg/m}^3$ Mo $K\alpha$ radiation $\lambda = 0.71073 \text{ \AA}$ $\theta = 1.91$ to 28.00° . $\mu = 11.540 \text{ mm}^{-1}$ Plate, colourless $0.56 \times 0.036 \times 0.04 \text{ mm}$ $R_{\text{int}} = 9.09$

23. Bis(Hexylamine) Tetraiodoplumbate

The crystal structure of bis(hexylamine) tetraiodoplumbate was previously characterized by Billing D.G *et al*; 2007. The hybrid structure was thermally and structurally characterized via a number of methods. This is an addition to the previously published data where the variable temperature photoluminescent and powder x-ray diffraction data was collected. The crystal had three phase transitions occurring at 268K, 354.9K and 371.3K. The initial transition exhibited thermochromic behaviour.

The inorganic layers shift their bond lengths and angles of the lead iodide units, I-Pb-I, according to the solid-solid phase transitions and the energy requirements at each specific temperature. The PXRD patterns exhibited evidence of the solid-solid transitions where peaks within the VT scan would disappear, appear or shift. The transitions are not so obvious in **Figure 68**. However **Figure 69(b)** which represents the top view of the PXRD scan clearly shows a transition in the bottom portion of the 3D scan.

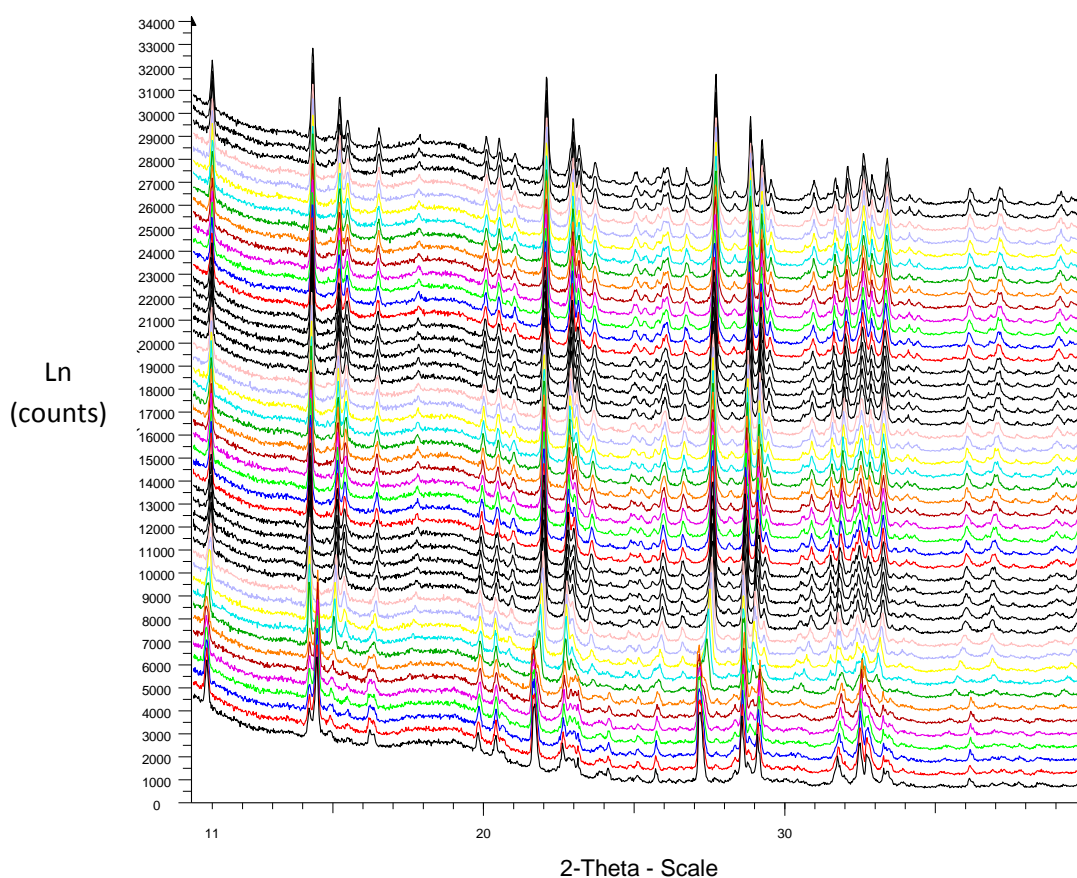
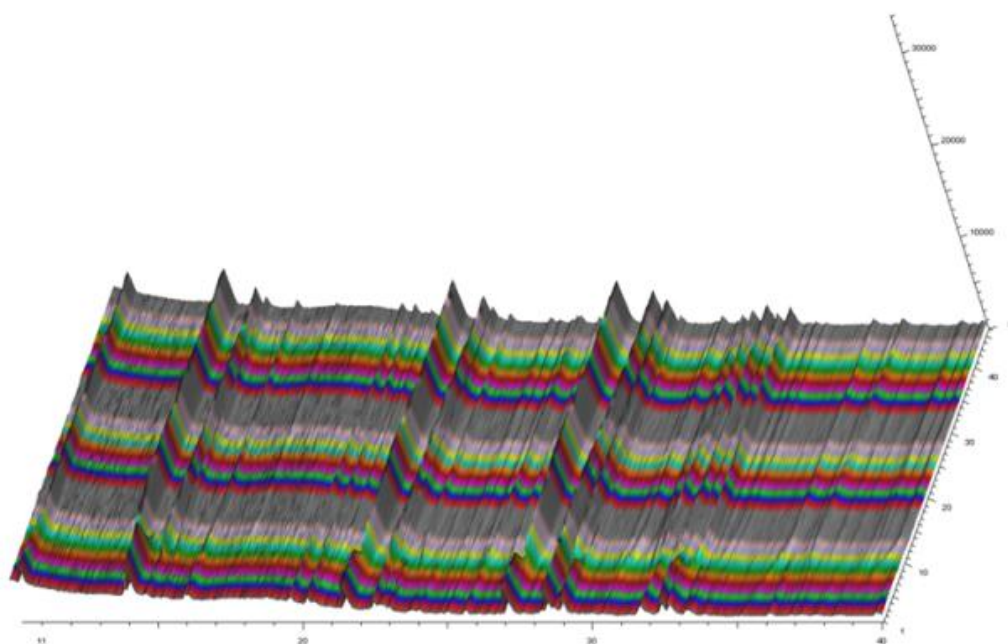
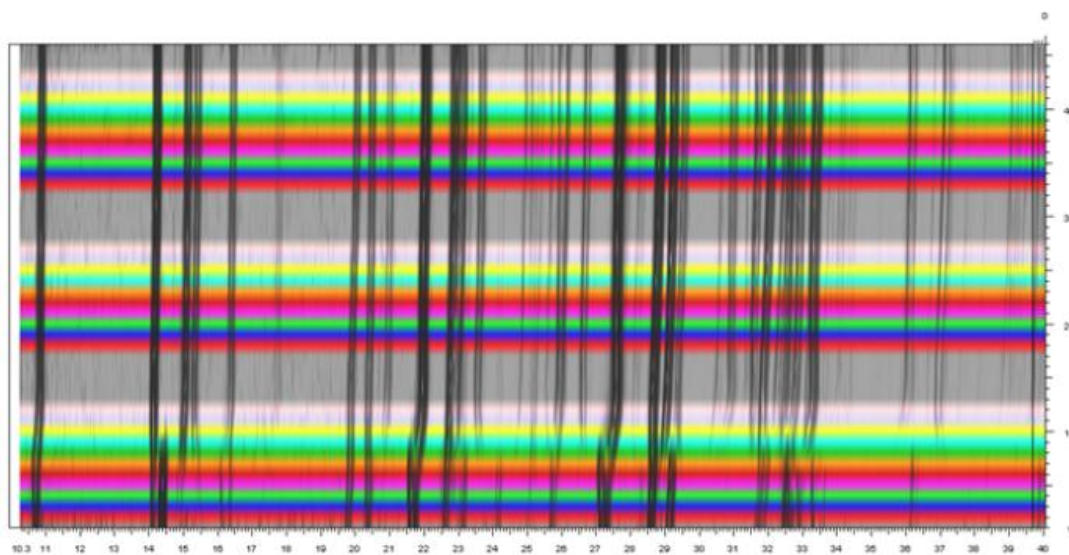


Figure 68: Variable temperature PXRD(VT-PXRD) scan of the hybrid between 2 theta values of 10 to 40 where each coloured line represents a different temperature.



(a)



(b)

Figure 69: Three dimensional VT-XRD scan of the hybrid structure (a) side view (b) top view

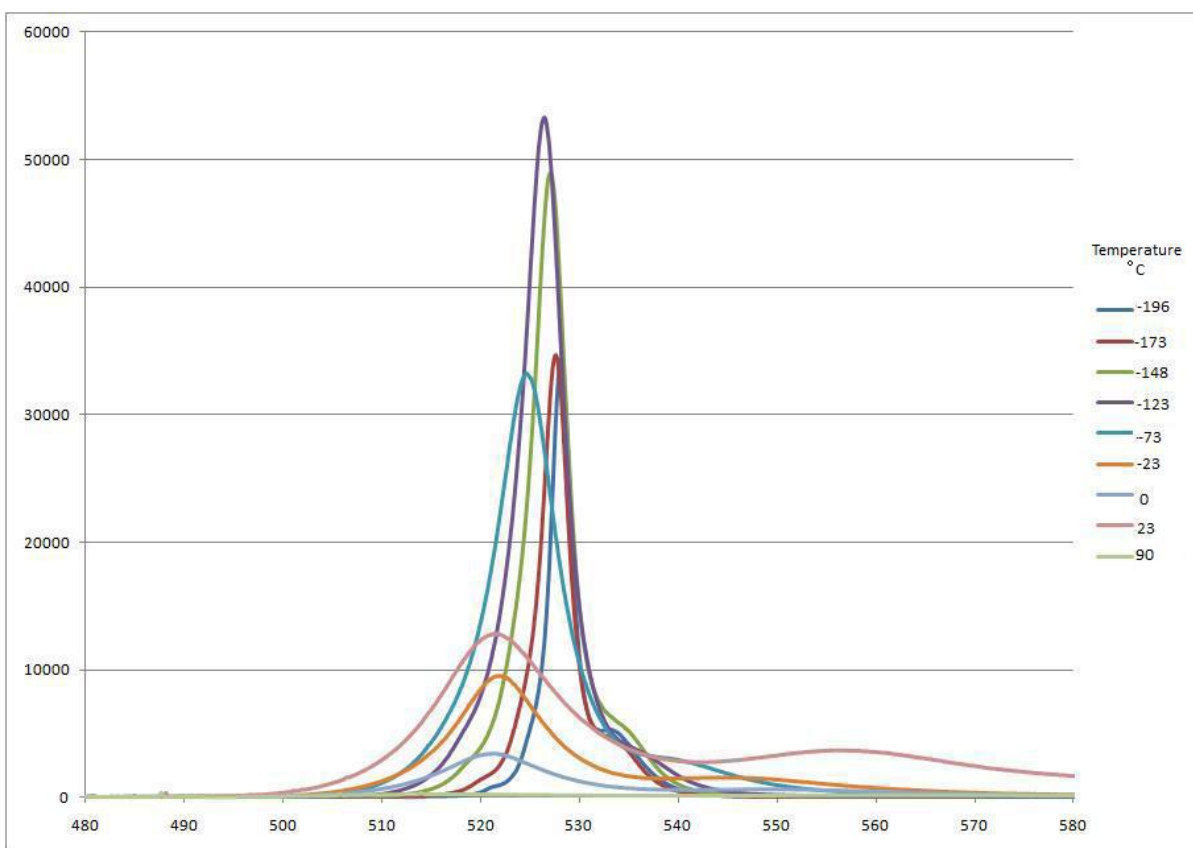


Figure 70: Variable temperature photoluminescent data of bis(*n*-hexylamine) tetraiodoplumbate

The crystal structure's photoluminescent capabilities were characterized in this study. Luminescence is the phenomenon where a material emits radiation in response to a previous excitation process. The excitation source consisted of an argon ion laser with a low power of approximately 0.20mW. A minimal amount of power is applied as the crystals degrade when exposed to high power sources. The laser-beam's diameter at the sample was approximately 1 μ m.

Structural properties such as the halide-metal-halide angles affect the optical properties of the hybrid. This would imply that each phase transition would have its own characteristic luminescent ability. It could then be concluded that the luminescent ability of bis(hexylamine) tetraiodoplumbate is temperature dependent refer to **Figure 70**.

The most energetic excitation peaks were identified at -123 $^{\circ}$ C and -148 $^{\circ}$ C. The hybrids are better photoluminescent materials at lower temperatures as the inorganic structure tends to be more ordered.

5. Discussion

5.1 Synthetic Methods

Organic-inorganic hybrids are extremely unstable structures particularly during synthesis. The environment in which the crystals are synthesized plays a crucial role in the synthesis or formation of the crystal.

5.2 Sample Characterization

Once the materials have been crystallized, structural characterization needs to take place. A great amount of care needs to be taken when analysing the samples as exposure to the atmosphere can cause decomposition. The samples were therefore mostly characterized below 0°C which ensured a slower degradation rate. Mercury and iodine containing crystals seemed to be the most susceptible to degradation due to the environmental factors.

The temperature at which the sample is characterized is also important as the crystals exhibit temperature dependent phase transitions. The crystals therefore have to be characterized at stable points between phase transitions. Thermal characterization such as DSC is therefore extremely important in determining the temperatures required for structural characterization.

5.3 Organic-Inorganic Hybrid Structures

All of the crystals characterized in this study formed the usual alternating layered structure. The inorganic component formed two dimensional layers which sandwiched the organic chains between the alternating metal halide layers. The packing characteristics of the organic component were greatly affected by the dimensionality of the inorganic metal halide unit. The hybrids rely on charge assisted hydrogen bonds for the structures stability.

A few of the crystal structures contained a varied degree of disorder (which were temperature related) and twinning. There was no confirmed evidence of any modulated structures found in this study. There was however a number of structures which were rather suspect when reviewing the raw data collected but will be left for future investigations.

5.4 Tetrahedral Coordination

A majority of the zinc, cobalt and mercury structures form isolated, tetrahedrally coordinated inorganic metal halide units. The isolated, zero dimensional units stack together to form layers which extend in two dimensions. The isolated inorganic tetrahedra cause a large charge density as there is no charge distribution between the metal-halide units.

The negative charge of the inorganic metal halide units are stabilized by the organic cations. The degree of packing efficiency of the organic chains is directly dependent on the charge

density of the inorganic component. The organic chains from alternating inorganic layers extend into the same space to produce intercalated species. Published data reveals that intercalation of the organic chains has only been identified for compounds containing zinc and cobalt (Ciajolo *et al.* 1977).

5.4.1 Zinc (II) Halide Structures

Inorganic The zinc-chloride units of the hybrid structures coordinated either as isolated tetrahedra or isolated octahedral units, though the majority of the structures and the bromide and iodide series tended to be tetrahedral. The octahedral structures discovered were similar to the structure discovered by R Deeth; 1984. The ability of the metal ion to change its coordination suggests the ability to change oxidation states. Future investigations should include the determination of the factors which induce the various oxidation states.

The zinc chloride hybrids had the ability to form tetrahedral and octahedral units. The size of the smaller chloride ion (when compared to bromide and iodide) could be an important factor in the ability to form the octahedral species.

The average zinc-halide bond lengths of the chloride series of crystals were directly proportional with the carbon chain length. Published results show that the chloride series is affected by the parity of the organic chains. The average metal-halide distance of the bromide and iodide hybrid structures was not influenced by the carbon chain length as the values remain relatively similar for each series. The bond lengths for all the halide structures are however affected by temperature.

Organic The organic chains of all of the zinc hybrids were intercalated. Most of the zinc hybrid structures contained carbon cations which were relatively planar. Bis(pentylamine) tetraiodozincate however contained a carbon chain with a non-planar carbon tail. The deviation in the carbon cation seemed to break the symmetry of the crystal cell therefore resulting in a low symmetry operator. Ultimately the position of the organic chain relative to the inorganic layer is dependent on the phase transitions and therefore the temperature.

Phase transitions

Tetrahedral coordination: The phase transitions of the tetrahedral chloride hybrids were similar as both hybrids (Butylammonium and hexylammonium) had two reversible phase transitions above 0°C. The butylammonium hybrid did however exhibit a third transition upon cooling which was situated between the two initial peaks. The transition was not identified but left for future investigation.

The bromide crystals can have as many as three or four transitions when thermally characterized via DSC between -70°C and 270°C. The phase transitions tend to occur above 0°C for this series of crystals. Only the heptylammonium and the nonylammonium hybrids showed evidence of any phase transition below 0°C. The phase transitions of the bromide

series of hybrids could therefore be dependent on the parity of the organic chains like the chloride series previously published.

The bis(n-hexamine)tetraiodozincate structure exhibited a low temperature phase transition below 0°C.

Octahedral coordination:The octahedral, butylammonium hybrid was not a stable structure as it decomposes during heating, no reversible phase transitions were identified. This hybrid structure is therefore less stable than the tetrahedral form.

The octahedral, octylammonium hybrid undergoes two phase transitions when characterized via DSC. These phase transitions are reversible and the crystal tends to be more stable than the shorter Butylamine chain length. There is an additional phase transition present below the limits of the DSC which was discovered by SC-XRD.

5.4.2 Cobalt (II) chloride structures

Three cobalt chloride structures were determined. The hexylammonium and decylammonium structures were isomorphous while the octylammonium structure tended to be an outlier. The asymmetric unit of the isomorphous structures consisted of a tetrahedrally coordinated metal halide and two cationic organic chains. The outlier structure consisted of three cationic organic chains, one tetrahedrally coordinated $[\text{CoCl}_4]^{-2}$ and one isolated Cl^- ion.

Inorganic The hexylammonium and Octylammonium's average metal halide bond length was directly proportional to the carbon chain length of the organic cation. The isolated chloride ion in the Octylammonium structure seemed to have an effect on the average metal halide bonding distance as it produced the largest average bond length and did not follow the trend seen in the other cobalt hybrids.

Organic The organic cations were intercalated for all structures containing cobalt (II).The internal rotation angles deviated slightly from a planar conformation. The Octylammonium hybrid however, contained an additional type of carbon chain which did not conform to the usual conformation.

Phase transitions All of the phase transitions occurred above room temperature for the cobalt chloride series of crystals. These hybrids were extremely stable as the crystals did not decompose upon heating and all phase transitions identified were reversible.

5.4.3 Mercury (II) Halide Structures

The mercury hybrids characterized in this study tended to be extremely unstable and exhibited some degree of disorder. The crystals decomposed when exposed to the atmosphere and high temperatures. This was evident in the iodide crystals as colour changes were evident when the crystal was removed from its reagent solution. Low

temperatures and an inert atmosphere would be required for further investigation of this series of hybrids.

Inorganic The average metal-halide bonding distance was directly proportional to the carbon chain length for all the structures discussed.

Organic Bis(n-butylammonium) tetrabromomercurate's organic component could not be solved as the structure was extremely disordered. The organic components of the iodide hybrids could be determined but no hydrogen atoms could be placed as it caused the structure refinement to become unstable. The organic component exhibited various degrees of disorder within the structure for all mercury containing crystals.

Phase transitions The hybrids were not thermally characterized via DSC as the structures were extremely unstable. A phase transition was however identified via SC-XRD for bis(n-butylammonium) tetrabromomercurate between room temperature and -50°C.

5.5 Octahedral Coordination

The lead and copper containing crystals tended to form structures where the inorganic metal halide component coordinates as corner sharing octahedra. The octahedra extend in two dimensions. The octahedral layer distributes the charge within the extended inorganic layer which implies that there is a lower charge density within the crystal system. The organic component has a lower packing efficiency as a result of the lower charge density. The organic cations extending from opposite inorganic layers do not form intercalated species.

5.5.1 Copper (II) Chloride Structures

Two hybrid structures were discovered in this study, Butylammonium and heptylammonium structures. The butylammonium hybrid structure had been previously characterized but not via SC-XRD.

Inorganic The average inorganic Cu-Cl bond length is directly proportional to the organic chain length for the copper structures. The axial chloride metal bonds are slightly longer than the other corner sharing metal-halide bonds. The copper hybrids exhibit Jahn-Teller distortions which reduce the unit cell's symmetry.

Organic The ammonium cations are inserted directly into the inorganic layer. This requires a slight deviation of the internal rotation angle of the polar head while the carbon chain portion remains relatively planar. The butylammonium organic chains are perpendicular with respect to the inorganic layer and parallel with respect to each other. The heptylammonium chains are tilted at an angle with respect to the inorganic layer and parallel with respect to each other.

Phase transitions The phase transitions of the butylammonium structure were previously studied and an order-disorder transition occurred at 51°C. The heptylammonium hybrid contained two phase transitions when heating the sample from -70°C one of which was below 0°C. The decomposition temperature was also determined at 240°C.

5.5.2 Lead (II) Halide Structures

The butylammonium and nonylammonium bromide crystals were characterized in this study. The butylammonium structure was disordered as the organic components could not be determined.

Inorganic The average inorganic Pb-Br bond lengths are directly proportional to the carbon chain lengths of the organic cation.

Organic The organic component could not be determined for the butylammonium hybrid. The nonylammonium hybrid on the other hand incorporated organic cations which were non-intercalated. The polar head of the cation is bent which allows for better hydrogen bonding. The organic chains therefore extend at an angle with respect to the inorganic layer but extend in a manner which is parallel with respect to each other.

Phase transitions Previous studies done on lead hybrid structures leads us to believe that the crystals undergo a number of phase transitions at low and high temperatures. Further investigation has to take place for this series of hybrid structures.

Photoluminescence The luminescent ability of the hybrid containing lead iodide was temperature dependent and therefore dependent on the solid-solid phase transitions of the hybrid.

6. Conclusion

Tetrahedral Coordination

- The isolated inorganic structures result in a large charge density. The organic components form intercalated chains as a result. The average metal-halide distance of the inorganic units is affected by carbon chain lengths in the hybrids of zinc(II) chloride, mercury and cobalt (II) chloride.
- The tetrahedral hybrids tend to have phase transitions above 0°C for all divalent metal systems. The exception to the rule included the odd numbered carbon chains of bis(n-heptylamine) tetrabromozincate and bis(n-nonylamine) tetrabromozincate.
- The stability of the hybrids could be ranked as Co>Zn>Hg in accordance with ease of structure refinement, order-disorder transitions and actual crystal stability during characterization.

Isolated Octahedral Coordination

- The zinc (II) chloride structures seemed to be the only hybrid which had the ability to either occur as isolated tetrahedral or octahedral units. The coordination was dependent on the experimental conditions, solutions and various environmental factors. This explanation would require further investigation.
- The zinc (II) chloride octahedral structures exhibited a number of phase transitions. The Butylammonium structure was unstable while the Octylammonium hybrid produced stable and reversible transitions. Could the length of the organic chain influence the stability of the octahedral units?

Corner Sharing Octahedral coordination

- The octahedrally coordinated hybrid structures tend to use high symmetry functions to complete their asymmetric units.
- The copper hybrids characterized in this study seem to behave in a manner which is similar to the zinc chloride series of crystals. The Butylammonium hybrid does not exhibit any phase transition below 0°C while the heptylammonium hybrid exhibited an additional phase transition which occurred below 0°C. This behaviour is relatively similar to the tetrahedrally coordinated zinc(II) chloride hybrids whose thermal and physical properties are dependent on the parity of the organic molecule.

7. References

- Aruta C., Licci F., Zappettini A., Bolzoni F., Rastelli F., Ferro P., Besagni T.; (2005) *Appl. Phys.* **A 81**, 963–968.
- Atkin P.W. (1978) *Physical chemistry, Oxford university press.*
- Barendregt F., Schenk H.; (1970) *Physica, Pays-Bas*, **49**, 465.
- Bats J.W., Fuess H., Salah A.B.; (1982) *Z KRISTALLOGR* **159**, 15.
- Beiser A., (1981) *Concepts of modern physics, McGraw-Hill International Book Comp 3rd edition.*
- Billing D.G., Lemmerer A. (2006) *Acta Crystallogr., Sect. C: Cryst. Struct. Commun.* , **62**, m238.
- Billing D.G., Lemmerer A.; (2007) *Acta Cryst.* **B63**, 735-747.
- Billing D.G., Lemmerer A.; (2008) *New. J. Chem.* **32**, 1736-1746.
- Black R.; (2009) Unpublished data, University of Witwatersrand, Johannesburg, RSA.
- Bloomquist D.R., Willet R.D., Dodgen H.W.; (1981) *J. Am. Chem. Soc.* **103**, 10 2610-2615.
- Brandenburg K.; (1999) *DIAMOND*. Version 2.1e. Crystal Impact GbR, Bonn, Germany.
- Bruker; (1998) *SMART-NT*. Version 5.050. Bruker AXS Inc., Madison , Wisconsin, USA.
- Bruker; (1999) *SAINT-plus*. Version 6.02 (including XPREP); Bruker AXS Inc., Madison , Wisconsin, USA.
- Bruker; (2005). *APEX2*. Version 2.0-1. Bruker AXS Inc., Madison, Wisconsin, USA.
- Ciajolo M.R., Corradini P., Pavone V.; (1977) *Acta Cryst.* **B33**, 553.
- Coelho A. A., (2000) *TOPAS v4.2: General Profile and Structure Analysis Software for Powder Diffraction Data* Karlsruhe.
- Cole L.B., Holt E.M.; (1990) *Acta Cryst.* **C46**, 1737.
- Criado J.J., Jimenez-Sanchez A., Cano F.H., Saez-Puche R., Rodriguez-Fernandez E.; (1999) *Acta Cryst.* **B55**, 947.
- Dam B., Janner A.; (1986) *Acta Cryst.* **B42** 69-77.
- Deeth R.J., Hitchman M.A., Lehmann G., Sachs H. (1984) *Inorg. Chem.*, **23**, 1310.
- Doudin B., Chapuis G.; (1990) *Acta Cryst.* **B46**, 175.
- Doudin B. and Chapuis G. , *Acta Cryst.* (1990). **B46**, 180—186.
- Doudin B., Chapuis G.; (1992) *Acta Cryst.* **C48**, 1218.
- Farrungia L.J.; (1999) *J. Appl. Cryst.* **32** 837-838.
- Farrungia L.J.; (1997) *J. Appl. Cryst.* **30** 565.
- Fenryan J., Reynhart E.C., Jurga S., Jurga K.; (1993) *Molecular physics* **78** no.5 1117-1128.
- Fu Z., Chivers T.; (2006) *Can. J. Chem.*, **84**, 140.
- Garland J.K., Emerson K., Pressprich M.R.; (1990) *Acta Cryst.* **C46**, 1603.
- Geselle M., Fuess H.; (1997) *Z. Kristallogr.-New Cryst. Struct.*, **212**, 241.
- Giacovazzo C. ed.; (1992) *Fundamentals of Crystallography*, IUCR & OUP, Oxford, UK.
- Glavcheva Z., Umezawa H., Okada S., Nakanishi H.; (2004) *Materials Letters* **58**, 2466-2471.
- Godwa B.T., Foro S., Terao H., Fuess H. (2009) *Acta Cryst sect e* **65**, m946.
- Gou N., Lin Y.H, Xi S.Q.; (1995) *Acta Cryst.* **C51**, 617.
- Gou N., Lin Y.H., Zeng G., Xi S.Q.; (1992) *Acta Cryst.* **C48**, 650.
- Gou N., Lin Y.H., Zeng G, Xi S.Q.; (1992b) *Acta Cryst.* **C48**, 542.
- Halvorson K., Willett R.D.; (1988) *Acta Cryst.*, **C44**, 2071.
- Herbst-Irmer R.; (2008) Twin Refinement with SHELXL, Twinning workshop, Stellenbosch.
- Hong X., Ishihara T., Nurmikko A.V.; (1992) *Solid State Communications* **84**, no6, 657-661.

Ishihara H., Dou S., Horiuchi K., Krishnan V.G., Paulus H., Feuss H., Weiss A.; (1997) *Z.Naturforsch.A.Phys. Sci.*; **52'** 550.

James B.D., Bakalova M., Liesegang J., Rieff W.M., Hockless D.C.R., Skelton B.W., White A.H.; (1996) *Inorg. Chim.Acta*,**247**, 169.

Kapustyanyk V.B., Korchak Y.M.; (2000) *J. Applied Spectroscopy*.**67** no6.

Kind .R, Plesco .S, Arend .H, Blinc.R, Zeks .B, Seliger. J, Lozar .B, Slak J., Levstik A., Filipic C., Zagar V., Lahajnar G., Milia F., Chapius G.; (1979) *J. Chem. Phys.***71**, 2118.

Knutson J.L., Martin J.D.; (2005) *Inorg.Chem.***44**, 4699-4705.

Korfer M., Fuess H., Bats J.W., Klebe G.; (1985) *Z.Anorg.Allg.Chem.* , **525**, 23.

Landee C.P., Willet R.D.; (1981) *Inorg.Chem.***20**, 2521.

Lemmerer A.; (2006) PhD Thesis, Phase Transitions and structural motifs of inorganic-organic lead halide hybrids; University of the Witwatersrand; Johannesburg; RSA.

Leoni S.; (2007) *Chem.Eur. J.***13** 10022-10029.

Mahmoudkhani A.H., Langer V.; (2002) *Acta Cryst.***E58**, M592.

Maris T., Bravic G., Chanh N.B., Leger J.M., Bissey J.C., Villesuzanne A., Zouari R., Daoud.; (1996) *J. Phys. Chem. Solids*, **57**, 1963.

Mattukat K.; (2009) Unpublished data, University of Witwatersrand, Johannesburg, RSA.

Meresse A., Daoud A. (1989)*Acta Crystallogr.,Sect.C:Cryst.Struct.Commun.* ,**45**,194.

Meyer M., Paciorek W.A., Schenk K.J., Chapius G., Depmeier W.; (1994) *Acta Cryst.***B50** 333-343.

Mitzi D.B .(1996) *Chem.Mater.* ,**8**,791.

Mitzi D.B.; (1999) *Prog.Inorg. Chem*,**48**, 1-121.

Mitzi D.B.; (2004) *J. Mater. Chem.*, **14**, 2355-2365.

Mousdis G.A., Gionis V., Papavassiliou G.C., Terzis A.; (1998) *J.Mater.Chem*, **8(10)**, 2259-2262.

Muller P., Refinement of disorder with SHELXL <http://shelx.uni-ac.gwdg.de/~peterm/tutorial/disord.htm>

Available <http://Shelx.uni-ac.gwdg.de/~peterm/tutorial/do-intro.htm> [accessed 19 October 2009]

Nagapetyan S.S., Dolzhenko Y., Arakelova E.R., Koshkin V.M., Struchkov Y.T., Shklover; (1988) *Zh. Neorg. Khim. (Russ.J.Inorg.Chem.)***33**,2806.

Nespolo M., Ferraris G. ; (2003) *Acta Cryst.***A60**, 89-95.

Pabst I., Korfer M., Fuess H., Bats J.W.; (1986) *Z.Kristallogr.* ,**174**, 167.

Papavassiliou G.C., Koutselas I.B., Terzis A., Whangbo M.H.; (1994) *Sol. State Comm.***vol91**, 9, 695-698.

Petricek V., Dusek M., Palatinus L.;(2006). *Jana2006*.The crystallographic computing system.Institute of Physics, Praha, Czech Republic.

Phelps D.W., Losee D.B., Hatfield W.E., Hodgson D.J.; (1976) *Inorg.Chem.*,**15**, 3147.

Reber C.; (2008) *Can. J. of Anal.Sci.and Spec.* **53**, 3 91-101.

Roberts S.A., Bloomquist D.R., Willet R.D., Dodgen H.W.; (1981) *J. Am. Chem. Soc.***103**, 10 2603-2610.

Salah A.B., Bats J.W., Kalus R., Fuess H., Daoud A.; (1982) *Z .Anorg.Allg. Chem*,**493**, 178.

Salah A.B., Daoud A., Miane J.L., Ravez J., Hagenmuller P.; (1984) *Rev.Chim.Miner.* , **21**, 795.

Sheldrick G.M.; (1997). SHELXS97 and SHELXL97. University of Göttingen, Germany.

Shikoh E., Ando Y., Era M., Miyazaki T.; (2001) *J. of Magnetism and magnetic materials* 226-230 2021-2022.

Shriver D.F. and Atkins P.W. (1999) *Inorganic Chemistry, Oxford University Press 3rd edition*.

Schubnell M. (2010) Mettler Toledo user meeting, Sandton.

Spek A.L.; (2003) *J. Appl. Cryst.***36**, 7-13.

Spengler R., Zouarf R., Safah A.B., Zimmermann H., Burzlaff (1998) *Acta Cryst secc* **54** , 980034.
Streuer W., Depmeier W.; (1989) *Acta Cryst.***B45**, 562-566.
Tachibana H., Hosaka N., Tokura Y.; (2001), *Polymer***42** 8311-8314.
Vincent B.R., Robertson K.N., Cameron T.S., Knop O.; (1987) *Can.J.Chem.*,**65**,1042.
Wagner T., Schonleber A.; (2009) *Acta Cryst.***B65**, 249-268.
Willet R.D., Riedel E.F., (1975) *Chem. Phys.* **8**, 112.
Xiao Z., Chen H., Shi M., Wu G., Zhou R., Yang Z., Wang M., Tang B., *Materials Science and Engineering*
B 117 (2005) 313–316.
Xu Z., Mitzi D.B., Dimitrakopoulos C.D., Maxcy K.R.; (2003) *Inorg.Chem.***42**, 2031-2039.
Zhang G., Zhang R.L., Zhao J., Gao X., Wang S., He S.; (2004) *Chin. J. Chem.*,**22**, 899.
Zuniga F.J., Chapuis G.; (1983) *Acta Cryst.***B39**, 620.
Zuniga F.J., Chapuis G.; (1981b) *Cryst. Struct.Commun.***10**, 53.
Zuniga F.J., Chapuis G.; (1981a) *Acta Cryst.***A37**, c103.